POWER FLOW CONTROLLABILITY AND FLEXIBILITY IN THE
TRANSMISSION EXPANSION PLANNING PROBLEM: A MIXED-INTEGER
LINEAR PROGRAMMING APPROACH

Ricardo Cunha Perez

Dissertação de Mestrado apresentada ao
Programa de Pós-graduação em Engenharia
Elétrica, COPPE, da Universidade Federal do
Rio de Janeiro, como parte dos requisitos
necessários à obtenção do título de Mestre em
Engenharia Elétrica.

Orientador: Djalma Mosqueira Falcão

Rio de Janeiro
Março de 2014

POWER FLOW CONTROLLABILITY AND FLEXIBILITY IN THE
TRANSMISSION EXPANSION PLANNING PROBLEM: A MIXED-INTEGER
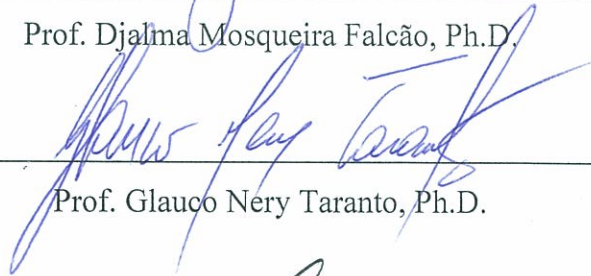LINEAR PROGRAMMING APPROACH

Ricardo Cunha Perez

DISSERTAÇÃO SUBMETIDA AO CORPO DOCENTE DO INSTITUTO ALBERTO
LUIZ COIMBRA DE PÓS-GRADUAÇÃO E PESQUISA DE ENGENHARIA
(COPPE) DA UNIVERSIDADE FEDERAL DO RIO DE JANEIRO COMO PARTE
DOS REQUISITOS NECESSÁRIOS PARA A OBTENÇÃO DO GRAU DE MESTRE
EM CIÊNCIAS EM ENGENHARIA ELÉTRICA.

Examinada por:

_____
Prof. Djalma Mosqueira Falcão, Ph.D.

_____
Prof. Glauco Nery Taranto, Ph.D.

_____
Eng. Mario Veiga Ferraz Pereira, D.Sc.

RIO DE JANEIRO, RJ - BRASIL
MARÇO DE 2014

To my first family; my second family;

last but not least, my Girlfriend Thatiana.

"Before engineers, we are human beings. The best academy is life"

Ricardo Perez

ACKNOWLEDGEMENTS

My Master Degree has helped me immensely to lay a foundation for my future professional life. I have received invaluable support from my advisors, family, girlfriend, friends and colleagues without whom this journey would not have been possible.

"If I have seen further, that is because I stood on the shoulders of giants" – Sir Isaac Newton. Despite the ironic historical meaning of the sentence, here it is applied in the literal sense. To achieve a goal as great as the master degree, two shoulders that sustain thee: the (i) professional and the (ii) personal.

On the first shoulder, I would first like to express sincere gratitude for my advisor Professor Djalma. His guidance and support has always helped me to think creatively and motivated. His dedication, patience, encouragement were determinants. I've got a great learning experience from our meetings not only academically but also personally.

I would also like to extend my gratitude to Professor Glauco Taranto for being a wonderful teacher, his support to my thesis work, serving on my master defense committee and finally for his valuable suggestions.

Additionally, I am extremely grateful for the help and support from all my PSR colleagues. Their suggestions, guidance, and help have helped immensely for this thesis work. As there are many important colleagues, the nomination would require a page.

I would like to thank Silvio Binato and Gerson Couto for teaching me a lot about transmission expansion planning and optimization problems. I would also like to thank Sergio Granville for helping me to develop the methodology, his contributions were more than fundamental.

Finally, I would like to extend a red carpet in gratitude to Dr. Mario Veiga Pereira. I am thankful for the dissertation topic, the ideas, encouragement, discussions and opportunity to carrying out this work. I have no words to represent the technical and personal contributions I've received from him. Priceless is too less a word.

On the second shoulder, first I thank my grandmother Reni for giving me spiritual enhancement and helping me grow as a human being in order to be able to produce this work. This is for you.

To my parents and brother for all the love, education, support and dedication without whom this work would not be developed. If I am able to be half of the parent you were to me, I'm satisfied.

I thank my second family, the "república" Ih Garai Rep!!® throughout the unconditional friendship, wonderful lived moments and for building me as an engineer in the professional side as on the personal side. This is a chosen and priceless family: "N.C.S.".

Last but for sure not least, I would like to thank the person who most followed day by day the execution of this work. Since studying with me, encouraging me, and even giving opinions about the work from her "medical" point of view. Definitely, I would not reach this goal without my future wife, Thatiana Correia. For all the love given to me that was the major factor in achieving this goal.

And finally, supporting both shoulders, I express gratitude to God, for giving me health and perseverance, without which I would never have achieved my goals.

CONTROLABILIDADE E FLEXIBILIDADE DE FLUXO DE POTÊNCIA NO PROBLEMA DE PLANEJAMENTO DA EXPANSÃO DA TRANSMISSÃO: UMA ABORDAGEM DE PROGRAMAÇÃO INTEIRA MISTA

Ricardo Cunha Perez

Março/2014

Orientador: Djalma Mosqueira Falcão

Programa: Engenharia Elétrica

A adição de equipamentos *FACTS* e *Distributed-FACTS* no sistema viabiliza maior controle do fluxo de potência ativa e maior flexibilidade operativa para acomodar diferentes cenários de despacho. Nesta dissertação, são propostas formulações baseadas em Programação Inteira Mista (PIM) para a incorporação desses dispositivos no problema de planejamento da expansão da transmissão. Este problema é formulado como um modelo de otimização baseado no fluxo de potência linearizado e nos limites de circuitos, onde o objetivo é minimizar os investimentos no sistema. A primeira formulação proposta é um modelo híbrido linear alternativo que evita a não-linearidade presente na Segunda Lei de Kirchhoff para linhas candidatas acrescentando ao mesmo tempo controlabilidade de fluxo ao sistema. A segunda formulação proposta modela Dispositivos Candidatos de Compensação Série (DCCSs) que são capazes de aumentar e/ou diminuir a reatância da linha de transmissão alvo e por consequência controlar o fluxo de potência na mesma. Os DCCSs podem ser conectados a uma linha existente ou candidata e apresentam um ponto de operação específico de acordo com cada cenário de despacho e condições operativas. As aplicações práticas das formulações propostas são demonstradas através de estudos de caso.

Abstract of Dissertation presented to COPPE/UFRJ as a partial fulfillment of the requirements for the degree of Master of Science (M.Sc.).

POWER FLOW CONTROLLABILITY AND FLEXIBILITY IN THE TRANSMISSION EXPANSION PLANNING PROBLEM: A MIXED-INTEGER LINEAR PROGRAMMING APPROACH

Ricardo Cunha Perez

March/2014

Advisor: Djalma Mosqueira Falcão

Department: Electrical Engineering

Adding FACTS and Distributed-FACTS to the system allows greater control of the active power flow and greater operational flexibility to accommodate different dispatch scenarios. In this dissertation, Mixed-Integer Linear Programming (MILP) formulations of the incorporation of these devices in the transmission expansion planning problem are proposed. This problem is formulated as an optimization model based on the linearized power flow and circuit limits where the objective is to minimize the investments in the transmission system. The first proposed formulation by this dissertation is an alternative hybrid linear model that avoids the nonlinearity present in the Kirchhoff's Voltage Law for candidate circuits adding at the same time power controllability to the system. The second proposed formulation models Candidate Series Compensation Devices (CSCDs) which are able to increase and/or decrease the line reactance and consequently control the power flow in the target transmission line. The CSCDs can be attached to an existing or candidate line and has a specific setpoint according to each dispatch scenario and operating conditions. Practical applications of the proposed formulations are demonstrated through several case studies.

TABLE OF CONTENTS

LIST OF FIGURES

LIST OF TABLES

1 INTRODUCTION

This introductory chapter begins with an exposition of the background and the motivation for the development of the research that lead to this dissertation. The objective and the technical contributions of this work are presented in section 1.2 and the chapter ends with a description of the organization of this document.

1.1 BACKGROUND AND MOTIVATION

There are several reasons to explain why transmission system loading is less than 100%. The first is related to redundancy in network design for reliability reasons. The second is owing to the need for a "capacity gap" to forearm against the uncertainties associated with the demand growth forecast. As a result of such uncertainties, transmission expansion plans tend to be "robust", i.e., with some overcapacity in relation to the plan which would be projected with perfect prediction of the future. A third reason is the need to establish alternative routes for the energy transport due to different patterns of energy production by the generators, in other words, different dispatch scenarios associated with the Renewable Energy Sources (RES). The most representative RES are: hydroelectricity, modern biomass, geothermal, biofuels, wind and solar power.

In hydrothermal systems as in the case of Brazil, the economic dispatches vary throughout the year due to the hydrology associated to the rivers located in different regions of the country. Therefore, the transmission expansion plan must be robust enough to meet the demand with completely different dispatch scenarios throughout the year.

Furthermore, the aforementioned issue concerning transmission expansion planning was not a big problem for the United States and most European countries. However, with the high penetration of intermittent renewables, such as wind and solar, the transmission expansion planning has become a task of extreme technical and economic importance, as it already is for Brazil.

Another important issue tied to the expansion planning task is the fact that the decision to add a candidate line into the expansion plan is binary, i.e., the line is added or not. In practice, it is not possible to construct a transmission line with any arbitrary

capacity. The reason is that the equipment that make up this line are generally produced in modules of different capacities. For example, to determine the nominal thermal rating (in MVA) of a transmission line with alternating current, the designer has at his disposal decision variables clearly discrete in nature, such as specifying the number of parallel circuits and the conductor arrangement to be used for each circuit.

The conjunction of the above mentioned facts leads to high investments in the transmission systems to meet different dispatch scenarios and low loading throughout the year.

Controllability and flexibility are important concepts for planning the operation and the expansion of the transmission system. In the operation context of the system, controllability refers to the ability to implement a direct or indirect control over relevant physical quantities to the network operation. For the purposes of this dissertation, these quantities are principally the line reactance and also the power flows in the circuits. Flexibility is the ability to accommodate different operating conditions (generation and load scenarios, network topology, etc.), using the existing resources in the network in order to maintain the adequacy of power supply and respect operating limits. Therefore, the controllability brings the flexibility.

Recent technological advances have revealed new devices that have as primary objective to increase the controllability and consequently the flexibility of the transmission system:

- FACTS (Flexible AC Transmission Systems): equipment based on power electronics or other static technologies, which aim to directly control physical quantities of the transmission system;

- Distributed-FACTS: allow direct control of the reactance and power flows in the transmission lines. Consist of modular equipment, coupled directly to the overhead transmission line cables. The distributed nature of the solution is the reason why the equipment is usually described as D-FACTS. The standardization associated to the modularity is one of the great advantages over the traditional FACTS devices, since traditional FACTS are manufactured for specific applications, resulting in higher costs and longer lead times. D-FACTS can fit a wide range of applications and are re-deployable. They have short lead times and do

not require line outages or substation modifications.

Introducing FACTS and D-FACTS in the system, the reactance of the transmission lines becomes variable, enabling thus a greater control of the active power flow in the circuits and a greater operational flexibility against different dispatch scenarios. The main purpose of this dissertation is to analyze these impacts in the transmission expansion planning and operation and also the associated financial impact.

1.2 OBJECTIVE AND CONTRIBUTIONS OF THIS DISSERTATION

Adding FACTS and Distributed-FACTS to the system allows greater control of the active power flow and greater operational flexibility to accommodate different dispatch scenarios.

This dissertation aims to show that a robust expansion plan compatible with all dispatch scenarios in the Business as Usual (BAU) case, i.e., traditional transmission equipment (lines and transformers), results in a lower average loading, needs more reinforcements in the system, and is more expensive. FACTS and D-FACTS are very important for transmission expansion planning by providing an operational flexibility to different dispatch scenarios and consequently increasing asset utilization and existing transmission capacity, capabilities that are vital in systems with high penetration of renewable energy sources. Therefore, the faculty of postponing transmission upgrades and saving transmission investments will be analyzed in this work.

In this dissertation, Mixed-Integer Linear Programming (MILP) formulations of the incorporation of these devices in the transmission expansion planning problem are proposed. This problem is formulated as an optimization model based on the linearized power flow and circuit limits where the objective is to minimize the investments in the transmission system.

The first proposed formulation by this dissertation is an alternative hybrid linear model that avoids the nonlinearity present in the Kirchhoff's Voltage Law (KVL) for candidate circuits adding at the same time power controllability to candidate circuits and consequently to the system. In the traditional formulation only the Kirchhoff's Current Law (KCL) and flow limit constraints for candidate circuits are enforced. Accordingly, the proposed formulation is an improvement of the traditional one because the KVL is

enforced but the susceptance presents an operating setpoint which can be between zero and the maximum susceptance value.

The second proposed formulation models Candidate Series Compensation Devices (CSCDs) which are able to increase and/or decrease the line reactance and consequently control the power flow in the target transmission line. This proposed formulation presents as contributions the following features:

- The CSCDs can be attached to an existing or candidate line;

- The maximum compensation level achieved by each CSCD is arbitrarily defined as input data;

- More than defining the susceptance (or reactance) variation range provided by the CSCD, the compensation type may also be set. The proposed formulation enables the application of three compensation types:

  o To facilitate reader's interpretation, a convention is now defined by this dissertation. **Positive compensation** is hereinafter defined as series compensation in order to increase (decrease) line susceptance (reactance) and consequently increase the power flow in the target transmission line;

  o **Negative compensation** is hereinafter defined as series compensation in order to decrease (increase) line susceptance (reactance) and consequently decrease the power flow in the target transmission line;

  o **Joint compensation** is hereinafter defined as series compensation which is able to increase or decrease the line susceptance (reactance) and consequently increase or decrease the power flow in the target transmission line.

- The proposed formulation has the capability of presenting a specific operating setpoint according to each dispatch scenario and operating conditions.

- Optimization solvers for Mixed Integer Programming (MIP) can be used to determine the optimal expansion plan, i.e., the problem can be solved

to global optimality with the use of widely employed and commercially available mixed-integer linear optimization solvers.

Finally, it is plausible to explain that the negative and the joint compensation types are enable by new Distributed-FACTS devices, which are deeply explained in the third chapter of this dissertation.

1.3 ORGANIZATION OF THE DISSERTATION

The remainder of this dissertation is organized as follows:

- Chapter 2 starts with an overview of the Brazilian Ten Year Plan for Energy Expansion 2022, i.e., a global overview about the generation and transmission system's expansion. Afterwards, the generation dispatch problem is presented. Its explanation begins with the geographical challenges imposed by the Brazilian territory and also with the hydro basins' localizations. Subsequently, the Renewable Energy Sources (RES) and the associated inflow uncertainties are presented. This chapter is then concluded with a brief explanation about how the dispatches are determined;

- Chapter 3 presents the power flow controllability and flexibility concepts, the devices that enable such control and finally their control capabilities;

- The transmission expansion planning problem is then presented in chapter 4. This chapter aims to show the challenges involved and also different ways for fulfilling the expansion planning task. Afterwards, this chapter gets more into detail the way in which the planning task will be performed in this dissertation. To achieve this goal, different transmission expansion planning methodologies will be defined and differentiated;

- Chapter 5 consists in the main contribution of this dissertation, because it contains the proposed Mixed-Integer Linear Programming (MILP) formulation of the incorporation of power flow controllability and flexibility in the transmission expansion planning model, i.e., the proposed formulation represents series compensation enabled by FACTS

and Distributed-FACTS devices in the DC Optimum Power Flow (OPF);

- The proposed formulation is applied to several case studies in chapter 6. The analysis of results of these case studies allows showcasing the applicability of the proposed formulation and discussing its features and characteristics;

- Conclusions and recommendations for future work are presented in chapter 7;

- Finally, the references are listed in chapter 8.

2 THE BRAZILIAN SYSTEM EXPANSION

2.1 INTRODUCTION

The Brazilian Ten Year Plan for Energy Expansion 2022 (PDE 2022 [1]) foresees investments of R$ 260.38 billion in the period 2013-2022 in new generation and transmission projects. The installed capacity expansion will be of R$ 199.96 billion, with emphasis on hydro and other renewables. Of this total, R$ 122 billion are based on planned power plants. In the transmission field, the investment forecast is of R$ 60.4 billion, of which R$ 37.8 billion in new lines and R$ 22.6 billion in substations. The Ministry of Mines and Energy has put on Thursday, October 24th, 2013, the document in public auction [1].

The PDE 2022 foresees the hiring of 63,361 MW of new capacity, with 26,605 MW that have to be hired in the next public auctions. Of this total 12,140 MW are from renewable sources such as wind, biomass and small hydro and 1,500 MW of thermal power starting on 2018, preferably natural gas. However, the fuel has to submit to enable the competitive procurement auctions.

Wind energy will be established from 2016 as the second largest renewable installed capacity in the country. The forecast is out of 3,898 MW in 2013 to 10,780 MW in 2016, increasing to 17,463 MW in 2022. Therefore, this energy source will be consolidated as the second most important, beating the thermal natural gas in 2019.

The PDE 2022 does not aggregate the solar source, but indicates this new source will become competitive in the next ten years with the reduction in prices of equipment. The document does not rule out the holding of auctions having this source to encourage the development of industry. Solar energy is listed in the A-3 and A-5, i.e., in the Brazilian public auctions to be held in the last two months of the year 2013.

In the Hydroelectric field, the PDE 2022 foresees the entry of hydro plants between 2018 and 2022 with 19,917 MW of total installed capacity. Five of these plants have a capacity exceeding 1 GW, with the greatest being São Luiz Tapajós, with 6,133 MW, in the Pará state, scheduled for 2019.

In the transmission field, an expansion of just over 104 thousand kilometers in 2012 to 155,736 km in 2022 is expected. The forecast of substation transformation capacity is out of 249,605 MVA to 352,833 MVA in the decade.

In conclusion, the Brazilian system features a large planned generation and transmission expansion especially in new areas with long distances that are currently being explored. These facts further emphasize the importance of this dissertation by allowing an assessment of transmission expansion plan, adding power flow controllability that will result in cost savings in the long-term transmission expansion planning task for a system with a large integration of Renewable Energy Sources (RES).

2.2   THE GENERATION DISPATCH PROBLEM

As explained in the introduction of this dissertation, there are several reasons to explain why transmission system loading is less than 100% and why the transmission expansion planning task is a complicated optimization problem. In summary, these reasons are: redundancy due to reliability reasons, uncertainties associated with the demand growth forecast, the binary nature of the decision to add a line or not and different dispatch scenarios associated with the renewable energy sources. The transmission expansion plan must be robust to meet all these requirements.

As can be seen, apart from complicated handling requirements, the transmission expansion planning also depends on the generation patterns associated with renewable energy sources which in turn depend on river flow, wind and irradiation, i.e., input data of a purely stochastic nature. This chapter aims to present the main concepts and characteristics of the generation dispatch problem. This problem has a high importance to this work, since the aim of this dissertation is to analyze methodologies to obtain flexible and therefore robust expansion plans to suit different dispatch scenarios with minimum cost.

The Brazilian system is hydrothermal. The figure presented below shows the localization of the hydro basins in Brazil.
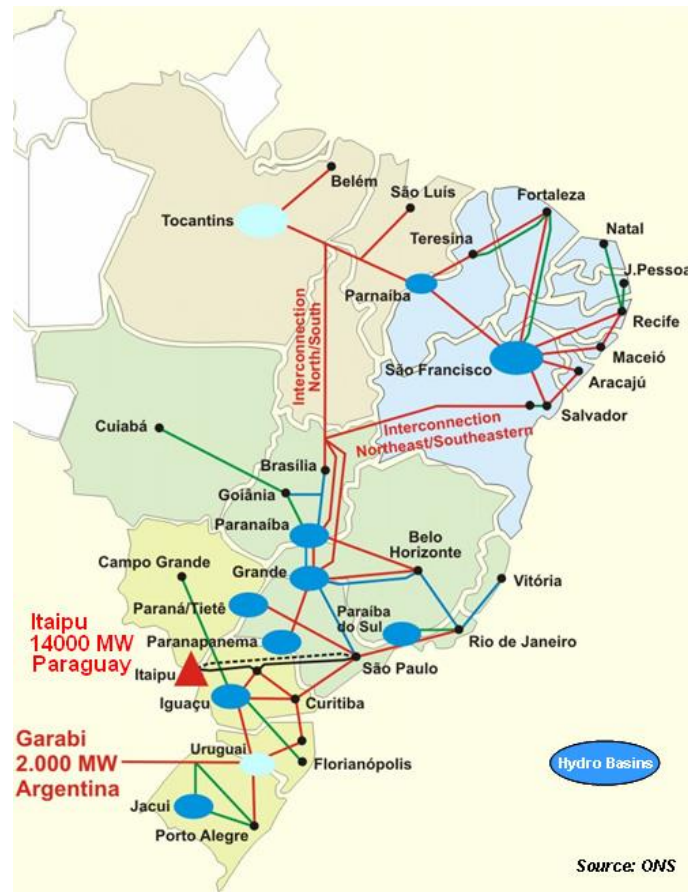
Figure 1: Hydro Basins in Brazil – adapted from ONS (www.ons.org.br)

As can be seen, the hydro basins are scattered throughout the territory with large distances between them. So, the economic dispatches vary throughout the year due to the hydrology associated to the rivers located in different regions of the country and the transmission system needs to meet not only the different dispatch scenarios but also the distance challenges.

Another interesting point about the Brazilian system is to analyze the contribution of the total hydroelectric generation for the supply and demand physical balance. This physical balance is presented below:

	2013	2014	2015	2016	2017	2018	2019	2020	2021	2022	2023	2024	2025	2026	2027	2028	2029	2030
Thermal	16.9	19.1	20.5	21.0	22.4	23.7	25.5	27.2	28.0	28.4	29.7	31.7	33.3	34.2	35.1	35.8	38.1	40.9
Hydro	48.6	51.1	52.9	53.9	56.4	59.0	59.8	60.7	63.0	65.5	67.3	68.7	70.1	72.7	75.0	77.4	78.9	79.5
Demand	63.8	66.7	69.3	71.8	74.2	76.6	79.3	82.0	84.9	87.8	90.7	93.8	97.1	100.3	103.6	106.5	110.2	113.5
% Hydro	74%	73%	72%	72%	72%	71%	70%	69%	69%	70%	69%	68%	68%	68%	68%	68%	67%	66%
% Thermal	26%	27%	28%	28%	28%	29%	30%	31%	31%	30%	31%	32%	32%	32%	32%	32%	33%	34%

Wind and Solar projects are considered as thermal power plants

Figure 2: Supply and demand physical balance

As indicated above, it is worth noting that just to show the hydro contribution to the physical balance, in this graphic, wind and solar projects are considered as thermal plants. Moreover, it is important to explain what the numbers in the chart represent. In order to ensure supply reliability, every energy contract in Brazil must be backed up by a physical plant capable of producing the contracted energy in a sustainable way. In order to be able to check this rule, the Ministry of Energy assigns to each power plant in Brazil a firm energy certificate (FEC) measured in [MWh/year] corresponding to its sustainable production capacity. The FEC is the maximum amount of energy that a generator can sell in energy contracts (which are the transactions in the Brazilian power market) [2]. So, the numbers shown in the chart represent the FEC for hydro and thermal plants.

As can be seen, there is a long-term reduction on the hydro contribution mainly because of two reasons: the majority of the high-potential projects have already been built and new hydro projects with reservoirs are impractical due to environmental barriers. Today in Brazil, the vast majority of new hydroelectric projects are run-of-river.

In order to show the problem of the high dispatch variability due to hydrology, further intensified by run-of-river new hydro plants, the historical inflow data from the FURNAS Power Plant is shown in the figure presented below:
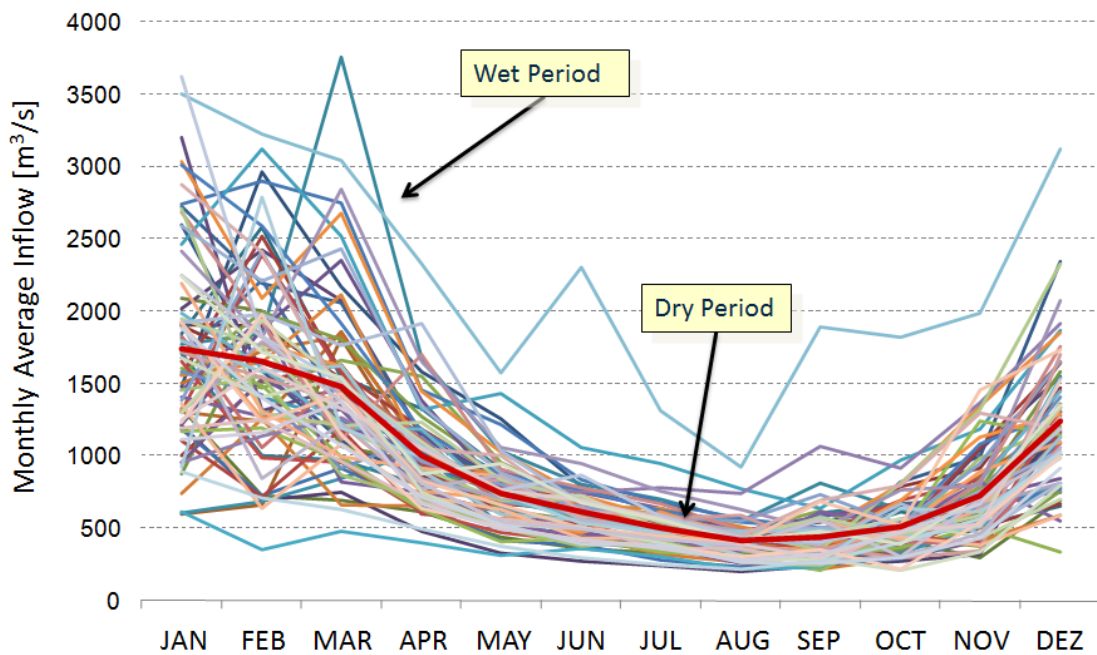
Figure 3: Historical Inflow Data – FURNAS Power Plant

Each line represents a historical inflow data realization and the red line represents the average. As can be seen the inflow data is very volatile, especially in the wet season.

Taking that information into account, the main consequence of not so many new hydro plants and the majority being run-of-river, is the loss of the regularization ability which is represented below:
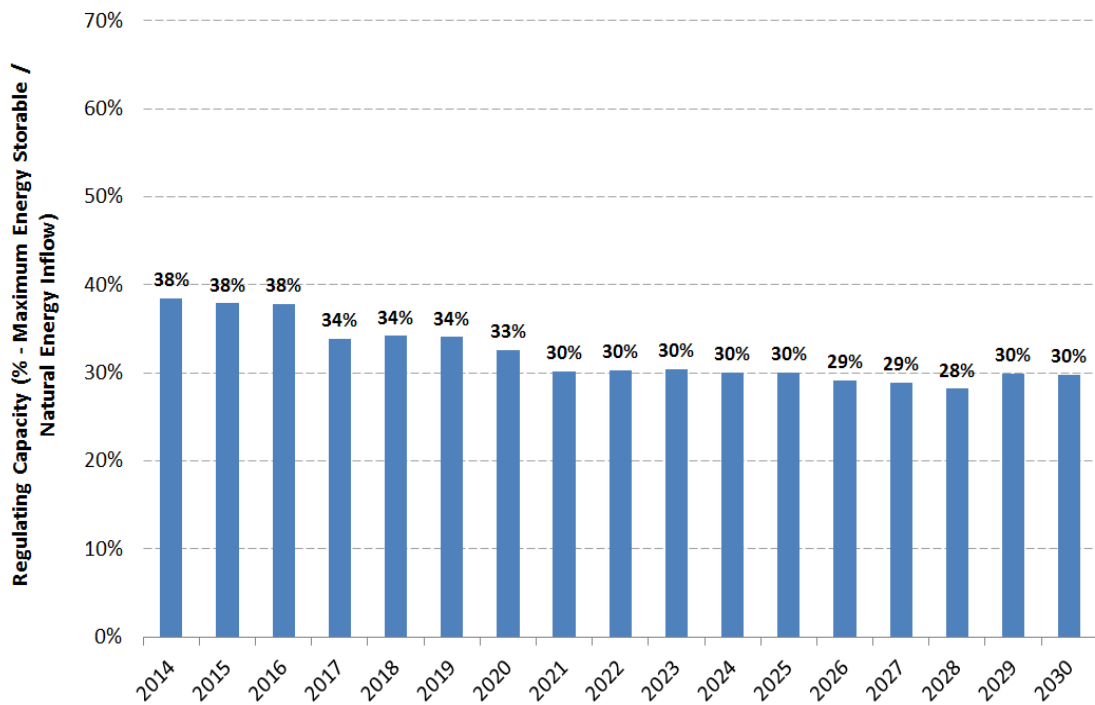
Figure 4: Evolution of the regularization capacity

This figure shows the regulating capacity, i.e., the ratio between the Maximum Energy Storable and the average of the Natural Energy Inflow (ESmax/ENA) which measures the percentage of natural energy inflow that could be stored and transferred for the following years.

With the regularization ability decreasing, it is more difficult to fulfill the role of energy reserve when requested. Accordingly, as the hydro inflow data is volatile, an expansion based on run-of-river hydro plants increases the importance of a robust and flexible transmission system.

In addition to that hydro contribution reduction and loss of regularization capacity, there is a fast expansion of installed wind capacity (worldwide and also in Brazil):

- World: from 283 GW in 2012 to 475 GW in 2016 (13.5% p.a.).

- Brazil: from 1.9 GW in 2012 to 10 GW in 2016 (48% p.a.).

Between this and that, we need to adapt the Brazilian's system expansion planning process to the wind power peculiarities.

For this purpose, first is shown below the wind speed variation curve during a month based on hourly data from the Triunfo Measuring Station in the state of Pernambuco (PE) [3]:
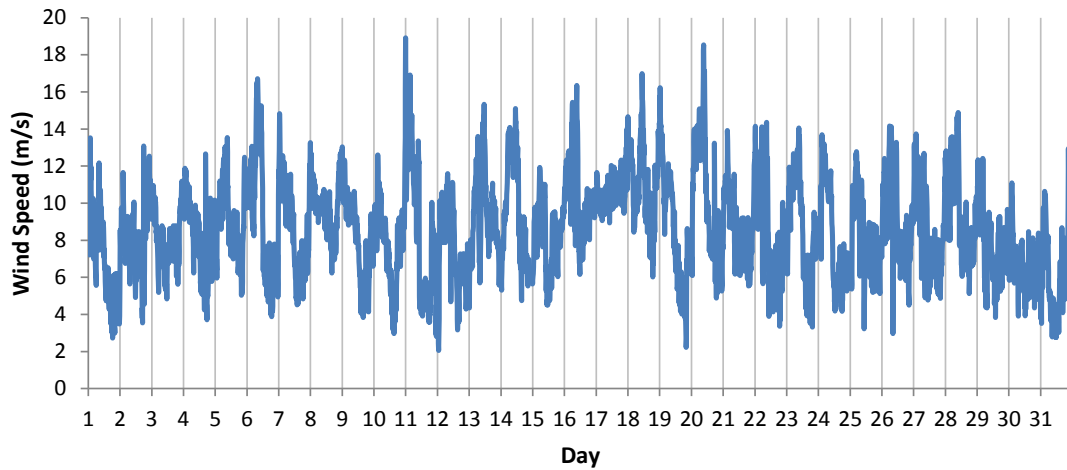
Figure 5: Wind speed variation during a month

As can be seen the wind inflow data is also volatile. Moreover, in addition to the monthly variability, it is also interesting to study the annual variability, i.e., the annual seasonality. To do this, although of course it would be preferable to work with data geographically sprayed as much as possible, the low availability of data requires a simplified representation based on representative samples of four "Wind Basins", regions that concentrate most of the technical and economic wind potential in Brazil (Bahia - BA, Ceará - CE, Rio Grande do Norte - RN and Rio Grande do Sul - RS). It is plausible to consider that the main effects of temporal and spatial variability are captured by this "basin" representation.

The figure presented below shows the seasonal generation profile according to each "wind basin". Besides these curves, the monthly sum of the Natural Energy Inflow (ENA) of all Brazilian hydros is also presented in order to compare the seasonal differences between wind and hydro [4], [5], [6]:
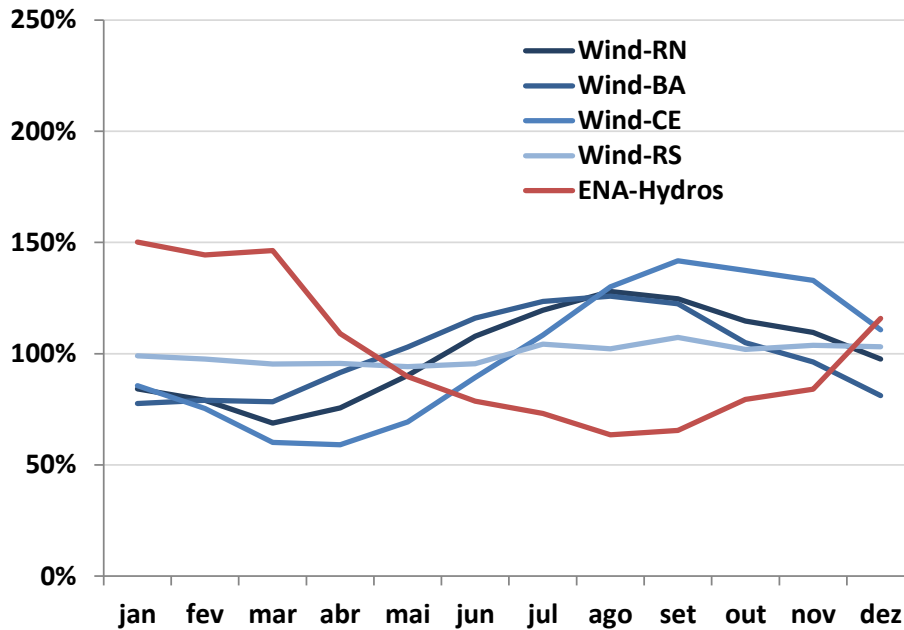
Figure 6: Seasonal generation profile according to each "wind basin"

The data analysis data revealed the following peculiarities: in terms of seasonal variability, it is observed that the RS basin presents an almost constant profile throughout the year, while the other three basins have reverse seasonality in comparison to the hydro's ENA. The CE basin presents the largest seasonal variability.

In addition to that, the correlation coefficient of the annual production time series of the four wind basins were also calculated and the results are presented in Table 1. These coefficients provide an estimate of the spatial correlation of wind generation. As can be seen, the wind production in the RS state is hardly correlated with each other because of the geographical distance, while the CE and RN basins have a very high correlation.

Table 1: Spatial correlation matrix of wind generation according to each "wind basin"

	RN	BA	CE	RS
RN	1.00	0.48	0.96	0.10
BA		1.00	0.37	0.14
CE			1.00	0.00
RS				1.00

14

As can be seen through the facts stated above, an advantage of a hydrothermal system with high wind park penetration is the reverse seasonality in comparison to the hydro's ENA. Another advantage is that hydroelectric plants have a fast power response, i.e., they can absorb with relative ease momentary fluctuations in wind generation.

On the other hand, it is also worth to emphasize the exacerbated uncertainties in hydro and wind generation. The figure presented below shows the hydro's ENA series in conjunction with the wind series from the CE basin, which presents the largest seasonal variability. These uncertainties make up the main reason why the transmission expansion planning is such a challenging task.
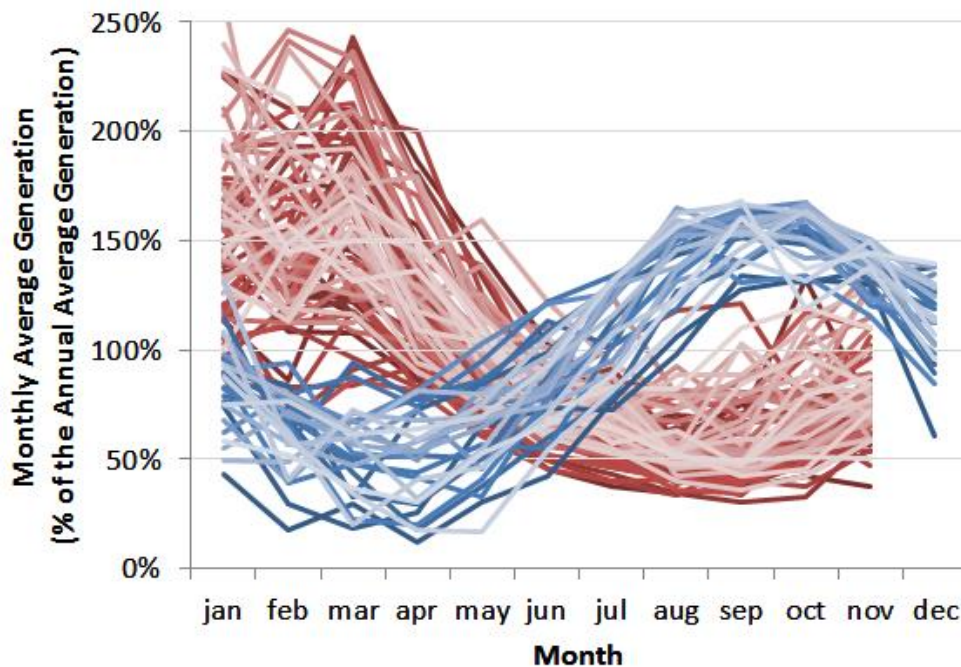
Figure 7: Exacerbated uncertainties in hydro and wind generation

2.3   DISPATCH SCENARIO DETERMINATION

As can be seen above, the dispatch scenario determination when many different RES are in the same system is a challenging task. Accordingly, the next question is how to determine the dispatch scenarios with so many aforementioned uncertainties.

The objective of hydrothermal scheduling is to determine an operation strategy of a hydrothermal system (as is the case of Brazil) that for each stage of the planning period produces generation targets for each plant. This strategy should minimize the expected value of the operation cost along the period, composed of fuel cost and

15

penalties for unserved load, while operating within area interchange limits. Different from thermal plants, hydro units do not have fuel costs, i.e., direct operating costs. As the energy can be stored in the reservoir, hydro plants may displace fuel cost today or in the future. This opportunity cost is called "water value". In Brazil, hydro plants are centrally dispatched by an Independent System Operator (ISO) based on their marginal water values, which are computed by a multi-stage stochastic optimization methodology, Stochastic Dual Dynamic Programming (SDDP) [7]. The SDDP algorithm has been applied to the scheduling of large-scale power systems in more than sixty countries, including detailing modelling of system components and transmission networks [8].

2.4 CONCLUSIONS

In hydrothermal systems as in the case of Brazil, the economic dispatches vary throughout the year due to the hydrology associated to the rivers located in different regions of the country.

In addition to that, there is a fast expansion of installed wind capacity. Both RES present a volatile inflow data and consequently exacerbated uncertainties. Therefore, the transmission expansion plan must be robust enough to meet the demand with completely different dispatch scenarios throughout the year meeting also the distance challenges associated to the size of the Brazilian territory.

The conjunction of the above mentioned facts leads to high investments in the transmission systems to meet different dispatch scenarios. These facts further emphasize the importance of operational flexibility in order to result in cost savings in the long-term transmission expansion planning task.

The next chapter will introduce the power flow controllability and flexibility concepts and also the devices that enable these features.

3 POWER FLOW CONTROLLABILITY AND FLEXIBILITY

According to the previous chapter of this dissertation, alternative routes for the energy transport due to different patterns of energy production by the generators need to be established while planning a network. It is a direct conclusion that system controllability and flexibility are features more than needed.

In the conventional free flow operation mode of a.c. transmission networks, the power flow on individual transmission circuits is determined by the characteristics of the transmission network itself. Moreover, for stable operation sufficient transmission margin must be available at all times to accommodate the almost instantaneous redistribution of power flow that results from a change in the operation setpoint or a power system disturbance.

The power flow in a transmission network is limited by a combination of the following factors [11], [12]:

• Steady-state and transient stability limits;

• Parallel flows (in meshed networks);

• Voltage limits;

• Thermal limits.

Accordingly, the power transfer capacity of the transmission system is limited due to several factors and therefore it is a great concern for the transmission expansion planning task, especially in systems with many different dispatch scenarios where a robust expansion plan is demanded.

Taking these statements into account, this chapter aims to present the concepts and features that the devices known as Flexible AC Transmission Systems (FACTS) and Distributed Flexible AC Transmission Systems (D-FACTS) contemplate. These devices are capable of interfering in the network and helping the power flow control, providing consequently the desired flexibility and controllability.

First, FACTS can be defined as AC transmission systems based on power electronics and other static controllers which aim to improve power flow control and increase the power transfer capability.

These devices hold the ability to [9], [11]:

- Improve voltage stability;

- Mitigate short circuit currents;

- Mitigate sub-synchronous resonance;

- Improve transient stability limit of the transmission line;

- Enhance the damping of the system;

- Improve the performance of converter stations at HVDC Systems' terminals;

- Improve the transient performance of the transmission system in regions with high penetration of intermittent renewable energy sources such as solar and wind power, due to their fast response;

- Increase active power flow control in transmission lines, enabling the operating flexibility desired in (i) hydrothermal systems with different dispatch scenarios throughout the year and (ii) systems with increasing RES since their variability is in an intra-daily and/or intra-hourly timescale;

- Reduce investments in transmission expansion due to the aforementioned operating flexibility.

Facing the points stated above, it is a direct conclusion that these devices are of vital importance to the improvement of systemic performance in both transient and steady-state operating conditions.

As the main objective of this dissertation is the transmission expansion planning task, focus will be given on the steady-state operating conditions. In steady-state operation, the three parameters that control the transmission line power flow are: impedance, voltage magnitude and phase angle at both buses (sending and receiving).

Conventional controllers can handle these parameters and maintain the system operation, but only for slow changes in loading conditions at steady state and other

limited applications, being in general not quickly enough to handle dynamic system conditions and being also unable to achieve representative changes in these parameters. It is shown below that the use of FACTS technology can change this situation. Conventional control is currently achieved through the use of mechanical devices, which necessarily impose a limit on the speed at which the action can be made. FACTS devices are based on solid-state control. They are able to control actions at much higher speed and consequently achieving also greater effects.

The facts stated above enhance even more the importance of operational flexibility and controllability of the transmission system provided by the FACTS and D-FACTS devices.

Therefore, this chapter is structured as follows: first a brief introduction of a transmission line power flow will be presented in order to better understand how the power flow control can be achieved. Afterwards, the FACTS and D-FACTS devices and their different functionalities will be presented. The chapter ends with presentation of the summary and the conclusions.

3.1 THE POWER FLOW

The power flow distribution in the AC transmission network is determined by the characteristics and physical parameters of the transmission circuits. Rather than operating the network in this conventional way, FACTS devices are able to control the power flow in a predetermined manner, increasing the operation flexibility, the utilization of the existing transmission lines and consequently the transmission capacity.

Their network interventions are much faster than the main usual control actions made by mechanical devices. They are capable of controlling the power flow by changing voltage magnitude, voltage angle or the line impedance.

Figure 8 illustrates the real and reactive power transferred via a transmission line.
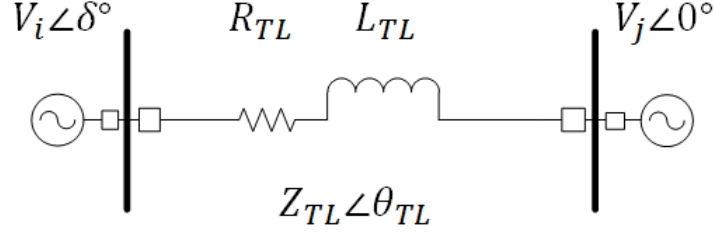
Figure 8: Power flow between two buses

The power flow through the line is determined by the following relationships:

$$P_{ij} = \frac{V_i V_j}{|Z_{TL}|} \cos(\theta_{TL} - \delta) - \frac{V_j^2}{|Z_{TL}|} \cos(\theta_{TL}) \tag{1}$$

$$Q_{ij} = \frac{V_i V_j}{|Z_{TL}|} \sin(\theta_{TL} - \delta) - \frac{V_j^2}{|Z_{TL}|} \sin(\theta_{TL}) \tag{2}$$

where:

P_{ij}	Real power flow between buses i and j;
Q_{ij}	Reactive power flow between buses i and j;
V_i, V_j	Voltage magnitudes at the two buses;
δ	Phase difference between the voltages at the two buses;
Z_{TL}	Transmission line impedance;
θ_{TL}	Angle of the transmission line impedance.

In high voltage transmission networks, the line reactance (X_{TL}) is much greater than the resistance (R_{TL}). Due to this typical high reactance-to-resistance (X_{TL}/R_{TL}) ratio, the aforementioned equations can be further simplified by neglecting the resistance (R_{TL}):

$$P_{ij} = \frac{V_i V_j}{X_{TL}} \sin(\delta) \tag{3}$$

$$Q_{ij} = \frac{V_i V_j}{X_{TL}} \cos(\delta) - \frac{V_j^2}{X_{TL}} \tag{4}$$

From the equations shown above, it is intuitive to see that the power flow control depends intrinsically of which part of the apparent power the system operator seeks to control. It is a common sense that the real power flow depends structurally on the phase angle difference, in other words, P_{ij} flows from the point i to j because the magnitude of voltage phase angle at i is greater than at j ($\delta_i > \delta_j$). The reactive power flows from i

to j when the voltage magnitude at the sending end is higher than the receiving end magnitude, i.e. $|V_i| > |V_j|$.

3.2 FACTS & D-FACTS EQUIPMENT CONTROL CAPABILITIES: DEFINITION AND DIFFERENTIATION

Having these initial and structural concepts in mind, this section aims to present the areas of compensation, the devices, their capabilities and specialties. The Table presented below summarizes the different areas of control capabilities [15].

Table 2: Different Areas of Control Capabilities

Control Capability	FACTS & D-FACTS Equipment
Shunt	SVC, STATCOM
Series	SSSC, TSSC, TCSC, Phase Shifter, DSR, DSC
Series & Shunt	UPFC

Where:

SVC	Static VAR Compensator;
$STATCOM$	Static Synchronous Compensator;
$SSSC$	Static Synchronous Series Compensator;
$TSSC$	Thyristor-switched Series Capacitor;
$TCSC$	Thyristor Controlled Series Capacitor;
DSR	Distributed Series Reactor;
DSC	Distributed Series Compensator;
$UPFC$	Unified Power Flow Controller.

All devices of interest of this dissertation will be timely explained in the document. It is also worth mentioning that the only D-FACTS devices presented in the Table 2 are: DSR and DSC.

The reader can notice that there is a "hybrid series-shunt equipment" called universal power flow controller (UPFC), which will be further explained later in this

document and can be used for accomplishing both functions with high flexibility but also higher associated costs.

In order to better understand the real effect of the different control capabilities shown in Table 2, Figure 9 presents the active power transfer capabilities according to compensation types as function of the power angle δ, having the voltage magnitude at the sending end equal to the receiving end magnitude, i.e. $|V_i| = |V_j|$ [10], [14].
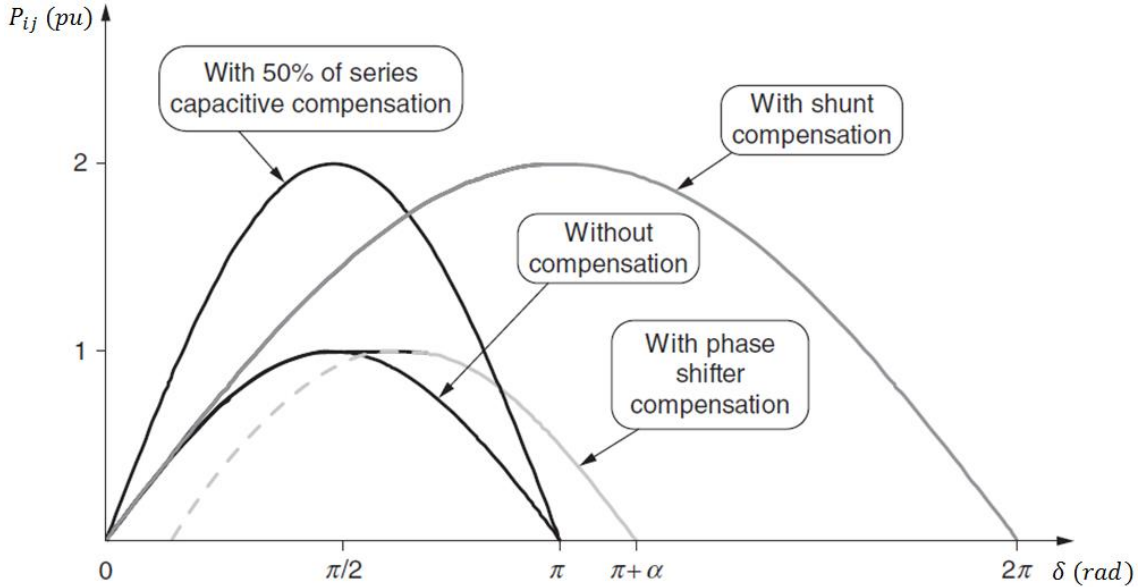
Figure 9: Power transfer capabilities according to compensation types – adapted from [13]

The normal operating region is where the power angle δ is below 90 degrees and the usual values stay around 30 degrees. It can be seen that the shunt compensator does not increase system's power transfer capability in a significant way in the normal operating region. The great importance of the shunt compensator is the voltage setpoint control and it is also the best option to increase the system stability margin [9], [14]. These are the main reasons shunt devices have been applied for worldwide VAR compensation and voltage support.

The literature shows that the phase shifter compensator is important to connect two systems with excessive or uncontrollable phase difference and also to simply control the power flow in a specific region, but it does not significantly increase the power transfer capability of the system [23], [24].

By analyzing Figure 9 and taking the aforementioned comments into account, it can be seen that in most practical applications and cases, series compensation is the best choice for increasing power transfer capability. A 50% series compensation presents a

significant increase in the line power transfer capability and therefore for controlling the active power flow on a line, series devices are much more effective.

As a consequence of the assumptions and facts described above, this dissertation will give focus to the FACTS and D-FACTS devices that are capable of realizing series compensation.

3.3 THE IDEAL SERIES COMPENSATION

A series compensator is basically used to increase or decrease the effective line reactance (X_{TL}), allowing consequently the desired real power flow control. The impedance change can be achieved by (i) a series injection of a passive reactance in the transmission line (capacitive or inductive) or by (ii) an active controlled voltage source V_C. Approach (i) is intuitive and presents a straight understanding by observing the direct impact that the reactance change has in the transmission line power flow in equation (3).

In the second approach, the ideal series compensator is modeled by a voltage source V_C connected in the middle of a lossless line as presented in the Figure 10 below:
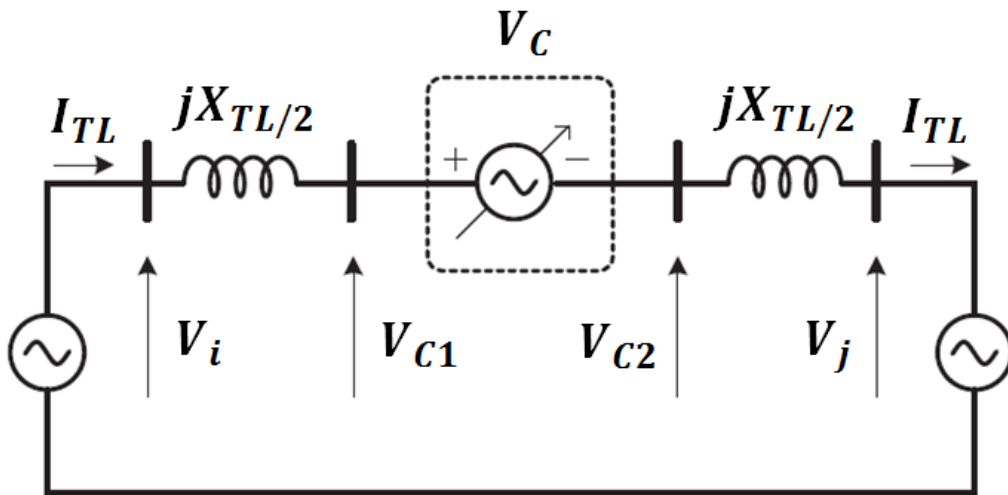
Figure 10: Controlled voltage source connected in the middle of a lossless line

The current flowing through the line (I_{LT}) is given by the following expression:

$$I_{LT} = \frac{(V_{ij} - V_c)}{jX_{TL}} \qquad (5)$$

If the voltage V_C is orthogonal to the line current I_{LT}, the series compensator will not provide or absorb active power, i.e. the power supply terminals V_C

23

will only be reactive. In this case, the voltage source V_C can be seen, from its terminals, as a capacitive or inductive equivalent reactance:

$$X_{eq} = X_{LT}(1 - s) \tag{6}$$

where $-1 < s < 1$ is the series compensation rate in per unit (p.u.). In other words, the final effect consists also in a line impedance change.

The compensation voltage is consequently given by:

$$V_C = I_{LT} * X_{eq} \tag{7}$$

And the transmitted active power is calculated as follows:

$$P_{ij} = \frac{V^2}{X_{LT}(1-s)} \sin(\delta) \tag{8}$$

Where V is the magnitude of the terminal voltages V_i and V_j. This equation shows that the transmitted active power can be increased considerably by varying the rate of the series compensation in the range $0 < s < 1$ and can be decreased by varying in the range $-1 < s < 0$. Figure 11 presented below represents the P-δ curve based on equation (8) and contains both variations (capacitive and inductive) of the line in impedance in terms the compensation level s.
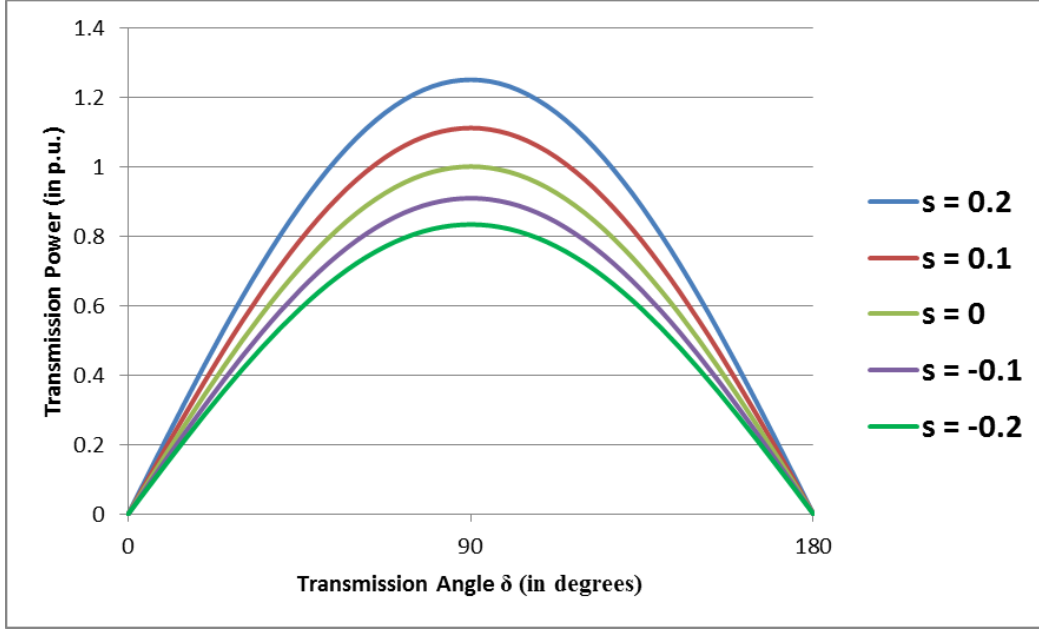
Figure 11: Series compensation effects on the P-δ curve

As can be seen in the figure presented above, if s is greater than zero (capacitive compensation), the power flow is increased and vice versa. Figure 11 represents exactly the effect of a passive impedance injection.

Moreover, as explained above, if the series compensation is indirectly achieved by a quadrature voltage injection through a voltage V_C that is orthogonal to the line current I_{LT}, the end effect is also a impedance injection, but there are some slight changes in the P-δ curves that are worth to be presented. In this case, the power flow equation depends on the injected quadrature voltage as follows [15]:

$$P_{ij} = \frac{V_i V_j}{X_{LT}} \sin(\delta) - \frac{V_i V_C}{X_{LT}} \cos(\delta/2) \left[\frac{\sin(\delta/2)}{\sqrt{\left(\frac{V_i + V_j}{2V_j}\right)^2 - \frac{V_i}{V_j} \cos^2(\delta/2)}} \right] \tag{9}$$

Assuming $V_i = V_j = V$, this equation can be simplified as follows:

$$P_{ij} = \frac{V^2}{X_{LT}} \sin(\delta) - \frac{V V_C}{X_{LT}} \cos(\delta/2) \tag{10}$$

To better illustrate the results of this type of series compensation, are presented below the phasor diagram for a capacitive reactance in Figure 12 and the P-δ curve in Figure 13 based on equation (10).
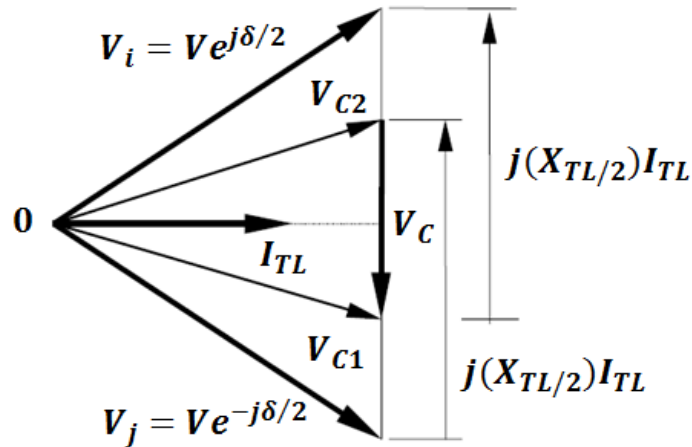
Figure 12: Phasor diagram of the series capacitive compensator
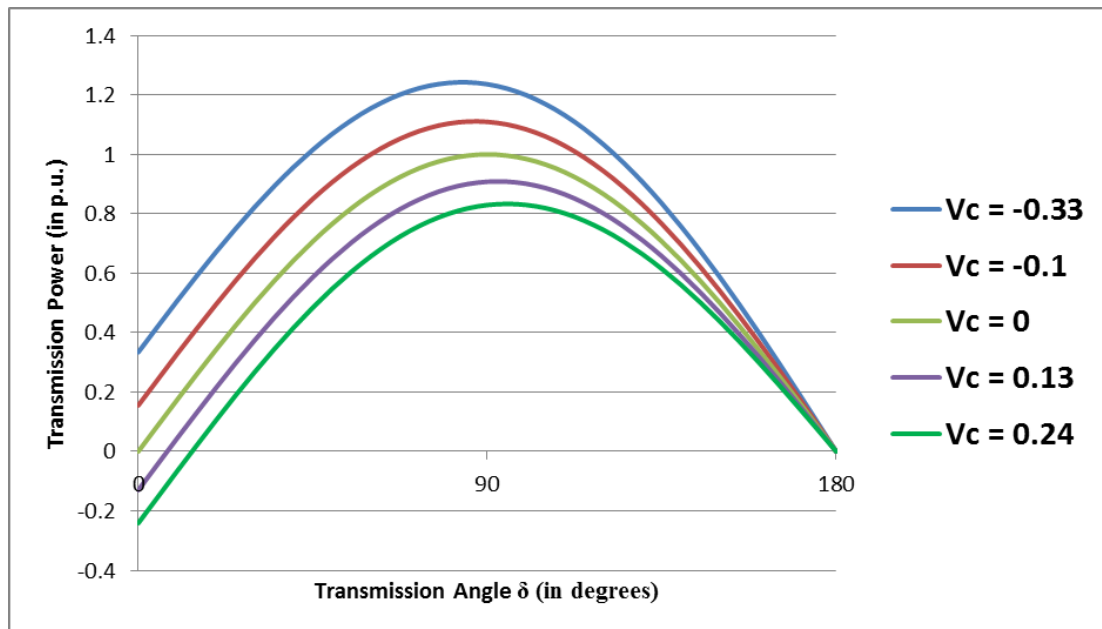
Figure 13: Quadrature voltage injection effects on the P-δ curve

As can be seen, a voltage lagging the line current by $90°$ would translate into a series capacitor while a voltage leading the line current would imply a series inductor. The shape of the figures 11 and 13 are slight different, but it is interest to emphasize that the end effect of this second approach is the same of the first one in the normal operating region $(0 < \delta < 90°)$, being only necessary to set the voltage value V_C to obtain the desired compensation level s. In Figure 13, the voltage V_C is set in order to achieve the same compensation as obtained in Figure 11.

3.4 FACTS DEVICES

As explained above, a series compensator is typically used to change (control) the power flow in a transmission line, i.e., increase and/or decrease the flow through an impedance injection that can be either (i) a passive impedance injection – defined hereafter as **Type 1** – or (ii) a quadrature voltage injection to indirectly achieve impedance injection – defined from now on as **Type 2**. In this section, the series compensator devices will be presented and categorized according to their types.

3.4.1 Thyristor-switched Series Capacitor (TSSC)

The power flow through long lines is mainly limited by reactive series impedance of the line. The fixed series capacitive compensation was introduced decades ago to cancel a portion of the reactive impedance of the line and therefore increase the capacity of power transmission.

The Thyristor-switched Series Capacitor (TSSC) introduces capacitor banks that are connected in series with the transmission line being the device consequently categorized as **Type 1**. Figure 14 shows the basic configuration of the device.
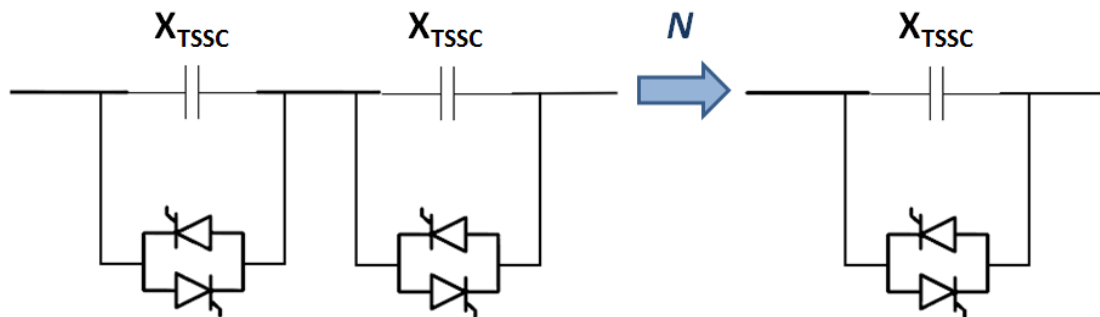
Figure 14: TSSC device configuration

The device has N capacitor banks (X_{TSSC}), each shunted by a thryistor switch. When these switches are closed, the capacitors are by-passed and when they are opened, the line reactance can be compensated stepwise from zero to maximum number of capacitors of the device ($N * X_{TSSC}$) [23].

This compensation system has the advantage of being really simple, but on the other hand, it doesn't allow continuous control. Beyond the stepwise compensation, depending on the switching frequency, harmonics and subharmonics may appear. The

capacitors design and also the whole project configuration must take these downsides into consideration.

For further technical information, the reader can consult [13], [14] and [23].

3.4.2 Thyristor Controlled Series Capacitor (TCSC)

Later, with further research on FACTS technology, it has been shown that the variable series compensation is quite effective in controlling power flow through the line and improving also the system stability. The controlled series compensation of transmission lines may be applied to obtain maximum utilization of the available transmission system by controlling the power flow through the lines. With the use of faster controllers, the controlled series compensation also allows minimizing the negative effects of disturbances in the system. The device is connected in series with a transmission line and has at least fifteen years of study and applications in the electrical system [16], [18].

Based on the aforementioned facts, the Thyristor Controlled Series Capacitor (TCSC) is the evolution of the TSSC device and also categorized as **Type 1**. The upgrade is based on the introduction of a small reactor in the path of the thyristor switch as shown in the figure presented below:
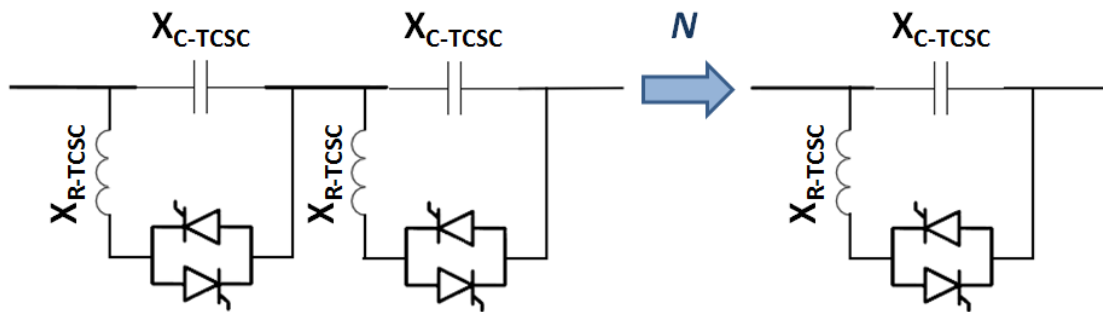
Figure 15: TCSC device configuration

The application of the small reactor X_{R-TCSC} results in an increased compensation capability, because by varying the conduction angle of the thyristors, the voltage on the capacitor can be increased beyond 1 p.u., reflecting consequently in an increased total capacitance [23]. This configuration has the advantage that the equivalent value of the series reactor can be continuously controlled by adjusting the firing angle of the thyristors, resulting consequently in an also continuously controllable

series capacitor. These capabilities justified and enabled practical applications of this device for power flow control and power oscillation damping that are worldwide under operation.

In order to understand better the TCSC effect on the system, the figure presented below illustrates the TCSC equivalent impedance [9], [10]:
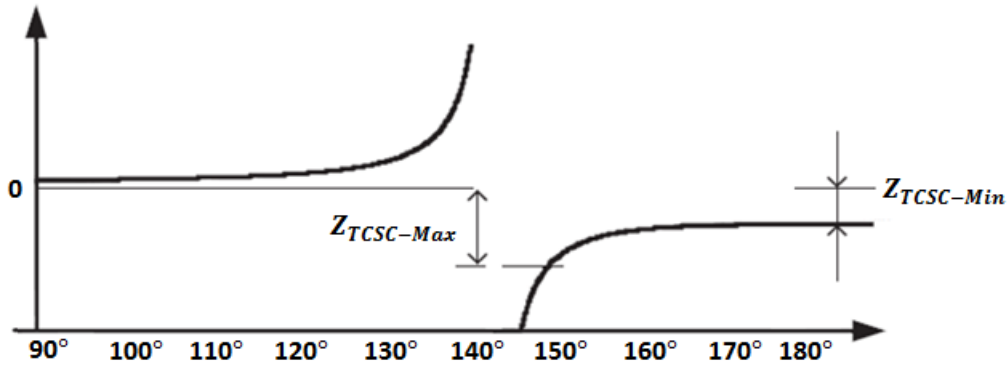
Figure 16: Effective TCSC circuit impedance

The figure shows the equivalent impedance of the TCSC (Z_{TCSC}) as a function of the firing-angle α. It can be seen that this device has both capacitive and inductive characteristic regions separated by a resonant region which is localized for α around 145°. In other words, the capacitive region is for $145° \leq \alpha \leq 180°$ and the inductive region is for $90° \leq \alpha \leq 145°$. In normal operation, the TCSC is controlled in the capacitive compensation region where its impedance injection varies from the minimum value $Z_{TCSC-Min}$ to the maximum value $Z_{TCSC-Max}$. The $Z_{TCSC-Max}$ is the maximum value because it is not safe for the system to operate in the resonance region.

As can also be seen in the figure, this device can also reach the inductive region (α is usually around 90° for these applications) to decrease power transfer capability through the transmission line, but this is not the main objective of the device.

The TCSC has a great operational flexibility as demonstrated above. On the other hand, there are several issues associated with the use of a series capacitor on a transmission line. Substantial changes are needed in the substation in order to incorporate a TCSC device, involving huge additional infrastructure requirements such as isolation platforms and complex protection schemes.

The TCSC is the most common series compensation FACTS device in practical applications [17]. More technical details about the TCSC devices and their practical applications can be found in the references [11], [14], [19], [20] and [21].

3.4.3 Static Synchronous Series Compensator (SSSC)

As previously explained in this document, a quadrature voltage injection can indirectly achieve impedance injection. A synchronous voltage-source inverter with a series transformer can achieve this goal [22]. The Static Synchronous Series Compensator (SSSC) is a voltage-source and has the ability to provide a constant reactive compensating voltage being consequently categorized as **Type 2**. The Figure presented below illustrates the circuit schematic from the referred device.
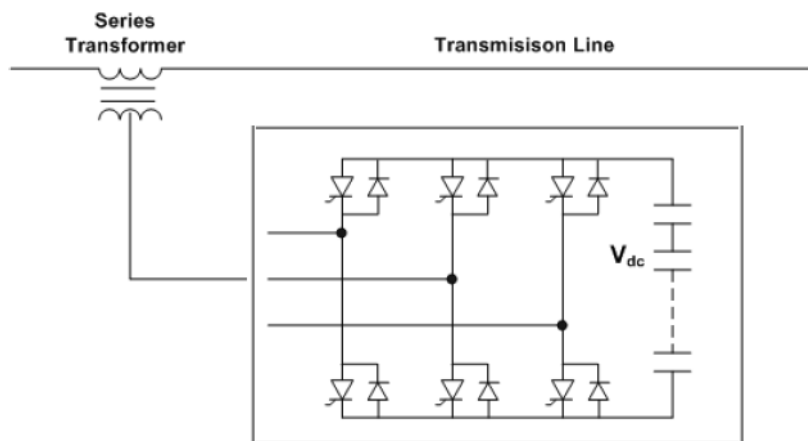
Figure 17: SSSC circuit schematic

This device controls the quadrature voltage injected independent of system conditions and therefore, by injecting a voltage at any angle to the line current, it has the ability of controlling independently the real and reactive power. The aforementioned Equation (10) shows the resultant power flow through a transmission line when the SSSC is compensating with a voltage V_C lagging the line current by 90°.

The figure presented below shows the comparison between the SSSC compensation with a voltage $V_C = -1.414$ and the TCSC compensation with $s = 0.5$. The voltage V_C is chosen in order to achieve the same power at $\delta = 90°$ that the TCSC would also provide [15], [22].
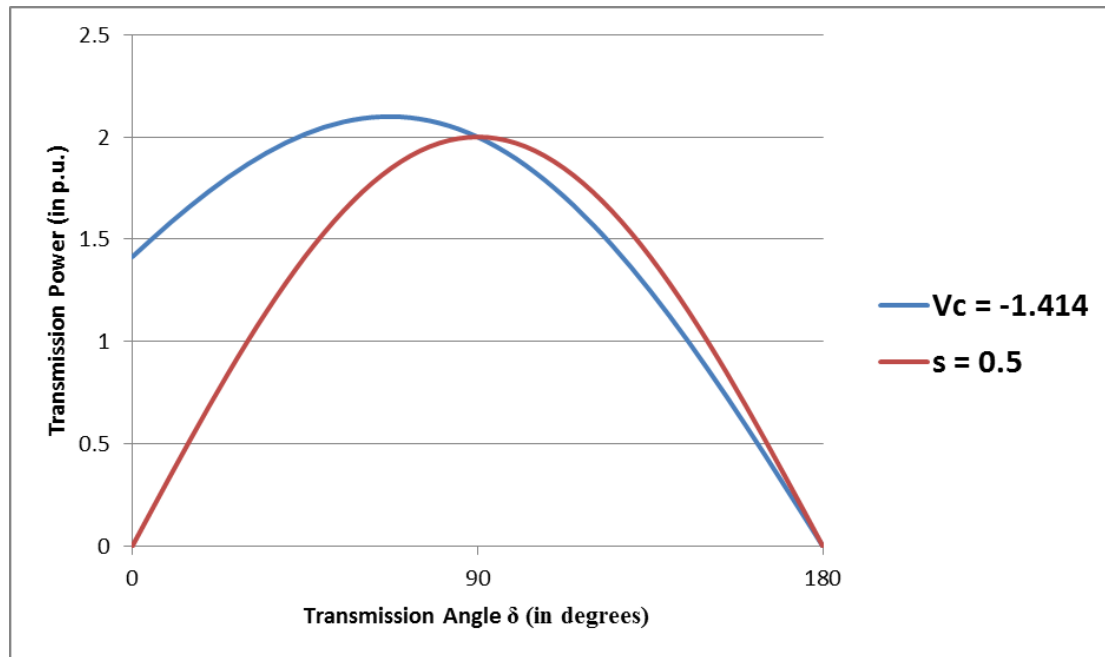
Figure 18: Comparison between the SSSC and the TCSC compensations

By analyzing figure presented above, it can be seen that choosing V_C in order to achieve the same power at $\delta = 90°$ that the TCSC would also provide, the SSSC has a greater impact on increasing the line power flow in the feasible operation angle range $0 \leq \delta \leq 90°$ [15], [23]. Moreover, another interesting advantage of this device is the ability to reduce line losses. By injecting a voltage out of phase with the transmission line current, these losses are supplied by the SSSC.

On the other hand, SSSC presents the high costs as the most important practical deployment limiters. The exchange of real power with the system demands the use of DC energy storage, as represented by the capacitors applied to the V_{dc} voltage in the SSSC circuit schematic figure. Finally, besides the DC energy storage, coupling transformers and inverters also present significant costs.

For further information about the SSSC device, the reader may consult [9], [11] and [22].

3.4.4 Phase Shifter

First of all, it is worth to present Figure 19 which consists in the representation of the ideal phase angle compensator [13]:
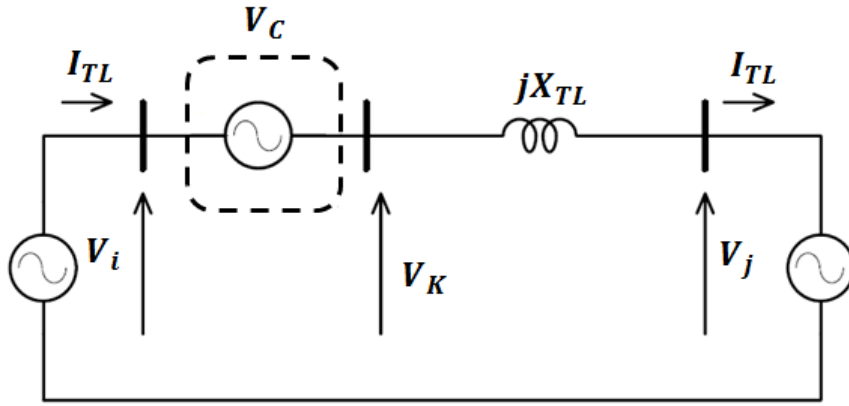
Figure 19: Ideal phase angle compensator schematic diagram

By analyzing Figure 19, if the voltage source V_C is added to the V_i and the resultant voltage V_K has the same magnitude of V_i but presenting an angle displacement of α degrees, the device is then called phase shifter [10], [14]. As the main objective is an angle displacement, the phase shifter will not be categorized as **Type 1** or **Type 2**.

To enhance the analysis of the effects provided by phase shifters, the phasor diagram of an ideal phase angle compensator is presented below [13]:
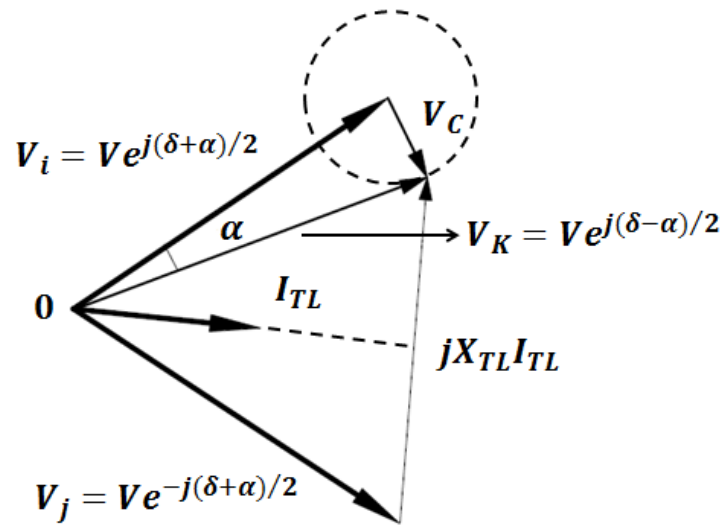
Figure 20: Phasor diagram of an ideal phase angle compensator

The resultant line power flow is:

$$P_{ij} = \frac{V_i V_j}{X_{TL}} \sin(\delta - \alpha) \tag{11}$$

From the abovementioned equation, it is intuitive to see that the active power still increases when the difference $(\delta - \alpha)$ reaches $90°$, in spite of the fact that the maximum $|P_{ij}|$ value is the same as there was no compensation. Both behaviors can also be seen in the Figure 9.

The nominal apparent power and the angle of the phase shifters affect their costs and sizes. Conventional ones can usually provide a continuous range of $\pm 25°$ [23].

Phase shifters are proven to be useful for controlling power flow in the system [24]. The system power angle can be better and faster controlled than in the traditional way (by controlling synchronous generator setpoints). On the other hand, Figure 9 shows that these devices do not have the ability to enhance the power transfer capability as the series compensators.

More technical details about the phase shifter can be found in the references [9], [10], [13], [23], [24] and [25].

3.4.5 Unified Power Flow Controller (UPFC)

The Unified Power Flow Controller (UPFC) is best represented as shown in Figure 21, where there are two voltage sources working simultaneously, one being a series and the other being a shunt voltage source. One of the main advantages of this topology is that the two sources can operate separately as two distinct reactive power compensators (one series and one shunt) and still compensating active power.
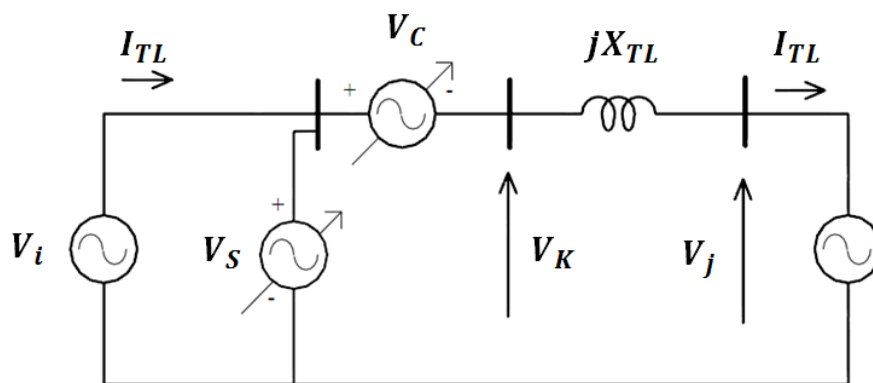
Figure 21: UPFC circuit schematic

Taking the UPFC circuit schematic into account, figure 22 presents the phasor diagram of a system containing an UPFC.
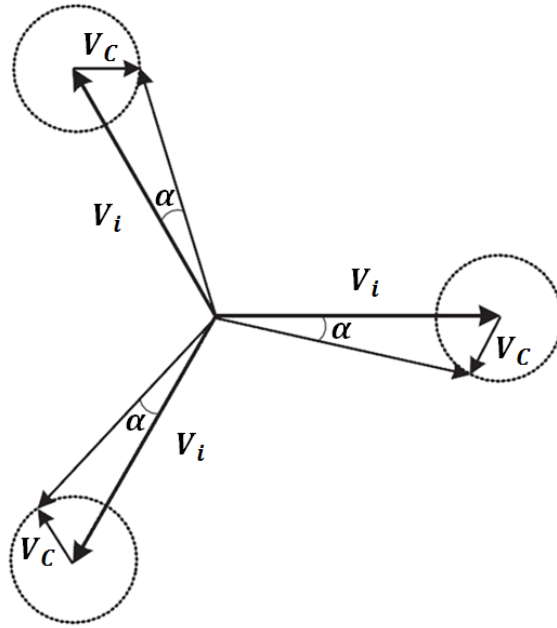
Figure 22: System operation with a UPFC

It can be seen that the injected voltage magnitude can be controlled from zero to a maximum value while the phase angle can vary from 0° to 360°. In other words, the UPFC can be operated in such a way as to produce any voltage phasor in series with the transmission line that fits inside the circles' areas. In fact, this structural concept turns the UPFC to be more generic than the phase-shifter and that is one of the greatest advantages of this device. As the UPFC achieves a series compensation through a voltage source V_C, it is categorized as **Type 2**, but it is worth to emphasize that this equipment is much more versatile than the other aforementioned series compensation devices by presenting also a shunt compensation.

Finally, in spite of the fact that the UPFC is the more generic and consequently more versatile power flow controller by presenting a series and a shunt voltage sources, its penetration into the market has been limited by the high installation and operation costs [23]. Its operation demands high technical level engineers to maintain and presents also a lifetime downside based on the low reliability of the power electronics.

For further technical information about the UPFC, the reader may consult [9], [10], [14], [23] and [26].

3.5 D-FACTS DEVICES

Distributed-FACTS allow direct control of the reactance and power flows in the transmission lines. Consist of modular equipment, coupled directly to the overhead transmission line cables. The distributed nature of the solution is the reason why the equipment is usually described as D-FACTS. The standardization associated to the modularity is one of the great advantages over the traditional FACTS devices, since traditional FACTS are manufactured for specific applications, resulting in higher costs and longer lead times. This technological differential should bring scale economic gains in the future.

The challenges regarding the practical application of FACTS devices (costs, centralized nature, substation project interference and space, etc.) led to the D-FACTS development by Professor Deepak Divan of Georgia Tech in cooperation with TVA, Southern Company, NRECA, Baltimore Gas and Electric, California Energy Commission, Southwire, Department of Energy, ARPA-E and NEETRAC [27]. Nowadays, the U.S. company Smart Wire Grid, Inc. (website: www.smartwiregrid.com) produces and commercializes the Smart Wire devices.

Since the D-FACTS devices are the newest ones presented in this dissertation, they deserve greater detail as the literature is not as plentiful as for other devices previously presented.

3.5.1 Distributed Series Reactors (DSRs) – Smart Wires

The Distributed Series Reactors have the ability to increase line impedance by injecting inductive reactance in series with the line. In meshed networks, the result of this action is to "push" current into other circuits of the network, i.e., divert power flow to underutilized transmission lines. This ability is achieved by injecting a pre-tuned value of magnetizing inductance of the Single-Turn Transformer (STT) shown in the figure 23 presented below.
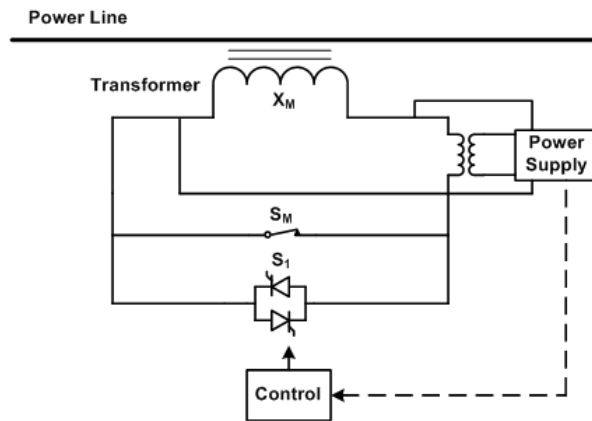
Figure 23: DSR circuit schematic – adapted from [28]

The quadrature voltage injection resultant from the DSR operation categorizes the device as **Type 2**. Each DSR can be configured at a predefined setpoint or dynamic controlled through telecommunication systems. The device is self-excited from the power line itself and enables the power flow control on each phase, i.e., it is consequently capable of phase balancing on transmission lines.

Each unit has two operation modes: injecting and monitoring. It normally stays in bypass mode until the inverter is activated. The monitoring mode is important, because the device automatically switches to this mode when it encounters a fault current, being consequently not needed changes in the line protection settings.

DSRs can fit a wide range of applications and are re-deployable. These devices can be installed in de-energized or live lines. They have short lead times and do not require substation modifications. Moreover, they do not see the line voltage and therefore insulation is not a big concern. They can be applied from 138 kV to 500 kV without significant redesign [27].

With regard to investment costs, it is estimated that today a 10kVA module costs $10,000. The typical impedance change consists in 50 µH per module. As an example, 50 µH per module per mile changes typical 138 kV conductor impedance by roughly 2% [29]. Therefore, a reasonable power flow control is achieved by using a large number of devices coordinated through a real-time telecommunication system. The figure presented below illustrates the communication design.
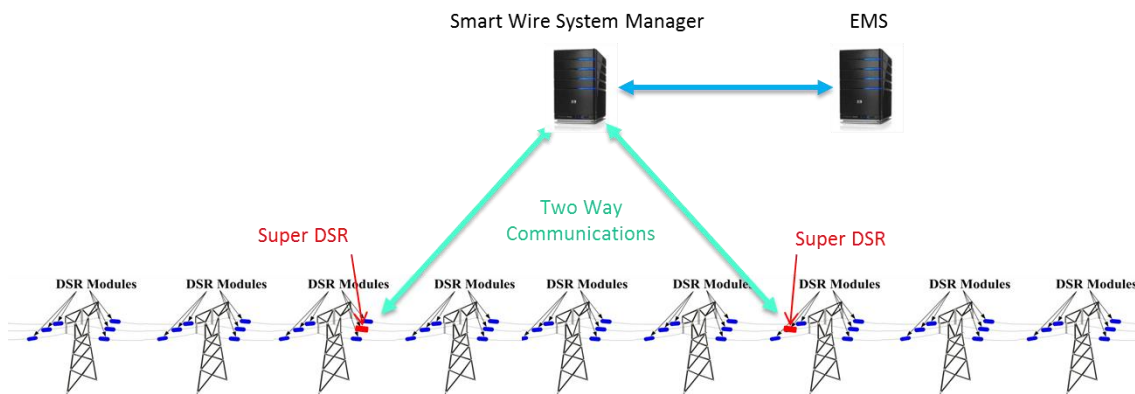
Figure 24: DSR's real-time communication system – adapted from [27]

As can be seen, the Super DSRs are responsible for interchanging data with the Smart Wire System Manager (SWSM) and the Energy Management System. Usually, wireless communications are used between the DSR and Super DSR, and also between Super DSR and the SWSM [27].

It is worth noting that the DSRs also contain useful sensors to monitor the condition of the line: line current, frequency, fault current and conductor temperature. The ambient temperature, sag and vibration monitoring are still in development. With this information available in the future, in conjunction with the other aforementioned sensors, more efforts will be made in order to produce an accurate Real-time Dynamic Thermal Rating (RTDR). As explained in [28], the maximum thermal capacity of the line dynamically changes, i.e., it is affected by climatic conditions which may vary significantly throughout the day or even in one hour. Nowadays utilities do not have accurate information in real time of the line thermal conditions of the line, making the operation very conservative. If RTDR curves could be inferred, there could be a power flow increase through a line by 10 to 30% for 90 to 98 % of the time compared to "state-of-art" techniques [28]. This would also increase the system power flow controllability and also transfer capability. Finally, it is important to emphasize that the RTDR inference is far away from being a trivial task due to the (i) uncertain and time variant ambient weather conditions and also (ii) conductor thermal dynamic nonlinearities.

More technical details about the DSRs and their practical applications can be found in the references [28], [29], [27], [24], [23] and [33].

3.5.2 Distributed Series Compensators (DSCs) – Active Smart Wires

Active Smart Wires consist of Distributed Series Compensators (DSCs) and have the ability to increase or decrease the line reactance. In meshed networks, the result of the line impedance increase is to "push" current into other circuits of the network, i.e., divert power flow to underutilized transmission lines and the result of the line impedance decrease is to "pull" current into the compensated line.

These devices are also called Distributed Static Series Compensators (DSSC) amd they consist of a small rated (10 kVA) single phase inverter and a STT as illustrated in the figure 25 presented below.
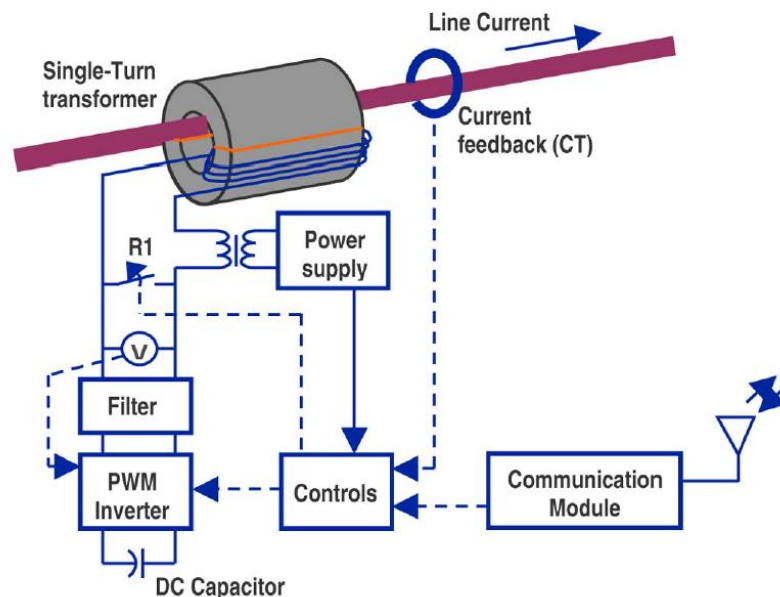
Figure 25: DSC circuit schematic – adapted from [15]

According to [31], once the device is in the injecting mode, the DSC can inject positive or negative inductance, or quadrature voltage being consequently categorized as **Type 2**.

The module is physically clamped around a transmission conductor, as well as the DSRs, enjoying all the aforementioned benefits of the distributed solution without insulation problems.

Assuming a 138 kV transmission line with a thermal capacity of 184 MVA, a 345 kV line with a capacity of 1195 MVA and a 765 kV line with a capacity of 6625 MVA, 1.4, 7.2, and 40 modules per mile per phase are respectively needed to

compensate 1% of the line reactance [31]. For the 138 kV transmission line under analysis, by installing 5 modules per mile per phase the impedance compensation can potentially change the line power flow by 10% and that roughly represents 18 MW of additional power flow capability. As mentioned in the previous section, as happens for the DSRs, a reasonable power flow control is achieved by using a large number of DSCs coordinated through communications.

For further technical information, the reader can consult [28], [15],[31] and [32].

3.6 SUMMARY AND CONCLUSIONS

Traditional solutions, i.e., construction of new lines are expensive to bear many different dispatch scenarios and reduce network utilization.

As explained in the introduction of this chapter, Shunt VAR compensation provides voltage support but do not significantly increase power flow control in the system. On the other hand, traditional Flexible AC Transmission Systems (FACTS) devices that provide series compensation are still options to enhance power flow control and transfer capability. The compensation level achieved by these devices can in fact increase system transfer capabilities. As the reader can see by analyzing figure 9, they can be projected to compensate 50% of a transmission line reactance. To enjoy the benefits of these devices, challenges regarding their practical application (costs, centralized nature, substation project interference and space, etc.) must be overcome.

Distributed control of transmission line reactance offers a new approach for controlling power flow in meshed systems. The distributed nature of the solution offers a high reliability, since the devices are re-deployable and the failure of one doesn't compromise system stability. This feature also helps the device dissemination, since the technological differential associated with the modularity can bring scale economic gains in the future. Moreover, there are no traditional FACTS devices capable of increasing and also decreasing the transmission line reactance. This flexibility achieved by the DSCs consists in a significant advantage although this technology is still under development and didn't achieve market utilization yet. On the other hand, it is worth to emphasize that the compensation level achieved by the D-FACTS solutions may not reach the compensation level achieved by traditional FACTS series compensators, since the number of devices needed would be significantly big. Another important issue is that the power flow control with D-FACTS devices directly depends on the

telecommunication systems, since the operation flexibility will be achieved only if the devices receive their operation setpoints according to each system condition.

In conclusion, there are a significant variety of new equipment revealed by recent technological advances with the ability to increase the controllability and consequently the flexibility of the transmission system, each one presenting specialties, advantages, disadvantages and practical challenges of deployment and implementation. More attention should be directed towards these devices, since the transmission expansion task is becoming more and more challenging. With the high penetration of intermittent renewables in the system, such as wind and solar, the transmission expansion planning is a task of extreme technical and economic relevance, because the transmission network needs to be robust enough to meet the demand with completely different dispatch scenarios throughout the year. These aforementioned facts enhance the importance of system's controllability and operation flexibility.

The next chapter of this dissertation will provide more details of the challenges involved in transmission expansion planning task.

4 THE TRANSMISSION EXPANSION PLANNING PROBLEM

The transmission expansion planning problem consists in finding the best options for expanding the network, under the technical and economic points of view.

The basic premise used for the elaboration of the criteria is that there will be no loss of load on the system or damage to the physical integrity of the equipment. The planned system must meet the performance levels established for the operation under steady state and transient operating conditions. The system's performance is tested for heavy, medium and low load conditions taking into account various generation dispatch scenarios and power flow exchange (between regions and/or systems) and it needs to support the different operating conditions without violating the criteria.

In order to propose an expansion plan which ensures that the load will be met within the limits of pre-established performance requirements, many studies are conducted for various scenarios involving different agents within a process that begins with the establishment of politician guidelines and macroeconomic indicators and results in the definition and grant of concession of a cast of transmission equipment to be implemented.

Therefore, it can be seen that the transmission expansion planning task is a complex process in which the network planners need to handle several uncertainties and consider different risk situations, taking into account many different interests from all agents. Some important aspects make this task at the same time crucial and very delicate.

Since the 1970s, several studies have been performed in order to automate the transmission planning task through the use of optimization techniques [34]. This task can be classified into different approaches as shown in the figure presented below [35].
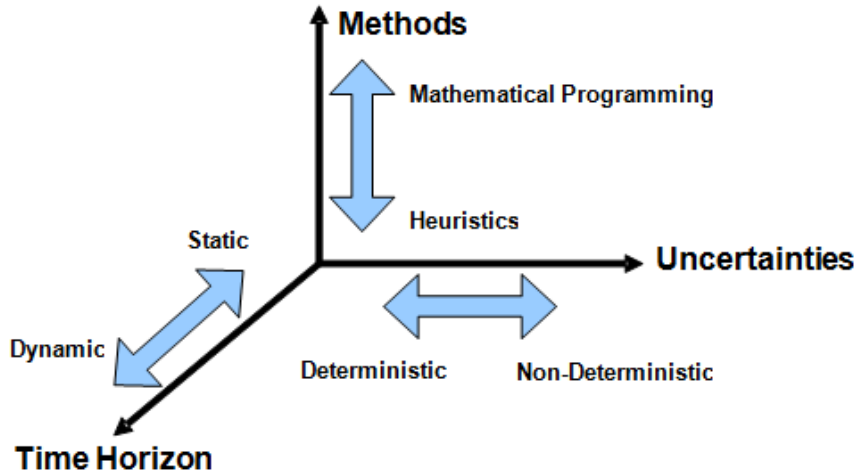
Figure 26: Classification of approaches to transmission expansion planning

Mathematical methods use classical optimization techniques such as linear, nonlinear and mixed-integer linear programming. Techniques such as Benders decomposition have also been used in the transmission expansion planning task [40], [41], [42].

More recently, heuristic and meta-heuristic models have become an alternative to mathematical optimization models. These algorithms use optimization techniques which, step by step, realize a process of generation, evaluation and selection of alternatives for new circuit allocations. These steps are performed until the algorithm is not able to find a better expansion plan, considering the criteria established in the objective function of the problem. The definition of reinforcements in these models is usually obtained by performing local searches guided by logical and/or sensitivities rules. These models have become an important alternative to mathematical models for demonstrating good potential to find feasible solutions, but not necessarily optimal, with an acceptable computational time. The main methods that have been applied to the transmission expansion planning problem are [34]: Genetic Algorithms (GA), object-oriented models, game theory, Simulated Annealing (SA), expert systems, fuzzy set theory and Greedy Randomized and Adaptive Search Procedure (GRASP).

Deterministic models are intended to define the expansion plan that meets the deterministic criteria (N-1 or N-2) and has the least overall costs. In these purely deterministic models, the aspects related to uncertainties are neglected. From the set of technically equivalent alternatives, the system planner chooses the one that has the least present value of costs [35], [36].

The non-deterministic models incorporate some external and internal uncertainties associated with the planning process into the analysis. The external uncertainties may involve: market projections, competitive market environment rules, environmental constraints, uncertainties associated with dispatch scenarios from RES, fuel costs, availability of new generations or large consumers, among others. Given these uncertainties, it is essential to obtain more flexible and robust expansion plans, able to withstand different future scenarios and consequently producing a better strategy for the system. The internal uncertainties involve uncertainties relating to the availability of the system equipment, i.e., system reliability. If only these uncertainties are considered, the objective is restricted to select the expansion plan able to meet the future load with the minimum cost and maximum reliability taking into account the criteria established by the system planner.

In the static planning, the planner seeks to obtain the optimal set of additions circuits for a given planning horizon. In this approach, the planner is not interested in determining when the circuits will be built, but in the optimal final network configuration for a given future situation.

In the dynamic or multi-stage planning, solving the expansion problem should provide the evolution of the network over a period of time basically answering three questions: which reinforcements will be needed, where and when they will be allocated in the system. In this case, the optimization model seeks to minimize the present value of all costs involved in its objective function. The current dynamic models still have limitations on the size and level of complexity of the systems. The characteristics of the problem provide a very large number of variables and constraints to be considered, requiring a huge computational effort to obtain the optimal solution.

In order to overcome this difficulty, these models have been simplified to provide better computational performance. One of the most common ways is to represent the problem by solving a sequence of static subproblems. To do so, it is usual to devise an expansion plan by means of two heuristic approaches: solving year by year a sequence of static expansion problems, the so-called forward approach, and solving backward in time starting from the horizon year solution, the backward approach. These are also called Pseudo-Dynamic Approaches [34], [37], [39].

In the forward approach, the static model is successively applied from the first to the horizon study year. For each intermediate year, the previous reinforcements are

considered part of the network. This approach has the advantage that all static problems solved usually require a small computational effort, since few yearly investments are made. On the other hand, this procedure typically takes "myopic" yearly decisions, without questioning previous year reinforcements. This procedure is not efficient in terms of economy of scale; nevertheless a feasible expansion plan is usually obtained once the horizon year static problem is solved.

On the other hand, especially if there are alternative voltage levels with different possibilities of voltage level routes of candidates, another solution approach can be devised, "polarizing" the expansion so as to focus on the horizon year configuration: a target (horizon year) solution is first obtained solving the static model. This static expansion model in general requires substantial computational effort if the load growth along the study period is significant; nevertheless the resulting horizon year optimal expansion "siting" and "sizing" decisions are obtained and must now be complemented by the "timing" of each added circuit in the plan. These reinforcements become a restricted candidate list that will thereon be considered since only the best "timing" of these candidates has to be decided (the remaining candidates are no longer dealt by the resulting restricted expansion model).

For more technical information about the transmission expansion planning methodologies, the reader should consult [34], [35], [38], [39] and [42].

Furthermore, the expansion planning of power systems should ideally be integrated, i.e. take into account the costs and benefits of reinforcements in generation plants, interconnections among regions and network circuits. Due to the complexity of this integrated planning problem, a hierarchy of the planning process is usually necessary and performed, based on the fact that the coupling of generation and interconnection reinforcement decisions is strong in terms of costs and mutual influence:

- The expansion along the study horizon of generation plants and interconnections among regions is decided by an optimization model with minimum total cost of investment and operation;

- The optimal hydrothermal schedule along the study horizon is determined by a Stochastic Dual Dynamic Programming tool [7],[8], as explained in chapter 2, and a simulation is performed to obtain the

dispatch of thermal and hydro plants for several dispatch scenarios;

- The network expansion is decided by the transmission expansion model taking into account the generation expansion and also the dispatch scenarios.

For further technical details about the aforementioned hierarchy and the integrated generation and transmission expansion planning process, the reader should consult [34], [37], [45] and [46].

If the reader seeks to know more about the whole process of the Brazilian electrical system planning, including the transmission expansion planning task, the references [1], [35] and [36] are recommended.

More than choosing the best method to determine the expansion plan, the transmission expansion planning task needs to be always up-to-date with the problems that the system will face in the future, its bottlenecks and especially new technologies that are being made available on the market. To address a specific problem in the system, different reinforcement solutions may be available, ranging from upgrading/uprating the existing assets to building new ones. The available options span from conventional technologies such as High Voltage Alternating Current (HVAC) overhead lines, transformers, cables to more innovative devices like High Voltage Direct Current (HVDC), Flexible Alternating Current Transmission Systems (FACTS) and finally the recent Distributed-FACTS. A combination of different solutions might also be important options.

Keeping the aforementioned argument in mind, as explained in the introduction of this document, the main objective of this dissertation is to incorporate power flow controllability and flexibility in the expansion model by adding Candidate Series Compensation Devices in order to evaluate the impacts in the transmission expansion planning task, especially when dispatch scenarios associated with RES are taken into account. To do so, Mixed-Integer Linear Programming (MILP) formulations of the incorporation of these devices in the transmission expansion planning problem are proposed.

Accordingly, the transmission expansion problem is formulated in this dissertation as an optimization model based on the linearized power flow and circuit

limits where the objective is to minimize the investments in the transmission system. Moreover, the static approach will be used and no security constraint will be imposed.

In the next section, the transmission expansion planning model is deeply analyzed. First, the DC Optimal Power Flow (OPF) basic equations will be shown. Afterwards, the different models and formulations will be presented and finally the static expansion planning model that will be applied to the test systems will be presented to the reader. The expansion model is first described for the network base case considering a single dispatch scenario; next we extend the formulation for multiple scenarios.

4.1 TRANSMISSION EXPANSION PLANNING MODEL

As explained in the previous section, optimization models are used in order to establish a preliminary expansion plan. The proposed transmission expansion planning model considers only the steady state of the network and adopts the linearized active power flow instead of the non-linear power flow due to the following reasons:

- The linearized model provides a good approximation for power flows in meshed high voltage networks due to the low typical resistance-to-reactance (*R/X*) ratio of overhead transmission lines;

- It avoids convergence problems that are common in non-linear power flow calculations, especially in systems lacking of reactive support which is the case of expansion planning study cases;

- Local nature of the VAr support requirements in power transmission expansion planning (which can be provided by shunt compensation, capacitors, SVCs, etc.);

- VAr support requirements present minor costs with respect to circuit investment costs (transmission lines, transformers, etc.);

- Optimization solvers for mixed integer programming can be used to determine the optimal expansion plan.

Once one or more options for network expansion are selected, more detailed studies should be performed with them:

- AC power flow studies and VAr Support dimensioning and planning;

- Dynamic studies;

- Short-circuit studies;

- Reliability studies.

Finally, Appendix A provides a description of the linearized power flow model determination and calculation.

4.2 DC OPTIMAL POWER FLOW BASIC EQUATIONS

In this section, the MILP formulation of the DC Optimal Power Flow (OPF) of an AC system is presented.

4.2.1 Kirchhoff's Current Law (KCL)

This law represents the active power balance in each AC bus (for notational simplicity, we suppose that each bus has generation and load):

$$\sum_{k \in \Omega_i} f_k + g_i = d_i, \forall\, i = 1, \dots, I \tag{12}$$

where:

i	Indexes the AC buses;
k	Indexes the circuits;
Ω_i	Set of circuits directly connected to bus i;
g_i	Generation of bus i;
d_i	Load of bus i;
f_k	Active power flow in the circuit k;
I	Number of buses;
K	Number of circuits.

The KCL can also be represented in matrix form as:

$$S\,f + g = d \tag{13}$$

where:

S	Incidence matrix of dimension $I \times K$;
f	K-dimensional vector of circuits flows

g I-dimensional vector of bus generations;

d I-dimensional vector of bus loads.

In the DC OPF formulation, the KCL usually contemplates also the bus load shedding:

$$S f + r = d - g \tag{14}$$

where:

r I-dimensional vector of variables representing the bus load shedding.

To do so, the equation presented below is also necessary:

$$r \le d \tag{15}$$

4.2.2 Kirchhoff's Voltage Law (KVL)

The For each AC circuit this law is expressed by:

$$f_k = \gamma_k \big(\theta(i_k) - \theta(j_k) \big) \tag{16}$$

where:

γ_k Circuit susceptance;

$\theta(i_k)$ Voltage angle of the circuit's terminal bus i_k;

$\theta(j_k)$ Voltage angle of the circuit's terminal bus j_k.

The KVL can also be represented in matrix form as:

$$f = |\gamma| \, S' \, \theta \tag{17}$$

where:

$|\gamma|$ Diagonal $K \times K$ matrix of circuit susceptances;

S' Transpose matrix of S;

θ I-dimensional vector of bus voltage angles.

4.2.3 Flow Limits

The For each AC circuit this law is expressed by:

$$-\overline{f_k} \le f_k \le \overline{f_k}, \forall\, k = 1, \ldots, K \tag{18}$$

where:

$\overline{f_k}$ K-dimensional vector of flow limits.

4.2.4 Dealing with Different Dispatch Scenarios

The DC OPF model was first described considering a single dispatch scenario. Next, a general formulation is extended for multiple dispatch scenarios. In this case, a general formulation having the KCL and KVL being represented in matrix form will be used in order to facilitate reader's interpretation and consequently highlight the impacts of the dispatch scenarios in the problem formulation:

$$Sf^n = d^n - g^n \tag{19}$$

$$f^n = |\gamma|\, S'\, \theta^n \tag{20}$$

$$-\overline{f_k} \le f_k^n \le \overline{f_k}, \forall\, k = 1, \ldots, K \tag{21}$$

Where the superscript $\blacksquare^n$ denotes the dispatch scenario n.

4.3 TRANSMISSION EXPANSION PLANNING PROBLEM: DIFFERENT MODELS AND FORMULATIONS

Based on the aforementioned equations and constraints, in this section, the different transmission expansion planning models will be presented. To facilitate the illustration of the following formulations and also to highlight the differences between them, generation limit constraints, bus load shedding constraints and finally the associated slack variables will not be presented.

4.3.1 Transportation Model

The Transportation Model Formulation is presented below:

$$Min \ \sum_{k=1}^{\Omega^1} c_k \, x_k \tag{22}$$

$$\sum_{k \in \Omega_i^0} f_k^0 + \sum_{k \in \Omega_i^1} f_k^1 + g_i = d_i, \forall \, i = 1, \dots, I \tag{23}$$

$$-\overline{f_k^0} \le f_k^0 \le \overline{f_k^0}, \forall \, k \in \Omega^0 \tag{24}$$

$$-\overline{f_k^1} x_k \le f_k^1 \le \overline{f_k^1} x_k, \forall \, k \in \Omega^1 \tag{25}$$

where:

Ω^0	Number of existing candidates;
Ω^1	Number of circuit candidates;
Ω_i^0	Set of existing circuits directly connected to bus i;
Ω_i^1	Set of candidate circuits directly connected to bus i;
$\blacksquare^0$	Superscript ^{0} denotes an existing circuit;
$\blacksquare^1$	Superscript ^{1} denotes a candidate circuit;

It can be seen that in this model the KVL is not enforced for existing and candidate circuits, only the flow limits. It is a very simplified model and present greatly reduced computational effort in comparison to the next formulations. The solutions obtained with this model, in general, are not feasible for the complete DC model, but it avoids the nonlinearity present in this model that will also be explained in the continuation of this chapter.

4.3.2 Hybrid Linear Model

The Hybrid Linear Model Formulation is presented below:

$$Min \ \sum_{k=1}^{\Omega^1} c_k \, x_k \tag{26}$$

$$\sum_{k \in \Omega_i^0} f_k^0 + \sum_{k \in \Omega_i^1} f_k^1 + g_i = d_i, \forall \, i = 1, \dots, I \tag{27}$$

$$f_k^0 = \gamma_k^0 \big(\theta(i_k) - \theta(j_k)\big), \ \forall \, k \in \Omega^0 \tag{28}$$

$$-\overline{f_k^0} \le f_k^0 \le \overline{f_k^0}, \forall \, k \in \Omega^0 \tag{29}$$

$$-\overline{f_k^1} x_k \le f_k^1 \le \overline{f_k^1} x_k, \forall \, k \in \Omega^1 \tag{30}$$

The KCL and flow limit constraints for existing and candidate circuits are enforced. On the other hand, only existing circuits must obey the KVL to avoid the nonlinearity present in the KVL for candidate circuits.

This model maintains the linearity and improves accuracy in comparison to the previous formulation since the existing branches are generally the majority of the network circuits.

4.3.3 Disjunctive Representation

When the KVL for candidate circuits is represented, note that there is a non-linearity in resulting from the product of the diagonal of matrix $|\gamma(x)|$ (the investment binary decision vector x) and the continuous bus angle vector θ that can also be represented as follows:

$$f_k^1 = \gamma_k \, x_k \left(\theta(i_k) - \theta(j_k)\right) \forall \, k \in \Omega^1 \tag{31}$$

The product of variables introduces a non-linearity to the problem. To circumvent this problem, it is used instead a mixed integer constraint which was proposed by [41], known as a disjunctive inequality:

$$-M(1 - x_k) \leq f_k^1 - \gamma_k\left(\theta(i_k) - \theta(j_k)\right) \leq M(1 - x_k) \forall \, k \in \Omega^1 \tag{32}$$

Where M is a very big constant ("big M"). The disjunctive constraints can be interpreted as follows: if $x_k = 1$, Kirchhoff's second law is enforced to the candidate circuit k, i.e., $f_k = \gamma_k\left(\theta(i_k) - \theta(j_k)\right)$. Otherwise, if $x_k = 0$, the disjunctive constraint is relaxed, since the circuit is nonexistent.

However, if M is arbitrarily big, the mathematical optimization problem becomes ill-conditioned. Therefore, we calculate for each candidate right-of-way the smallest value of M capable of enforcing in equation (31) the same behavior as in (32). Initially suppose that there is an existent circuit having reactance γ_k^0, capacity f_k^0 and the same bus terminals as candidate circuit k. The maximum angle difference between these bus terminals is f_k^0/γ_k^0; therefore one can set $M_k = \gamma_k \left(f_k^0/\gamma_k^0\right)$. For a new corridor with bus terminals i_k and j_k (and no existing circuit connect these bus terminals), the maximum angle difference can be derived considering each path from i_k to j_k composed by existing circuits. For each such circuit, its maximum angle

difference is the ratio mentioned earlier, and summing these terms results in the maximum angle difference between i_k and j_k. Since there may be several paths connecting buses i_k and j_k the smallest value of M_k will be the candidate's reactance times the length of the shortest path between i_k and j_k (a circuit "length" is the ratio of its capacity and its reactance) [42]. The length of the shortest path between any pair of buses is calculated by Dijkstra's algorithm. Note that the value of M_k for candidate k depends on the network topology and the reactance of existing circuits. More details about the "big M" and its calculation can be found in Appendix B of this dissertation.

Using this disjunctive formulation any mixed linear integer (MIP) solver (Branch-and-Bound or Branch-and-Cut algorithm) can be used to find the optimal solution, whereas using the non-linear equation results in non-convexity of the model formulation (a non-linear mixed integer solver will stop at a local optimal solution).

The use of the above mentioned disjunctive formulations to solve benchmark problems found in the transmission expansion literature was proved to be very effective, they were solved faster and the optimal solution was obtained and proven for the first time [40], [42].

The final transmission expansion planning problem having the disjunctive representation is presented below:

$$Min \ \sum_{k=1}^{\Omega^1} c_k \, x_k \tag{33}$$

$$\sum_{k \in \Omega_i^0} f_k^0 + \sum_{k \in \Omega_i^1} f_k^1 + g_i = d_i, \forall \ i = 1, \dots, I \tag{34}$$

$$f_k^0 = \gamma_k^0 \big(\theta(i_k) - \theta(j_k) \big), \ \forall \ k \in \Omega^0 \tag{35}$$

$$-M(1 - x_k) \le f_k^1 - \gamma_k \big(\theta(i_k) - \theta(j_k) \big) \le M(1 - x_k) \ \forall \ k \in \Omega^1 \tag{36}$$

$$-\overline{f_k^0} \le f_k^0 \le \overline{f_k^0}, \forall \ k \in \Omega^0 \tag{37}$$

$$-\overline{f_k^1} x_k \le f_k^1 \le \overline{f_k^1} x_k, \forall \ k \in \Omega^1 \tag{38}$$

4.3.4 Dealing with Different Dispatch Scenarios

The DC OPF model was first described considering a single dispatch scenario. Next the formulation is extended for multiple dispatch scenarios. In this case, the

Disjunctive Representation will be used in order to facilitate reader's interpretation and consequently highlight the impacts of the dispatch scenarios in the problem formulation:

$$Min \sum_{k=1}^{\Omega^1} c_k x_k \tag{39}$$

$$\sum_{k \in \Omega_i^0} f_{k0}^n + \sum_{k \in \Omega_i^1} f_{k1}^n + g_i^n = d_i^n, \forall i = 1, \dots, I \tag{40}$$

$$f_{k0}^n = \gamma_{k0} \left(\theta^n(i_k) - \theta^n(j_k) \right), \ \forall k \in \Omega^0 \tag{41}$$

$$-M(1 - x_k) \leq f_{k1}^n - \gamma_k \left(\theta^n(i_k) - \theta^n(j_k) \right) \leq M(1 - x_k) \ \forall k \in \Omega^1 \tag{42}$$

$$-\overline{f_k^0} \leq f_{k0}^n \leq \overline{f_k^0}, \forall k \in \Omega^0 \tag{43}$$

$$-\overline{f_k^1} x_k \leq f_{k1}^n \leq \overline{f_k^1} x_k, \forall k \in \Omega^1 \tag{44}$$

When multiple dispatch scenarios are considered, the superscript $\blacksquare^n$ denotes the dispatch scenario n, the subscript $\blacksquare_0$ will hereinafter denote an existing circuit and the subscript $\blacksquare_1$ will hereinafter denote a candidate circuit.

It can be seen that the variable x_k associated to the construction of the candidate circuits is responsible for coupling the dispatch scenarios in the OPF formulation. In other words, the KCL, KVL and flow limits are represented for each dispatch scenario and the variable x_k is responsible for coupling the dispatch scenarios and therefore obligates the OPF model to meet all scenarios taken into account.

4.3.5 Objective Function

In this work, the following Objective Function will be applied for the transmission expansion planning problem:

$$Min \sum_{k=1}^{\Omega^1} c_k x_k + \delta r^n \tag{45}$$

where:

Ω^1	Number of circuit candidates;
k	Indexes the circuit candidates;
c_j	Annualized value of candidate's investment cost;
x_j	Binary variable related to building candidate j.
δ	High penalty cost in order to avoid loss of load when feasible solutions exist.

r^n I-dimensional vector of variables representing the bus load shedding in each dispatch scenario n.

This formulation that includes a penalty for load shedding is useful because it accelerates the OPF convergence and it is also a measure of how far the problem is from a feasible solution in cases where load shedding is inevitable.

4.4 CONCLUSIONS

The Transportation Model is the simplest and easiest to solve. For a long time it was the only software used in planning transmission expansion due to the greatly reduced computational effort in comparison to the next formulations. On the other hand, the solutions obtained with this model, in general, are not feasible for the complete DC model.

The Hybrid Model maintains the linearity and improves accuracy in comparison to the Transportation Model, but it is also not a complete model, since it does not represent the KVL for candidate circuits.

Finally, the DC model with the Disjunctive Representation is currently the most used in practice, because it presents a better accuracy and already exist optimization programs that are capable of producing solutions for this model even for large systems [46].

5 THE INCORPORATION OF POWER FLOW CONTROLLABILITY AND FLEXIBILITY IN THE TRANSMISSION EXPANSION PLANNING MODEL

5.1 INTRODUCTION

This chapter consists in the main contribution of this dissertation, because it contains the proposed MILP formulation of the incorporation of power flow controllability and flexibility in the transmission expansion planning model, i.e., the proposed formulation enables to represent series compensation (SC) enabled by FACTS and D-FACTS devices in the DC OPF.

In order to facilitate the interpretation by the reader, the inclusion of the penalty for load shedding in the objective function will not presented in the following equations despite being represented within the model. This is done so that the problem is presented in a clearer way in order to highlight the proposed formulation.

5.2 HYBRID LINEAR MODEL: ALTERNATIVE PROPOSAL

As can be seen in the previous chapter, the hybrid model contemplates the KCL, enforces flow limit constraints for existing and candidate circuits, but enforces the KVL law only for existing circuits to avoid the nonlinearity present in the KVL for candidate circuits.

The first proposed formulation by this dissertation is an alternative hybrid linear model that also avoids the nonlinearity present in the KVL for candidate circuits adding at the same time power controllability to candidate circuits and consequently to the system. As will be seen, this alternative proposal for the Hybrid Model is an improvement of the methodology published in [48].

First, it contains all equations from the traditional hybrid linear model which are presented below:

$$Min \sum_{k=1}^{\Omega^1} c_k\, x_k \tag{46}$$

$$\sum_{k \in \Omega_i^0} f_k^0 + \sum_{k \in \Omega_i^1} f_k^1 + g_i = d_i, \forall\, i = 1, \dots, I \tag{47}$$

$$f_k^0 = \gamma_k^0\big(\theta(i_k) - \theta(j_k)\big), \ \forall\, k \in \Omega^0 \tag{48}$$

$$-\overline{f_k^0} \le f_k^0 \le \overline{f_k^0}, \forall\, k \in \Omega^0 \tag{49}$$

$$-\overline{f_k^1} x_k \le f_k^1 \le \overline{f_k^1} x_k, \forall\, k \in \Omega^1 \tag{50}$$

In addition to that, the KVL for candidate circuits needs to be represented:

$$f_k^1 = \gamma_k^1\, x_k \big(\theta(i_k) - \theta(j_k)\big) \ \forall\, k \in \Omega^1 \tag{51}$$

Or just:

$$f_k^1 - \gamma_k^1\, x_k\, \Delta\theta_{ij} = 0 \ \forall\, k \in \Omega^1 \tag{52}$$

Where $\Delta\theta_{ij} = \theta(i_k) - \theta(j_k)$. As explained in the previous chapter, the disjunctive representation introduces the disjunctive constraints in order to circumvent the nonlinearity present in this equation. On the other hand, our goal in this formulation is not to fully represent the KVL as the disjunctive formulation does, but to propose a hybrid model that avoids this nonlinearity and at the same time adds power flow controllability for the candidate circuits. To this end, the hybrid model needs to contain differences in the problem formulation in order to contemplate the following constraint:

$$0 \le \gamma_k^1 \le \overline{\gamma_k^1} \tag{53}$$

Multiplying the terms of the above constraint by $\left|\Delta\theta_{ij}\right|$,

$$\gamma_k^1\left|\Delta\theta_{ij}\right| \le \overline{\gamma_k^1}\left|\Delta\theta_{ij}\right| \tag{38}$$

Considering that $\gamma_k^1\left|\Delta\theta_{ij}\right| = \left|\gamma_k^1\Delta\theta_{ij}\right|$ which may be replaced by variable $\left|f_k^1\right|$, then the KVL can be reformulated as follows:

$$\left|f_k^1\right| \le \overline{\gamma_k^1}\left|\Delta\theta_{ij}\right| \tag{54}$$

Where $\overline{\gamma_k^1}$ represents now that the susceptance may vary from zero to $\overline{\gamma_k^1}$. This formulation is interesting because it represents the susceptance variation and also avoids

the nonlinearity present when the variable x_k is in the equation. On the other hand, the absolute function is nonlinear. To solve this nonlinearity, the following decomposition is needed:

$$f_{k1} = f_{k1}^+ - f_{k1}^- \tag{55}$$

$$f_{k1}^+ \leq \overline{\gamma_k^1} \Delta\theta_k^+ \tag{56}$$

$$f_{k1}^- \leq \overline{\gamma_k^1} \Delta\theta_k^- \tag{57}$$

$$\Delta\theta_k = \Delta\theta_k^+ - \Delta\theta_k^- = \Delta\theta_{ij} = \theta_i - \theta_j \tag{58}$$

It is worth noting that the superscripts $\blacksquare^+$ or $\blacksquare^-$ denote the parts of the decomposition according to $\Delta\theta_k^+$ or $\Delta\theta_k^-$ and the subscript $\blacksquare_1$ denotes a candidate circuit.

The extension of this formulation to multiple scenarios is straightforward and presented below:

$$f_{k1}^n = f_{k1}^{n+} - f_{k1}^{n-} \tag{59}$$

$$f_{k1}^{n+} \leq \overline{\gamma_k^1} \Delta\theta_k^{n+} \tag{60}$$

$$f_{k1}^{n-} \leq \overline{\gamma_k^1} \Delta\theta_k^{n-} \tag{61}$$

$$\Delta\theta_k^n = \Delta\theta_k^{n+} - \Delta\theta_k^{n-} = \Delta\theta_{ij}^n = \theta_i^n - \theta_j^n \tag{62}$$

Where the superscript $\blacksquare^n$ denotes the dispatch scenario n.

If these equations are introduced into the model, there is still no guarantee that the KVL for candidate circuits will be respected. This problem occurs because there is no constraint that forces that only one of the variables $\Delta\theta_k^{n+}$ and $\Delta\theta_k^{n+}$ can be nonzero in the optimal solution of the problem. This problem is deeply detailed and explained in Appendix C which is entitled "WHY IS THE $\Delta\theta^+$ OR $\Delta\theta^-$ UNIQUE EXISTENCE ASSURANCE IMPORTANT?". In this Appendix, a numerical explanation is given by using the first test system with 3 buses which is used in the case study chapter (next chapter of this dissertation).

Now, if we consider the proposed first set of flow direction unique existence assurance constraints for the hybrid candidate circuits:

$$\Delta\theta_k^{n+} \leq K \times z_k^n \tag{63}$$

$$\Delta\theta_k^{n-} \leq K \times (1 - z_k^n) \tag{64}$$

$$z_k^n \in \{0,1\}$$

Where K is a big constant that does the same job as the big M in the disjunctive representation, the KVL for candidate circuits is enforced, the resultant susceptance γ_k^1 will be inside the limits $\left\{0, \overline{\gamma_k^1}\right\}$ and will depend on the dispatch scenario and system operating conditions.

As introduced above, K is a very big constant which can be interpreted as follows: if $z_k^n = 1$, $\Delta\theta_k^{n+}$ is nonzero and $\Delta\theta_k^{n-}$ is zero. Otherwise, if $z_k^n = 0$, $\Delta\theta_k^{n-}$ is nonzero and $\Delta\theta_k^{n+}$ is zero.

It is worth to emphasize that the aforementioned constraints add an integer variable to the MIP problem and this problem consequently demands more computational effort to reach the optimal solution.

Moreover, the decision to use $\Delta\theta_k^{n+}$ or $\Delta\theta_k^{n+}$ directly depends on the power flow direction. In other words, if the circuit flow is from i to j, $\Delta\theta_k^{n+}$ is nonzero and $\Delta\theta_k^{n-}$ is zero and if the circuit flow is from j to i, $\Delta\theta_k^{n-}$ is nonzero and $\Delta\theta_k^{n+}$ is zero. Taking this information into account, this dissertation proposes also a tighter formulation to accelerate the optimal power flow model. The second set of constraints proposed to outline this problem is presented below:

$$\Delta\theta_k^{n+} \leq K(1 - z_k^{n-}) \tag{65}$$

$$\Delta\theta_k^{n-} \leq K(1 - z_k^{n+}) \tag{66}$$

$$z_k^{n+} \geq f_{k1}^{n+}/\overline{f_{k1}} \tag{67}$$

$$z_k^{n-} \geq f_{k1}^{n-}/\overline{f_{k1}} \tag{68}$$

$$z_k^{n+} + z_k^{n-} \leq x_k \tag{69}$$

$$z_k^{n+}, z_k^{n-} \in \{0,1\} \tag{70}$$

This alternative formulation adds two integer variables to the MIP problem. It might look that the addition of one more integer variable in each Right-Of-Way (ROW) containing a candidate circuit could demand even more computational effort, but in this formulation the utilization of the integer variables is now intrinsically linked with the direction of the circuit power flow and therefore the OPF formulation becomes more adherent to the reality and physical flow distribution through the lines.

After presenting this alternative proposal for the Hybrid Model, in the next section, the proposed MILP formulation of the series compensation attached to an existing circuit is presented.

5.3 MILP FORMULATION OF THE SERIES COMPENSATION ATTACHED TO AN EXISTING CIRCUIT

As described in chapter 3 entitled "POWER FLOW CONTROLLABILITY AND FLEXIBILITY", there are devices able to: (i) only decrease the line reactance, (ii) only increase the line reactance and (iii) decrease or increase the line reactance. The proposed formulation is general and therefore encompasses all three forms of compensation. All forms will be explained in this chapter.

In addition to all previous defined variables, before presenting the formulation, it is plausible to present the variables' notation in order to facilitate reader's interpretation.

5.3.1 Nomenclature

γ_0	Existing transmission line nominal series susceptance;
γ'	Line susceptance variation $\Delta\gamma$ enabled by the series compensation;
γ_{min}	Minimum susceptance achieved by the compensated line;
γ_{max}	Maximum susceptance achieved by the compensated line;
γ_{min}^{SC}	Minimum susceptance achieved by the series compensation device;
γ_{max}^{SC}	Maximum susceptance achieved by the series compensation device;
$\bar{\gamma}$	Susceptance variation range;
γ_{ROW}	Susceptance associated to the Right-Of-Way in which there are an existing circuit and a series compensation device attached to it;
$\blacksquare^+$	Superscript $^+$ denotes the positive part of the decomposition;
$\blacksquare^-$	Superscript $^-$ denotes the negative part of the decomposition;

$\blacksquare^n$	Superscript ^{n} denotes the dispatch scenario n;
$\blacksquare_{k0}$	Subscript $_0$ denotes an existing circuit k;
$\blacksquare_{k1}$	Subscript $_1$ denotes a candidate circuit k;

f_{ROW}^n	Resulting active power flow associated to the Right-Of-Way in which there are an existing circuit and a series compensation device attached to it according to the dispatch scenario n;
δ_k^n	Resulting delta-flow caused by the series compensation device k in the dispatch scenario n;
δ_{k1}^n	Delta-flow caused by a positive series compensation in the dispatch scenario n from device k;
δ_{k2}^n	Delta-flow caused by a negative series compensation in the dispatch scenario n from device k.
η^1	Number of Candidate Series Compensation Devices (CSCDs).

In the DC OPF formulation, rather than the line reactance, the susceptance is usually used in the formulation and therefore will also be used in this formulation. Moreover, it is plausible to present that the first representation of FACTS devices in the DC OPF was proposed by [47].

A traditional FACTS device and a set of (Active) Smart Wires allow a line susceptance change of $\alpha\%$, being α a limited value according to the project and operation limits.

Thus, in the proposed formulation, the variable v_k will represent the series compensation (SC) construction and the objective function will be defined as follows:

$$Min \ \sum_{k=1}^{\Omega^1} c_k x_k + \sum_{k=1}^{\eta^1} c_k v_k + \delta r^n \tag{71}$$

Where v_k is the binary variable related to building CSCD k.

All existing circuits that have a Candidate Series Compensation Device, defined hereinafter as CSCD, will present flow variation δ_k^n as can be seen in the KCL:

$$S(f_k^n + \delta_k^n) = d^n - g^n \quad \forall \ n = 1, \dots, N \tag{72}$$

The resulting active power flow in a Right-Of-Way that contains an existing line with a CSCD will be:

$$f_{ROW}^n = f_{k0}^n + \delta_k^n \tag{73}$$

For the existing circuit, the KVL equation is straightforward:

$$f_{k0}^n - \gamma_0 \Delta\theta_{ij}^n = 0 \tag{74}$$

On the other hand, if the candidate SC is built, there will be a susceptance variation:

$$\gamma_{ROW} = \gamma_0 + \gamma' \tag{75}$$

Where γ' represents the line susceptance variation $\Delta\gamma$ enabled by the series compensation and is bounded by:

$$\gamma_{min}^{SC} \leq \gamma' \leq \gamma_{max}^{SC} \tag{76}$$

The definition of the above mentioned limits depends on the susceptance variation range provided by the candidate SC device and also on the compensation type. To facilitate the interpretation, a convention is now defined by this dissertation. **Positive compensation** is hereinafter defined as series compensation in order to increase (decrease) line susceptance (reactance) and consequently increase the power flow in the target transmission line. The delta-flow associated with this type of compensation will be denoted by δ_{k1}^n. **Negative compensation** is hereinafter defined as series compensation in order to decrease (increase) line susceptance (reactance) and consequently decrease the power flow in the target transmission line. The delta-flow associated with this type of compensation will be denoted by δ_{k2}^n.

5.3.2 Positive Compensation

For positive compensation, the line susceptance variation range will be:

$$0 \leq \gamma_{k1} \leq \gamma_{max}^{SC} \tag{77}$$

Where γ' is represented by γ_{k1} for the positive compensation.

The KVL for the candidate SC must be obeyed:

$$\delta_{k1}^n - \gamma_{k1}^n \Delta\theta_{ij}^n = 0 \tag{78}$$

This equation presents a nonlinearity associated to the multiplication of γ_{k1} by $\Delta\theta$, because both can vary. The following equation should be used to outline this problem:

$$|\delta_{k1}^n| \leq \overline{\gamma}_{k1}|\Delta\theta_k^n| \tag{79}$$

$$\overline{\gamma}_{k1} = \gamma_{max}^{SC} \tag{80}$$

Equation (79) solves the nonlinearity of equation (78). On the other hand, the absolute function is a nonlinear function. To solve this nonlinearity, the following decomposition is needed:

$$\delta_{k1}^n = \delta_{k1}^{n+} - \delta_{k1}^{n-} \tag{81}$$

$$\Delta\theta_k^n = \Delta\theta_k^{n+} - \Delta\theta_k^{n-} = \Delta\theta_{ij}^n = \theta_i^n - \theta_j^n \tag{82}$$

This decomposition was also used for the hybrid alternative proposal.

5.3.2.1 KVL for Positive Compensation

The Kirchhoff's Second Law for the CSCD is defined as follows:

$$\delta_{k1}^{n+} \leq \overline{\gamma}_{k1}\Delta\theta_k^{n+} \tag{83}$$

$$\delta_{k1}^{n-} \leq \overline{\gamma}_{k1}\Delta\theta_k^{n-} \tag{84}$$

It is worth noting that $\overline{\gamma}_{k1}$ will determine the susceptance variation range, i.e., the maximum series compensation level. As explained in chapter 3, the series compensation devices are projected in order to compensate $X\%$ of the line reactance. So, in order to incorporate the maximum compensation level in the model, we just need to convert the maximum reactance compensation level into a susceptance variation range.

5.3.2.2 *Flow Direction Unique Existence Assurance Constraints*

The delta-flow δ_{k1}^n will obey the KVL only if there are constraints that ensure that only $\Delta\theta_k^{n+}$ or $\Delta\theta_k^{n-}$ is different from zero in the optimal solution of the problem. Appendix C entitled "WHY IS THE $\Delta\theta^+$ OR $\Delta\theta^-$ UNIQUE EXISTENCE ASSURANCE IMPORTANT?" deals with this issue.

The first set of constraints proposed to outline this problem is presented below:

$$\Delta\theta_k^{n+} \leq K \times z_k^n \tag{85}$$

$$\Delta\theta_k^{n-} \leq K \times (1 - z_k^n) \tag{86}$$

$$z_k^n \in \{0,1\} \tag{87}$$

It is worth to emphasize that the aforementioned constraints add an integer variable to the MIP problem and this problem consequently demands more computational effort to reach the optimal solution.

The decision to use $\Delta\theta_k^{n+}$ or $\Delta\theta_k^{n-}$ directly depends on the power flow direction in the circuit in which the CSCD is connected. In other words, if the existing circuit flow is from i to j, $\Delta\theta_k^{n+}$ is nonzero and $\Delta\theta_k^{n-}$ is zero and if the existing circuit flow is from j to i, $\Delta\theta_k^{n-}$ is nonzero and $\Delta\theta_k^{n+}$ is zero. Taking this information into account, this dissertation proposes also a tighter formulation to accelerate the optimal power flow model:

$$\Delta\theta_k^{n+} \leq K(1 - z_k^{n-}) \tag{88}$$

$$\Delta\theta_k^{n-} \leq K(1 - z_k^{n+}) \tag{89}$$

$$z_k^{n+} \geq \delta_{k1}^{n+}/\overline{f_{k0}} \tag{90}$$

$$z_k^{n-} \geq \delta_{k1}^{n-}/\overline{f_{k0}} \tag{91}$$

$$z_k^{n+} + z_k^{n-} \leq v_k \tag{92}$$

$$z_k^{n+}, z_k^{n-} \in \{0,1\} \tag{93}$$

This alternative formulation adds two integer variables to the MIP problem. It might look that the addition of one more integer variable in each Right-Of-Way containing a SC candidate device could demand even more computational effort, but in

this formulation the utilization of the integer variables is now intrinsically linked with the direction of the circuit power flow and therefore the OPF formulation becomes more adherent to the reality and physical flow distribution through the lines.

Furthermore, only one set of the constraints (88), (89) and (92) per ROW is needed, but still one set of the constraints (90) and (91) is needed for all CSCDs in every ROW in order to cover all combinations of z_k^{n+} and z_k^{n-}. This fact is also valid for the negative and joint compensation types.

5.3.2.3 KCL for Positive Compensation

The positive series compensation presents as main objective the increase of the line susceptance and consequently the power flow increase through the existing line. As this compensation will result in a δ_{k1}^n that has the same direction of the existing line power flow f_0^n, both flows must have the same signals in the bus balance equation illustrated as follows:

$$f_{ROW}^n = f_{k0}^n + \delta_{k1}^n \tag{94}$$

5.3.2.4 Flow Limit Constraint for Positive Compensation

The existing circuit flow limit constraint (without series compensation) is presented below:

$$-\overline{f_{k0}} \le f_{k0}^n \le \overline{f_{k0}} \tag{95}$$

The above mentioned equation needs to be replaced by:

$$-\overline{f_{k0}} \le f_{k0}^n + \delta_{k1}^n \le \overline{f_{k0}} \tag{96}$$

As the SC devices are coupled in series with the line, the flow limit in the Right-Of-Way should be respected taking the CSCD into account.

5.3.2.5 Flow Existence Constraints for Positive Compensation

As the "construction" of the SC device is decided by the MIP problem, the δ_{k1}^n should exist only if the CSCD is built. Therefore, the following equations are needed:

$$\delta_{k1}^{n+} \le \overline{f_{k0}}\, v_k \tag{97}$$

$$\delta_{k1}^{n-} \le \overline{f_{k0}}\, v_k \tag{98}$$

5.3.3 Negative Compensation

For negative compensation, the line susceptance variation range will be:

$$0 \leq \gamma_{k2} \leq -\gamma_{min}^{SC} \tag{99}$$

The DC OPF formulation for the negative compensation is basically equal to the positive compensation formulation. The only differences are the aforementioned line susceptance variation range and also the inclusion of the negative compensation in the bus balance equations. The negative compensation formulation is presented below:

$$\overline{\gamma}_{k2} = -\gamma_{min}^{SC} \tag{100}$$

$$\delta_{k2}^n = \delta_{k2}^{n+} - \delta_{k2}^{n-} \tag{101}$$

$$\Delta\theta_k^n = \Delta\theta_k^{n+} - \Delta\theta_k^{n-} = \Delta\theta_{ij}^n = \theta_i^n - \theta_j^n \tag{102}$$

5.3.3.1 KVL for Negative Compensation

$$\delta_{k2}^{n+} \leq \overline{\gamma}_{k2}\Delta\theta_k^{n+} \tag{103}$$

$$\delta_{k2}^{n-} \leq \overline{\gamma}_{k2}\Delta\theta_k^{n-} \tag{104}$$

5.3.3.2 Flow Direction Unique Existence Assurance Constraints

As explained in the positive compensation section, the delta-flow δ_{k2}^n will obey the KVL only if there are constraints that ensure that only $\Delta\theta_k^{n+}$ or $\Delta\theta_k^{n-}$ is different from zero in the optimal solution of the problem. The first set of constraints proposed to outline this problem is presented below:

$$\Delta\theta_k^{n+} \leq K \times z_k^n \tag{105}$$

$$\Delta\theta_k^{n-} \leq K \times (1 - z_k^n) \tag{106}$$

$$z_k^n \in \{0,1\} \tag{107}$$

The second set of constraints proposed to outline this problem is presented below:

$$\Delta\theta_k^{n+} \leq K(1 - z_k^{n-}) \tag{108}$$

$$\Delta\theta_k^{n-} \leq K(1 - z_k^{n+}) \tag{109}$$

$$z_k^{n+} \geq \delta_{k2}^{n+}/\overline{f_{k0}} \tag{110}$$

$$z_k^{n-} \geq \delta_{k2}^{-}/\overline{f_{k0}} \tag{111}$$

$$z_k^{n+} + z_k^{n-} \leq v_k \tag{112}$$

$$z_k^{n+}, z_k^{n-} \in \{0,1\} \tag{113}$$

5.3.3.3 KCL for Negative Compensation

The negative series compensation presents as main objective the decrease of the line susceptance and consequently the power flow decrease through the existing line. As this compensation will result in a δ_{k2}^{n} that has the opposite direction of the existing line power flow f_0^n, this behavior needs to be represented in the bus balance equation as illustrated below:

$$f_{ROW}^n = f_{k0}^n - \delta_{k2}^n \tag{114}$$

5.3.3.4 Flow Limit Constraint for Negative Compensation

The flow limit constraint for negative compensation is defined as follows:

$$-\overline{f_{k0}} \leq f_{k0}^n - \delta_{k2}^n \leq \overline{f_{k0}} \tag{115}$$

5.3.3.5 Flow Existence Constraints for Negative Compensation

$$\delta_{k2}^{n+} \leq \overline{f_{k0}} \, v_k \tag{116}$$

$$\delta_{k2}^{n-} \leq \overline{f_{k0}} \, v_k \tag{117}$$

5.3.4 Joint Compensation: Positive and Negative

This section describes the DC OPF formulation for series compensation devices that are able to compensate in both directions: positive and negative. It is plausible to remind that the only device that is able to achieve a joint compensation is the Active Smart Wire (ASW) which is still being developed for market applications.

As explained in chapter 3, the series compensation devices are projected in order to compensate $X\%$ of the line reactance. So, in order to incorporate the maximum compensation level in the model, we just need to convert the maximum reactance

compensation level into a susceptance variation range. Moreover, the ASW will be projected in order to compensate the same $X\%$ in both directions and that characteristic will be contemplated by the model. On the other hand, it is worth to emphasize that the model is agnostic to the change $X\%$ be the same or different in both directions, i.e., the proposed formulation is prepared for all these situations.

For the joint compensation, the line susceptance variation range will be:

$$\gamma_{min}^{SC} \leq \gamma' \leq \gamma_{max}^{SC} \tag{118}$$

Now, the following equation needs to be represented:

$$\delta_k^n - \gamma'^n \Delta\theta_k^n = 0 \tag{119}$$

The aforementioned equation is nonlinear, because γ'^n and $\Delta\theta_k^n$ vary. Moreover, as γ'^n may now be negative, the following equation may not be directly represented:

$$|\delta_k^n| \leq \overline{\gamma}_k |\Delta\theta_k^n| \tag{120}$$

Consequently, another decomposition is needed. δ_k^n will be decomposed in two terms: a positive compensation term (δ_{k1}^n) part and a negative compensation term (δ_{k2}^n):

$$\delta_k^n = \delta_{k1}^n - \delta_{k2}^n \tag{121}$$

Where δ_{k1}^n represents the susceptance variation in the range $0 \leq \gamma_{k1} \leq \gamma_{max}^{SC}$ and δ_{k2}^n represents the susceptance variation in the range $0 \leq \gamma_{k2} \leq -\gamma_{min}^{SC}$. The end effect is that the joint compensation is nothing more than a superposition of the positive and the negative compensation:

$$\delta_k^n = \delta_{k1}^n - \delta_{k2}^n \tag{122}$$

$$\overline{\gamma}_{k1} = \gamma_{max}^{SC} \tag{123}$$

$$\delta_{k1}^n = \delta_{k1}^{n+} - \delta_{k1}^{n-} \tag{124}$$

$$\overline{\gamma}_{k2} = -\gamma_{min}^{SC} \tag{125}$$

$$\delta_{k2}^n = \delta_{k2}^{n+} - \delta_{k2}^{n-} \tag{126}$$

$$\Delta\theta_k^n = \Delta\theta_k^{n+} - \Delta\theta_k^{n-} = \Delta\theta_{ij}^n = \theta_i^n - \theta_j^n \tag{127}$$

5.3.4.1 KVL for Joint Compensation

$$\delta_{k1}^{n+} \leq \overline{\gamma}_{k1}\Delta\theta_k^{n+} \tag{128}$$

$$\delta_{k1}^{n-} \leq \overline{\gamma}_{k1}\Delta\theta_k^{n-} \tag{129}$$

$$\delta_{k2}^{n+} \leq \overline{\gamma}_{k2}\Delta\theta_k^{n+} \tag{130}$$

$$\delta_{k2}^{n-} \leq \overline{\gamma}_{k2}\Delta\theta_k^{n-} \tag{131}$$

As explained in the positive compensation section, $\overline{\gamma}_{k1}$ and $\overline{\gamma}_{k2}$ will determine the susceptance variation ranges according respectively to the positive and negative compensation, i.e., the maximum series compensation level. Accordingly, the proposed MILP formulation can be applied if $\overline{\gamma}_{k1}$ is equal to $\overline{\gamma}_{k2}$ or not.

5.3.4.2 Flow Direction Unique Existence Assurance Constraints

The first set of constraints proposed to outline this problem is presented below:

$$\Delta\theta_k^{n+} \leq K \times z_k^n \tag{132}$$

$$\Delta\theta_k^{n-} \leq K \times (1 - z_k^n) \tag{133}$$

$$z_k^n \in \{0,1\} \tag{134}$$

The second set of constraints proposed to outline this problem is presented below:

$$\Delta\theta_k^{n+} \leq K(1 - z_k^{n-}) \tag{135}$$

$$\Delta\theta_k^{n-} \leq K(1 - z_k^{n+}) \tag{136}$$

$$z_k^{n+} \geq \delta_{k1}^{n+}/\overline{f_{k0}} \tag{137}$$

$$z_k^{n-} \geq \delta_{k1}^{n-}/\overline{f_{k0}} \tag{138}$$

$$z_k^{n+} \geq \delta_{k2}^{n+}/\overline{f_{k0}} \tag{139}$$

$$z_k^{n-} \geq \delta_{k2}^{n-}/\overline{f_{k0}} \tag{140}$$

$$z_k^{n+} + z_k^{n-} \leq v_k \tag{141}$$

$$z_k^{n+}, z_k^{n-} \in \{0,1\} \tag{142}$$

It is worth noting that Appendix C which is entitled "WHY IS THE $\Delta\theta^+$ OR $\Delta\theta^-$ UNIQUE EXISTENCE ASSURANCE IMPORTANT?", also contains interesting details about these set of constraints in the case of the joint compensation.

5.3.4.3 KCL for Joint Compensation

Both compensation terms (positive and negative) are introduced in the bus balance equation as follows:

$$f_{ROW}^n = f_{k0}^n + \delta_{k1}^n - \delta_{k2}^n \tag{143}$$

5.3.4.4 Flow Limit Constraint for Joint Compensation

Both compensation terms (positive and negative) are introduced in the flow limit constraint as illustrated below:

$$-\overline{f_{k0}} \leq f_{k0}^n + \delta_{k1}^n - \delta_{k2}^n \leq \overline{f_{k0}} \tag{144}$$

5.3.4.5 Flow Existence Constraint for Joint Compensation

The effects of the CSCD for joint compensation need to be eliminated in case the CSCD is not "constructed". So, the following constraints are needed:

$$\delta_{k1}^{n+} \leq \overline{f_{k0}} v_k \tag{145}$$

$$\delta_{k1}^{n-} \leq \overline{f_{k0}} v_k \tag{146}$$

$$\delta_{k2}^{n+} \leq \overline{f_{k0}} v_k \tag{147}$$

$$\delta_{k2}^{n-} \leq \overline{f_{k0}} v_k \tag{148}$$

5.4 MILP FORMULATION OF THE SERIES COMPENSATION ATTACHED TO A CANDIDATE CIRCUIT

5.4.1 Precedence Constraint

If the CSCD is attached to a candidate line, there must be a precedence constraint that ensures that the CSCD can only be built if the line is. This equation is represented below:

$$v_k \leq x_k \tag{149}$$

5.4.2 Flow Limit Constraint – CSCD Attached to a Candidate Circuit

The flow limit constraint also needs to be altered as illustrated below:

$$-\overline{f_{k1}}x_k \leq f_{k1}^n + \delta_{k1}^n - \delta_{k2}^n \leq \overline{f_{k1}}x_k \tag{150}$$

Where:

$$f_{k1}^n = f_{k1}^{n+} + f_{k1}^{n-} \tag{151}$$

Where f_{k1}^{n+} represents the power flowing from i to j through the candidate circuit and f_{k1}^{n-} represents the power flowing from j to i.

The candidate circuit flow is formulated by the disjunctive representation based on equation (36). Furthermore, it is plausible to emphasize that the disjunctive representation does not require the separation into a positive flow f_{k1}^{n+} and a negative flow f_{k1}^{n-}. However, equation (151) shows that the candidate circuit flow is decomposed in two parts. This is done because it consists in a tighter formulation, where the linear is closer to the integer solution (tighter linear relaxation), presenting thus a smaller integrality gap and the Branch and Bound solution processing effort should be much lower [38].

5.4.3 Flow Direction Unique Existence Assurance Constraints – CSCD Attached to a Candidate Circuit

If the first or the second proposed set of constraints are used, no changes are required when the CSCD is connected to a candidate line, i.e., both may be directly applied. On the other hand, if the second set is used, another proposed improvement may be done.

As explained above, the decision to use $\Delta\theta_k^{n+}$ or $\Delta\theta_k^{n-}$ directly depends on the power flow direction in the circuit in which the CSCD is connected. In other words, if the candidate circuit flow is from i to j, $\Delta\theta_k^{n+}$ is nonzero and $\Delta\theta_k^{n-}$ is zero and if the candidate circuit flow is from j to i, $\Delta\theta_k^{n-}$ is nonzero and $\Delta\theta_k^{n+}$ is zero. Taking this information into account, this dissertation proposes also a tighter formulation to accelerate the optimal power flow model when the CSCD is attached to a candidate line:

5.4.3.1 Positive Compensation

For the positive compensation, there is a guarantee that f_{k1}^{n+} or f_{k1}^{n-} will never be greater than $\overline{f_{k1}}$. So the following set of constraints can be used:

$$\Delta\theta_k^{n+} \leq K(1 - z_k^{n-}) \tag{152}$$

$$\Delta\theta_k^{n-} \leq K(1 - z_k^{n+}) \tag{153}$$

$$z_k^{n+} \geq f_{k1}^{n+}/\overline{f_{k1}} \tag{154}$$

$$z_k^{n-} \geq f_{k1}^{n-}/\overline{f_{k1}} \tag{155}$$

$$z_k^{n+} + z_k^{n-} \leq x_k \tag{156}$$

$$z_k^{n+}, z_k^{n-} \in \{0,1\} \tag{157}$$

The candidate circuit flows f_{k1}^{n+} and f_{k1}^{n-} can directly be used instead of the CSCD flow variables (δ_{k1}^{n+} and δ_{k1}^{n-}). In other words, when the candidate circuit is added to the network, the integer variable associated to the flow direction definition for the CSCD (z_k^{n+} or z_k^{n-}), will directly be activated.

Furthermore, just one set of the aforementioned constraints is needed for every ROW, i.e., one set per ROW covers all combinations of z_k^{n+} and z_k^{n-}. This is a valuable contribution of the proposed formulation because for existing circuits, only one set of the constraints (88), (89) and (92) per ROW is needed, but still one set of the constraints (90) and (91) is needed for all CSCDs in every ROW in order to cover all combinations of z_k^{n+} and z_k^{n-}. This fact is also valid for the negative and joint compensation types.

5.4.3.2 Negative Compensation

For the negative compensation, there is no guarantee that f_{k1}^{n+} or f_{k1}^{n-} will never be greater than $\overline{f_{k1}}$, because only the resultant flow in the ROW, i.e., $f_{k1}^n - \delta_{k2}^n$, must respect the flow limit $\overline{f_{k1}}$. On the other hand, the CSCD flow (δ_{k2}^{n+} or δ_{k2}^{n-}) mathematically respects the thermal limit $\overline{f_{k1}}$, as $\overline{f_{k1}}$ represents a conservative upper bound for both flow variables. So the following set of constraints is proposed:

$$\Delta\theta_k^{n+} \leq K(1 - z_k^{n-}) \tag{158}$$

$$\Delta\theta_k^{n-} \leq K(1 - z_k^{n+}) \tag{159}$$

$$z_k^{n+} \geq f_{k1}^{n+}/2\overline{f_{k1}} \tag{160}$$

$$z_k^{n-} \geq f_{k1}^{n-}/2\overline{f_{k1}} \tag{161}$$

$$z_k^{n+} + z_k^{n-} \leq x_k \tag{162}$$

$$z_k^{n+}, z_k^{n-} \in \{0,1\} \tag{163}$$

As will be seen in the next chapter, especially in the case study entitled "3-Bus System: Negative Compensation Circuit 1-3", the circuit flows f_{k1}^{n+} and f_{k1}^{n-} can be greater than $\overline{f_{k1}}$ for the negative compensation and therefore, by multiplying $\overline{f_{k1}}$ by 2, we guarantee that the aforementioned equations (160) and (161) will not be used as a false upper bound (flow limit) by the OPF model.

5.4.3.3 Joint Compensation

Exactly the same constraints used for the negative compensation can be used for the joint compensation. This is interesting because only 5 constraints are necessary, instead of the 7 that are required when the CSCD is connected to an existing line.

Finally, it is worth to emphasize that the aforementioned enhancement cannot be applied to existing lines in the proposed formulation by this dissertation, as the existing line flows are represented by free variables (the candidate circuit flow f_{k1}^{n} is decomposed in f_{k1}^{n+} and and f_{k1}^{n-}, as explained above).

6 CASE STUDIES AND DISCUSSION OF RESULTS

6.1 INTRODUCTION

In this chapter, the proposed MILP formulations of the transmission expansion problem are applied to a number of case studies:

- The case studies of section 6.2 consist in didactic examples to illustrate the flexibility and the range of application of the proposed MILP formulations;

- Those of section 6.3 consist in a benchmark of the proposed formulation against the traditional transmission expansion planning task, i.e., Business as Usual (BAU). They enable the comparison of the solutions obtained with the proposed MILP formulation taking CSCDs into account with the BAU cases, allowing an impact analysis realization to measure the importance of power flow controllability and flexibility;

- Those of section 6.4 show the impacts on the transmission expansion planning task from a real system, the Brazilian system.

Finally, it is plausible to present that all simulations were made with an Intel Quad-Core 2.4 GHz, 64 bits with 8 GB of RAM.

6.2 CASE STUDY CS1 – 3-BUS SYSTEM: DIDACTIC EXAMPLE

This is the simplest test system, with 3 buses, 2 existing branches and 1 candidate circuit. The main objective of this didactic example is to illustrate numerically the proposed formulation and its results.

$g(1) \leq 60$
BUS_1

$\gamma(1,2) = 10$
$f(1,2) \leq 40$

$g(2) \leq 40$
BUS_2

$\gamma(1,3) = 5.556$
$f(1,3) \leq 40$

$\gamma(2,3) = 10$
$f(2,3) \leq 80$

BUS_3

$d(3) = 100$
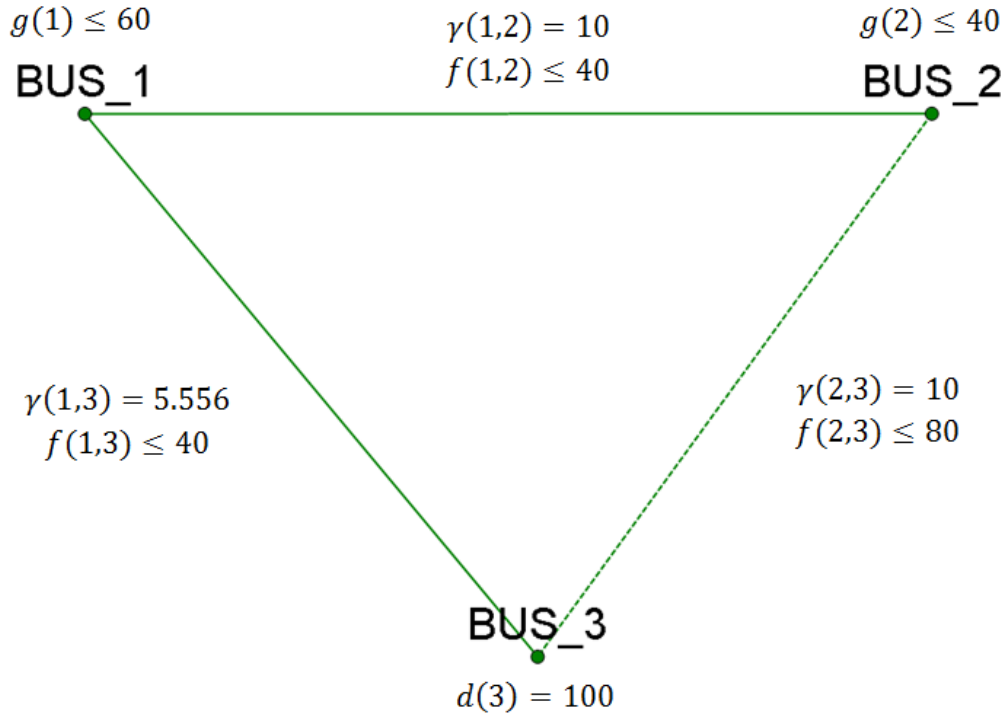
Figure 27: 3-Bus test system

Where:

$g(i)$ Generation at bus i;

$d(i)$ Load at bus i;

$\gamma(i,j)$ Transmission line between buses i and j nominal series susceptance;

$f(i,j)$ Power flow between buses i and j;

As can be seen in the figure presented above, existing transmission lines are represented through a continuous line while the candidate line is represented through a dashed line.

The first example is to show the proposed hybrid formulation by this dissertation.

6.2.1 3-Bus System: Hybrid Model Proposal for Circuit 2-3

In this example, candidate circuit 2-3 is a hybrid. The expansion planning problem is formulated as follows. In order to facilitate the interpretation by the reader, the slack variables associated to bus generations and load shed in buses without load

74

will not presented in the following equations despite being represented within the model.

$$Objective\ Function = Min\{\delta \times r(3) + c_1 \times x_1\} \tag{164}$$

Subject to:

Bus balance equations respectively for buses 1, 2 and 3**:**

$$-f(1,2) - f(1,3) = -60 \tag{165}$$

$$f(1,2) - f(2,3)^+ + f(2,3)^- = -40 \tag{166}$$

$$f(1,3) + r(3) + f(2,3)^+ - f(2,3)^- = 100 \tag{167}$$

KVL for existing circuits 1-2 and 1-3:

$$f(1,2) = 10 \times (\theta(1) - \theta(2)) \tag{168}$$

$$f(1,3) = 5.556 \times (\theta(1) - \theta(3)) \tag{169}$$

Flow limits for the existing circuit 1-2 and 1-3:

$$-40 \leq f(1,2) \leq 40 \tag{170}$$

$$-40 \leq f(1,3) \leq 40 \tag{171}$$

Angle constraint for the candidate circuit 2-3:

$$\Delta\theta(2,3) = \Delta\theta(2,3)^+ - \Delta\theta(2,3)^- \tag{172}$$

KVL upper bound for candidate circuit 2-3:

$$f(2,3)^+ \leq 10 \times \Delta\theta(2,3)^+ \tag{173}$$

$$f(2,3)^- \leq 10 \times \Delta\theta(2,3)^- \tag{174}$$

Flow direction unique existence assurance constraints for the hybrid candidate circuit 2-3:

$$z(2,3)^+ \geq f(2,3)^+ / 80 \tag{175}$$

$$z(2,3)^- \geq f(2,3)^- / 80 \tag{176}$$

$$\Delta\theta(2,3)^+ \leq K(1 - z(2,3)^-) \tag{177}$$

$$\Delta\theta(2,3)^- \leq K(1 - z(2,3)^+) \tag{178}$$

$$z(2,3)^+ + z(2,3)^- \leq x_1 \tag{179}$$

$$z(2,3)^+, z(2,3)^- \in \{0,1\}$$

Flow limit constraints for the hybrid candidate circuit 2-3:

$$f(2,3)^+ \leq 80 \times x_1 \tag{180}$$
$$f(2,3)^- \leq 80 \times x_1 \tag{181}$$

The results are presented below:

$g(1) = 60 \ MW$

$g(2) = 40 \ MW$

$d(3) = 100 \ MW$

$f(1,2) = 16 \ MW$

$f(1,3) = 40 \ MW$

$f(2,3)^+ = 56 \ MW$

$f(2,3)^- = 0 \ MW$

$r(3) = 4\ MW$

$\theta_1 = 0°$

$\theta_2 = -0{,}917°$

$\theta_3 = -4{,}125°$

$\Delta\theta(2,3)^+ = 3{,}209°$

$\Delta\theta(2,3)^- = 0°$
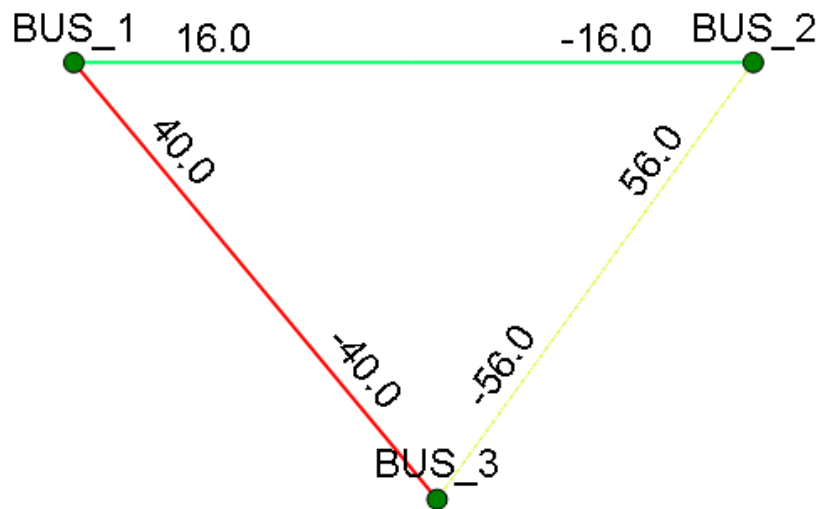
Figure 28: 3-Bus test system: power flow with the hybrid candidate circuit 2-3

As can be seen in the figure presented above, even with the addition of the proposed hybrid candidate circuit 2-3, it is still necessary to shed load (4 MW) in order to respect system operating limits.

The purpose of this example is not to eliminate all overloads and load shedding, because for those applications candidate series compensation devices (CSCDs) will be proposed. The main objective of this example is to show that the proposed hybrid formulation works properly and avoids the ill-condition that high big M constants may cause to the problem.

6.2.2 3-Bus System: Positive Compensation Circuit 1-2

If the expansion planning model is applied in the 3-Bus test system having the candidate circuit 2-3 modeled through the disjunctive representation based on equation (36), i.e., with big M constants, candidate circuit 2-3 will be added to system in order to minimize the load shed.

If we neglect the thermal limit of the lines, the resultant power flow will be as follows:
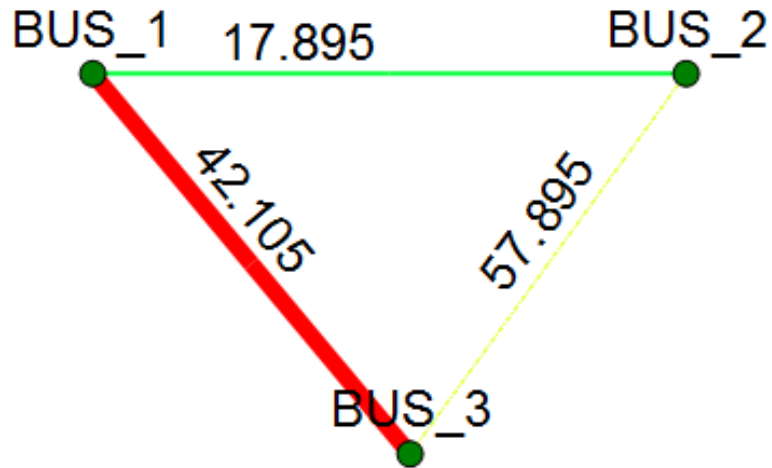
Figure 29: 3-Bus test system

The circuit power flow values are mapped in the color spectrum from blue to red, i.e., a "color scheme" is used to represent the circuit loading. Highlighted-red circuits represent overloaded circuits. As can be seen, even with circuit 2-3 in the network there is still an overload of approximately 2 MW in circuit 1-3. To solve this problem, candidate series compensation devices (CSCDs) will be proposed as follows.

First, a candidate series compensation device will be attached to circuit 1-2. This candidate only enables 50% positive compensation and is represented through a blue dashed line in the following figure:
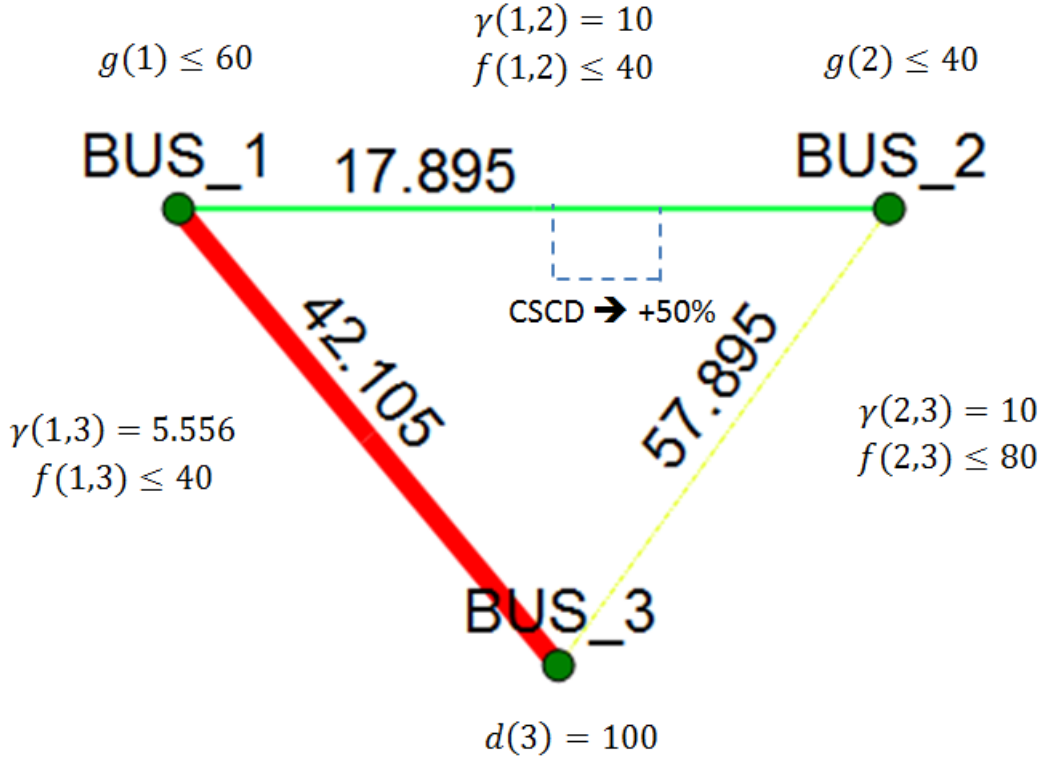
Figure 30: 3-Bus test system with positive compensation circuit 1-2

Before formulating the expansion problem, we need to calculate $\overline{\gamma}_{k1}$ regarding the compensation level:

$$X_{Min}(1,2) = X(1,2) \times (1 - Max.\ Compensation/100) \tag{182}$$

$$X_{Min}(1,2) = 0.1 \times \left(1 - \frac{50}{100}\right) = 0.05\ H \tag{183}$$

$$\gamma_{Max}(1,2) = \frac{1}{X_{Min}(1,2)} = 20\ S \tag{184}$$

$$\overline{\gamma}_{k1}(1,2) = \gamma_{Max}(1,2) - \gamma(1,2) = 20 - 10 = 10\ S \tag{185}$$

Where H represents the reactance unit $Henry$ and S represents the susceptance unit $Siemens$.

In figure 30, the power flow distribution takes into account the candidate circuit 2-3 in the network, just to show that even with this addition, there is an overload. On the other hand, the expansion planning problem will be formulated having the transmission line candidate circuit between buses 2-3 (which will be modeled through the disjunctive representation) and the Candidate Series Compensation Device (CSCD) between buses 1-2. It is worth to remember that a positive compensation, in the convention proposed

by this master thesis, represents a susceptance increase (reactance decrease) enabling consequently an increase in the transmission line power flow. Moreover, in order to facilitate the interpretation by the reader, the slack variables associated to bus generations and load shed in buses without load will not presented in the following equations.

Accordingly, the proposed MILP formulation by this dissertation is presented below.

$$Objective\ Function = Min\{\delta \times r(3) + c_1 \times x_1 + c_2 \times v_1\} \tag{186}$$

Subject to:

Bus balance equations respectively for buses 1, 2 and 3**:**

$$-f(1,2) - f(1,3) - \delta_{k1}^n(1,2)^+ + \delta_{k1}^n(1,2)^- = -60 \tag{187}$$

$$f(1,2) - f(2,3)^+ + f(2,3)^- + \delta_{k1}^n(1,2)^+ - \delta_{k1}^n(1,2)^- = -40 \tag{188}$$

$$f(1,3) + r(3) + f(2,3)^+ - f(2,3)^- = 100 \tag{189}$$

KVL for existing circuits 1-2 and 1-3:

$$f(1,2) = 10 \times (\theta(1) - \theta(2)) \tag{190}$$

$$f(1,3) = 5.556 \times (\theta(1) - \theta(3)) \tag{191}$$

Flow limits for the existing circuit 1-3:

$$-40 \le f(1,3) \le 40 \tag{192}$$

Angle constraint for the candidate circuit 2-3:

$$\Delta\theta(2,3) = \Delta\theta(2,3)^+ - \Delta\theta(2,3)^- \tag{193}$$

KVL upper bound for candidate circuit 2-3:

$$f(2,3)^+ \leq 10 \times \Delta\theta(2,3)^+ \tag{194}$$

$$f(2,3)^- \leq 10 \times \Delta\theta(2,3)^- \tag{195}$$

KVL lower bound for candidate circuit 2-3:

$$f(2,3)^+ - 10 \times \Delta\theta(2,3)^+ \geq -M(1 - x_1) \tag{196}$$

$$f(2,3)^- - 10 \times \Delta\theta(2,3)^- \geq -M(1 - x_1) \tag{197}$$

As can be seen, the candidate circuit 2-3 KVL lower bound is formulated through the disjunctive representation. For further details about the big M determination, the reader should consult Appendix B of this dissertation. Moreover, it is worth to emphasize that this formulation does not require the separation into a positive flow $f(2,3)^+$ and a negative flow $f(2,3)^-$. However, this is a tighter formulation, where the linear is closer to the integer solution, i.e., the integrality gap is smaller.

The candidate circuit flow limit constraints are:

$$f(2,3)^+ \leq 80 \times x_1 \tag{198}$$

$$f(2,3)^- \leq 80 \times x_1 \tag{199}$$

Angle constraint for the CSCD 1-2:

$$\Delta\theta(1,2) = \Delta\theta(1,2)^+ - \Delta\theta(1,2)^- \tag{200}$$

KVL for the CSCD 1-2 with $\overline{\gamma}_{k1}(1,2) = 10$:

$$\delta_{k1}^n(1,2)^+ \leq 10 \times \Delta\theta(1,2)^+ \tag{201}$$

$$\delta_{k1}^n(1,2)^- \leq 10 \times \Delta\theta(1,2)^- \tag{202}$$

Flow direction unique existence assurance constraints for the CSCD 1-2:

$$z(1,2)^+ \geq \delta_{k1}^n(1,2)^+ / 40 \tag{203}$$

$$z(1,2)^- \geq \delta_{k1}^n(1,2)^- / 40 \tag{204}$$

$$\Delta\theta(1,2)^+ \leq K(1 - z(1,2)^-) \tag{205}$$

$$\Delta\theta(1,2)^- \leq K(1 - z(1,2)^+) \tag{206}$$

$$z(1,2)^+ + z(1,2)^- \leq v_1 \tag{207}$$

$$z(1,2)^+, z(1,2)^- \in \{0,1\}$$

CSCD flow limits:

$$\delta_{k1}^n(1,2)^+ \leq 40 \times v_1 \tag{208}$$

$$\delta_{k1}^n(1,2)^- \leq 40 \times v_1 \tag{209}$$

ROW 1-2 flow limit, where ROW 1-2 is composed of the existing circuit 1-2 and the CSCD 1-2):

$$-40 \leq f_0^n + \delta_{k1}^n(1,2)^+ - \delta_{k1}^n(1,2)^- \leq 40 \tag{210}$$

The results are presented below:

$g(1) = 60 \, MW$

$g(2) = 40 \, MW$

$d(3) = 100 \, MW$

$f(1,2) = 10.303 \, MW$

$f(1,3) = 39.394 \, MW$

$\delta_{k1}^n(1,2)^+ = 10.303 \, MW$

$$\delta_{k1}^{n}(1,2)^{-} = 0 \ MW$$

$$\gamma' = 10 \ S$$

It is worth to emphasize that γ' represents the line susceptance variation $\Delta\gamma$ enabled by the series compensation.

$$Compensation \ Level = 50\%$$

$$f(2,3)^{+} = 60.606 \ MW$$

$$f(2,3)^{-} = 0 \ MW$$

$$r(3) = 0 \ MW$$

$$\theta_1 = 0.5903°$$

$$\theta_2 = 0°$$

$$\theta_3 = -3.47247°$$

$$\Delta\theta(1,2)^{+} = 0.5903°$$

$$\Delta\theta(1,2)^{-} = 0°$$

$$\Delta\theta(2,3)^{+} = 3.47247°$$

$$\Delta\theta(2,3)^{-} = 0°$$

Figure 31: 3-Bus test system: power flow with the positive compensation circuit 1-2

As can be seen in the figure presented above, the addition of the proposed CSCD in the network eliminates the overload in the circuit 1-3.

Moreover, as the MILP proposed formulation is flexible and enables the OPF to find the best compensation level setpoint for each dispatch scenario according to system conditions, it is worth to analyze the final compensation setpoint for this specific dispatch scenario. The easier way to see the end effect of the series compensation is to calculate the final susceptance and reactance of the ROW 1-2. The power flow in the equation shown below must be in p.u. and the angle in radians:

$$\gamma(1,2) = (2 * 0{,}1033)/(0{,}5903 * 0{,}01745) = 20 \ S \tag{211}$$

$$x(1,2) = \frac{1}{20} = 0{,}05 = 5\% \tag{212}$$

As can be seen, the resultant susceptance value is twice the initial and the reactance is half. So, the existing circuit 1-2 is compensated at his maximum level (50%).

In order to see if the OPF would find another compensation level under other operating conditions, while maintaining the dispatch scenario only to use the data in this example and therefore facilitating the exemplification, the following example is shown.

If the thermal limit of circuit1-2 was 20 MW instead of 40 MW, the CSCD would not be able to achieve the maximum compensation level of 50% because there would be an overload in circuit 1-2. Running the proposed expansion model with this new thermal capacity, the following results are obtained:
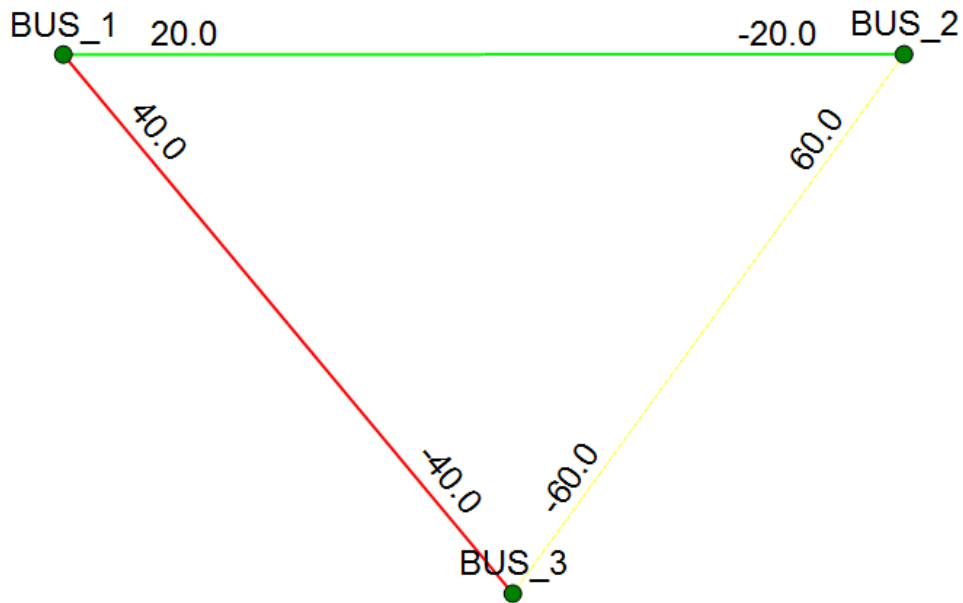
Figure 32: 3-Bus test system with positive compensation circuit 1-2 and new thermal limit for circuit 1-2

The numerical results are presented below:

$$f(1,2) = 12 \; MW$$

$$f(1,3) = 40 \; MW$$

$$\delta_{k1}^n(1,2)^+ = 8 \; MW$$

$$\delta_{k1}^n(1,2)^- = 0 \; MW$$

$$YLT(2,3)^+ = 60 \; MW$$

$$YLT(2,3)^- = 0 \; MW$$

$$\gamma' = 6.67 \; S$$

$$Compensation \; Level = 40\%$$

In this case, the angle difference between buses 1 and 2 is:

$$\Delta\theta(1,2) = 0.012 \text{ rad} = 0.687° \tag{213}$$

The flow in the ROW 1-2 is equal to:

$$f(1,2) + \delta_{k1}^n(1,2)^+ - \delta_{k1}^n(1,2)^- = 20 \text{ MW} \tag{214}$$

The existing circuit 1-2 power flow is:

$$f(1,2) = 12 \text{ MW} \tag{215}$$

The CSCD 1-2 power flow is:

$$\delta_{k1}^n(1,2)^+ = 8 \text{ MW} \tag{216}$$

So, the resultant susceptance and reactance in the ROW 1-2 respectively are:

$$\gamma(1,2) = (0.2/0.012)^\wedge - 1 = 16.666666666667 \, S \tag{217}$$

$$x(1,2) = \frac{1}{16.666666666667} = 0.06 = 6\% \tag{218}$$

The OPF model takes into account that if the circuit 1-2 is more compensated, an overload would be generated. Consequently, circuit 1-2 is 40% compensated and that is the maximum compensation that can be achieved respecting the actual system operating conditions.

6.2.3 3-Bus System: Negative Compensation Circuit 1-3

In order to solve the same overload, a candidate series compensation device (CSCD) will be attached to circuit 1-3. This candidate only enables 50% negative compensation and is represented through a blue dashed line in the following figure:
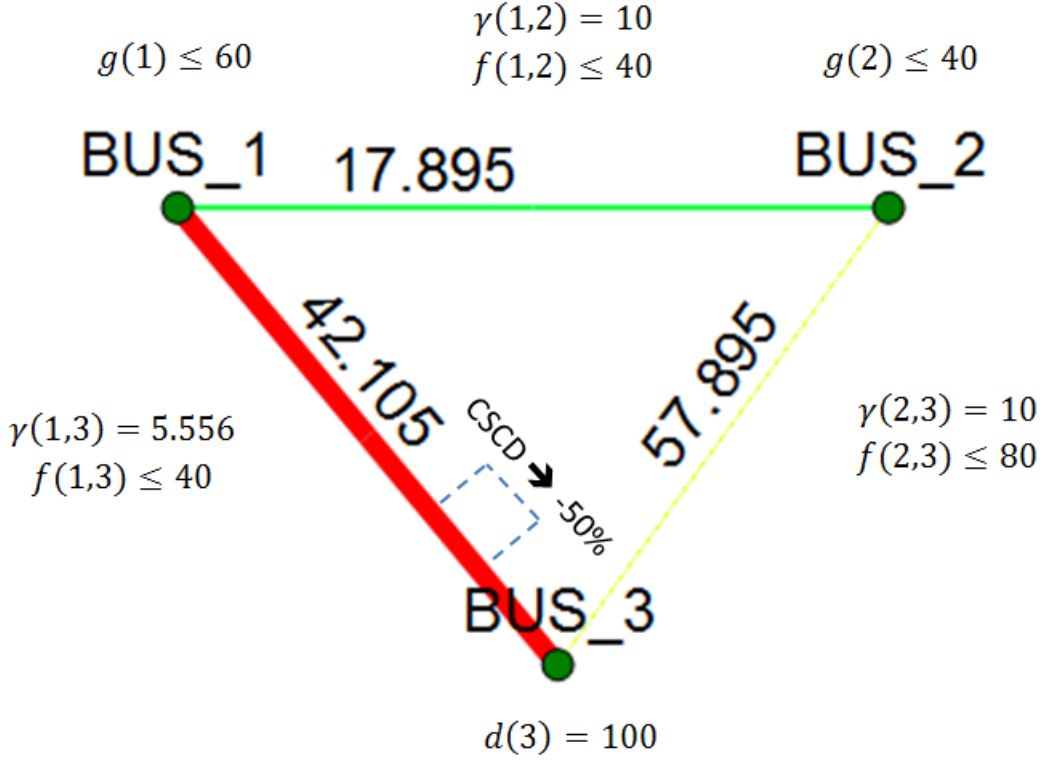
Figure 33: 3-Bus test system with positive compensation circuit 1-3

Before formulating the expansion problem, we need to calculate $\overline{\gamma}_{k2}$ regarding the compensation level:

$$X_{Max}(1,3) = X(1,3) \times (1 + Max.\ Compensation/100) \tag{219}$$

$$X_{Max}(1,3) = 0.18 \times \left(1 + \frac{50}{100}\right) = 0.27\ H \tag{220}$$

$$\gamma_{Max}(1,3) = \frac{1}{X_{Max}(1,3)} \cong 3.7\ S \tag{221}$$

$$\overline{\gamma}_{k2}(1,3) = \gamma(1,3) - \gamma_{Min}(1,3) = 5.5556 - 3.7 \cong 1.85\ S \tag{222}$$

The expansion planning problem proposed MILP formulation considering a transmission line candidate circuit between buses 2-3 and a series compensation candidate device between buses 1-3 is presented below. It is worth to remember that a negative compensation, in the convention proposed by this master thesis, represents a susceptance decrease (reactance increase) enabling consequently a decrease in the transmission line power flow.

$$Objective\ Function = Min\{\delta \times r(3) + c_1 \times x_1 + c_2 \times v_1\} \tag{223}$$

Subject to:

Bus balance equations respectively for buses 1, 2 and 3:

$$-f(1,2) - f(1,3) + \delta_{k2}^n(1,3)^+ - \delta_{k2}^n(1,3)^- = -60 \tag{224}$$

$$f(1,2) - f(2,3)^+ + f(2,3)^- = -40 \tag{225}$$

$$f(1,3) + r(3) + f(2,3)^+ - f(2,3)^- - \delta_{k2}^n(1,3)^+ + \delta_{k2}^n(1,3)^- = 100 \tag{226}$$

KVL for existing circuits 1-2 and 1-3:

$$f(1,2) = 10 \times (\theta(1) - \theta(2)) \tag{227}$$

$$f(1,3) = 5.556 \times (\theta(1) - \theta(3)) \tag{228}$$

Flow limits for the existing circuit 1-3:

$$-40 \leq f(1,3) \leq 40 \tag{229}$$

Angle constraint for the candidate circuit 2-3:

$$\Delta\theta(2,3) = \Delta\theta(2,3)^+ - \Delta\theta(2,3)^- \tag{230}$$

KVL upper bound for candidate circuit 2-3:

$$f(2,3)^+ \leq 10 \times \Delta\theta(2,3)^+ \tag{231}$$

$$f(2,3)^- \leq 10 \times \Delta\theta(2,3)^- \tag{232}$$

KVL lower bound for candidate circuit 2-3:

$$f(2,3)^+ - 10 \times \Delta\theta(2,3)^+ \geq -M(1 - x_1) \tag{233}$$

$$f(2,3)^- - 10 \times \Delta\theta(2,3)^- \geq -M(1 - x_1) \tag{234}$$

Candidate circuit flow limits:

$$f(2,3)^+ \leq 80 \times x_1 \tag{235}$$

$$f(2,3)^- \leq 80 \times x_1 \tag{236}$$

Angle constraint for the CSCD 1-3:

$$\Delta\theta(1,3) = \Delta\theta(1,3)^+ - \Delta\theta(1,3)^- \tag{237}$$

KVL for the CSCD 1-3 with $\overline{\gamma}_{k2}(1,3) = 1.851$:

$$\delta_{k2}^n(1,3)^+ \leq 1.851 \times \Delta\theta(1,3)^+ \tag{238}$$

$$\delta_{k2}^n(1,3)^- \leq 1.851 \times \Delta\theta(1,3)^- \tag{239}$$

Flow direction unique existence assurance constraints for the CSCD 1-3:

$$z(1,3)^+ \geq \delta_{k2}^n(1,3)^+ / \, 40 \tag{240}$$

$$z(1,3)^- \geq \delta_{k2}^n(1,3)^- / \, 40 \tag{241}$$

$$\Delta\theta(1,3)^+ \leq K(1 - z(1,3)^-) \tag{242}$$

$$\Delta\theta(1,3)^- \leq K(1 - z(1,3)^+) \tag{243}$$

$$z(1,3)^+ + z(1,3)^- \leq v_1 \tag{244}$$

$$z(1,3)^+, z(1,3)^- \in \{0,1\}$$

CSCD flow limits:

$$\delta_{k2}^n(1,3)^+ \leq 40 \times v_1 \tag{245}$$

$$\delta_{k2}^n(1,3)^- \leq 40 \times v_1 \tag{246}$$

ROW 1-3 flow limit, where ROW 1-3 is composed of the existing circuit 1-3 and the CSCD 1-3):

$$-40 \leq f_0^n - \delta_{k2}^n(1,3)^+ + \delta_{k2}^n(1,3)^- \leq 40 \tag{247}$$

The results are presented below:

$g(1) = 60\ MW$

$g(2) = 40\ MW$

$d(3) = 100\ MW$

$f(1,2) = 25.957\ MW$

$f(1,3) = 51.0638\ MW$

$\delta_{k2}^n(1,3)^+ = 17.0213\ MW$

$\delta_{k2}^n(1,3)^- = 0\ MW$

$\gamma' = 1.85\ S$

$Compensation\ Level = 50\%$

$f(2,3)^+ = 65.957\ MW$

$f(2,3)^- = 0\ MW$

$r(3) = 0\ MW$

$\theta_1 = 5.266°$

$\theta_2 = 3.779°$

$\theta_3 = 0°$

$\Delta\theta(1,3)^+ = 5.266°$

$\Delta\theta(1,2)^- = 0°$

$\Delta\theta(2,3)^+ = 3.779°$
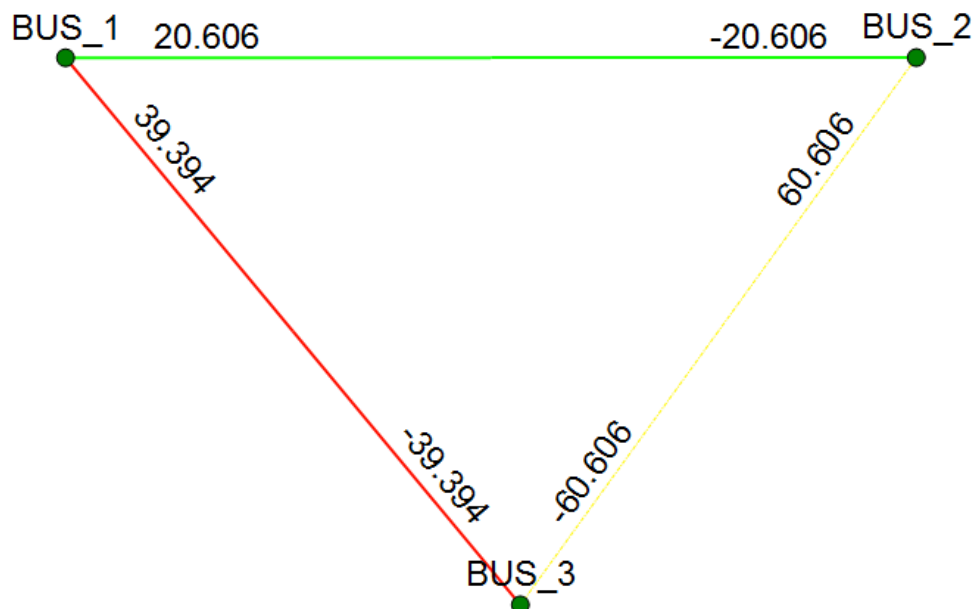
$\Delta\theta(2,3)^- = 0°$
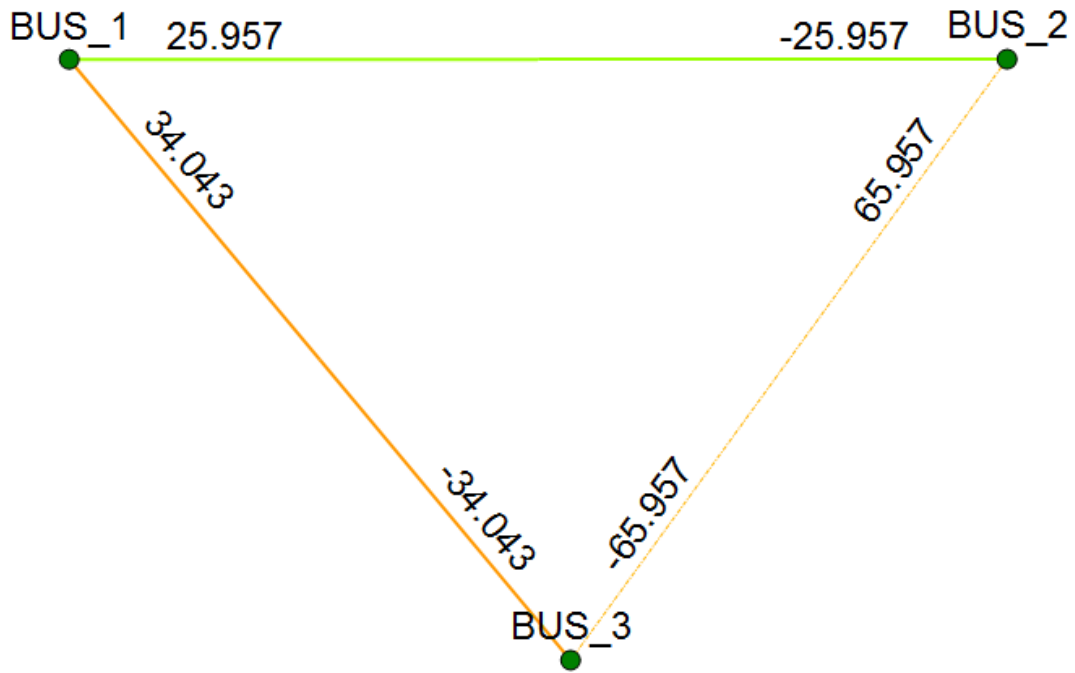
Figure 34: 3-Bus test system: power flow with the negative compensation circuit 1-3

As can be seen in the figure presented above, the addition of the proposed CSCD in the network eliminates the overload in the circuit 1-3.

Moreover, another interesting point is that the flow $f(1,3)$ exceeds $40\,MW$. This point is very important for the correct representation of the flow limit constraint (247), as well as for the correct representation of the improvement in the flow direction unique existence assurance constraints in the case of a CSCD attached to a candidate line.

6.2.4 3-Bus System: Positive Compensation Circuit 2-3

In this example, a CSCD will be attached to candidate circuit 2-3. This candidate only enables 50% positive compensation and is represented through a blue dashed line in the following figure:
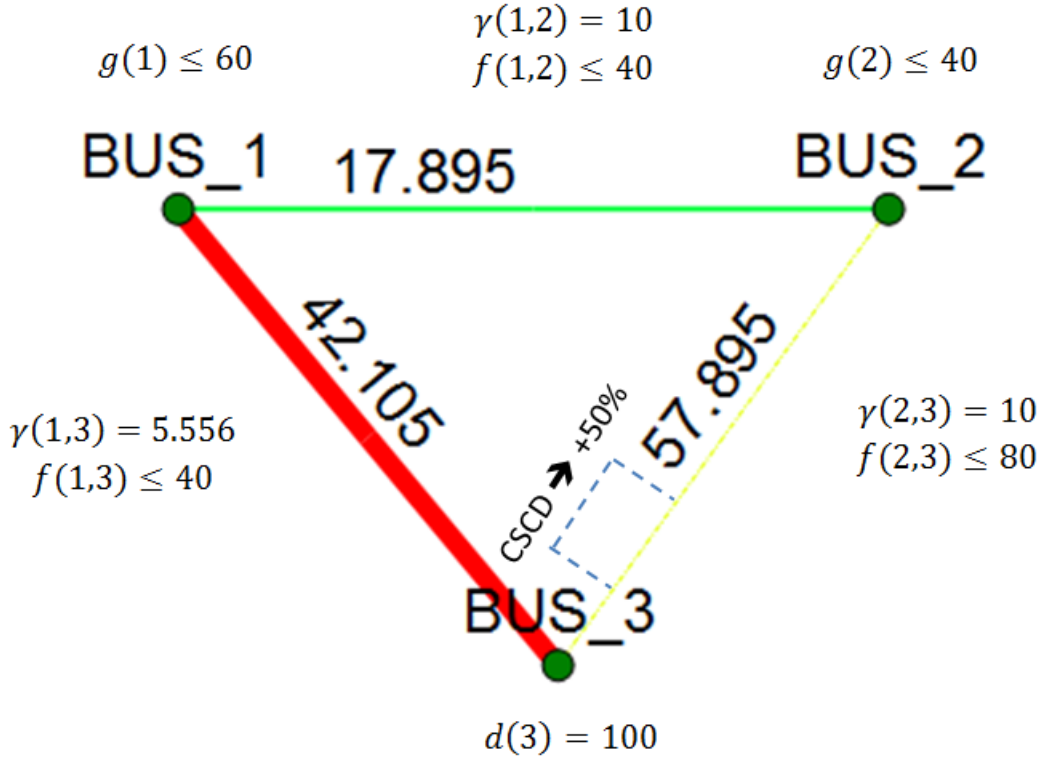
Figure 35: 3-Bus test system with positive compensation circuit 2-3

As $\gamma(1,2)$ is equal to $\gamma(2,3)$, the CSCD 2-3 has the same $\overline{\gamma}_{k1}$ as the CSCD 1-2. The expansion planning problem is formulated as follows:

$$Objective\ Function = Min\{\delta \times r(3) + c_1 \times x_1 + c_2 \times v_1\} \tag{248}$$

Subject to:

Bus balance equations respectively for buses 1, 2 and 3:

$$-f(1,2) - f(1,2) - f(1,3) = -60 \tag{249}$$

$$f(1,2) - f(2,3)^+ + f(2,3)^- - \delta_{k1}^n(2,3)^+ + \delta_{k1}^n(2,3)^- = -40 \tag{250}$$

$$f(1,3) + r(3) + f(2,3)^+ - f(2,3)^- + \delta_{k1}^n(2,3)^+ - \delta_{k1}^n(2,3)^- = 100 \tag{251}$$

KVL for existing circuits 1-2 and 1-3:

$$f(1,2) = 10 \times (\theta(1) - \theta(2)) \tag{252}$$

$$f(1,3) = 5.556 \times (\theta(1) - \theta(3)) \tag{253}$$

Flow limits for the existing circuit 1-3:

$$-40 \leq f(1,3) \leq 40 \tag{254}$$

Angle constraint for the candidate circuit 2-3:

$$\Delta\theta(2,3) = \Delta\theta(2,3)^+ - \Delta\theta(2,3)^- \tag{255}$$

KVL upper bound for candidate circuit 2-3:

$$f(2,3)^+ \leq 10 \times \Delta\theta(2,3)^+ \tag{256}$$

$$f(2,3)^- \leq 10 \times \Delta\theta(2,3)^- \tag{257}$$

KVL lower bound for candidate circuit 2-3:

$$f(2,3)^+ - 10 \times \Delta\theta(2,3)^+ \geq -M(1 - x_1) \tag{258}$$

$$f(2,3)^- - 10 \times \Delta\theta(2,3)^- \geq -M(1 - x_1) \tag{259}$$

As the angle constraint for ROW 2-3 is already represented, no additional angle constraint for the CSCD 2-3 is needed.

The KVL for the CSCD 2-3 with $\overline{\gamma}_{k1}(2,3) = 10$:

$$\delta_{k1}^n(2,3)^+ \leq 10 \times \Delta\theta(2,3)^+ \tag{260}$$

$$\delta_{k1}^n(2,3)^- \leq 10 \times \Delta\theta(2,3)^- \tag{261}$$

Flow direction unique existence assurance constraints for the CSCD 2-3:

$$z(2,3)^+ \geq f(2,3)^+ / \overline{f_{1k}} \tag{262}$$

$$z(2,3)^- \geq f(2,3)^- / \overline{f_{1k}} \tag{263}$$

$$\Delta\theta(2,3)^+ \leq K(1 - z(2,3)^-) \tag{264}$$

$$\Delta\theta(2,3)^- \leq K(1 - z(2,3)^+) \tag{265}$$

$$z(2,3)^+ + z(2,3)^- \leq x_1 \tag{266}$$

$$z(2,3)^+, z(2,3)^- \in \{0,1\}$$

As explained in the previous chapter, as the candidate transmission line 2-3 already defines power flow direction of the ROW 2-3, equations (262) and (263) can directly be represented using the candidate circuit 2-3 power flow.

CSCD flow limits:

$$\delta_{k1}^n(2,3)^+ \leq 80 \times v_1 \tag{267}$$

$$\delta_{k1}^n(2,3)^- \leq 80 \times v_1 \tag{268}$$

ROW 2-3 flow limit, where ROW 2-3 is composed of the candidate circuit 2-3 and the CSCD 2-3:

$$f(2,3)^+ + \delta_{k1}^n(2,3)^+ \leq 80 \times x_1 \tag{269}$$

$$f(2,3)^- + \delta_{k1}^n(2,3)^- \leq 80 \times x_1 \tag{270}$$

Finally, the precedence constraint is presented below:

$$v_1 \leq x_1 \tag{271}$$

The results are presented below:

$$g(1) = 60 \; MW$$

$$g(2) = 40 \; MW$$

$d(3) = 100\ MW$

$f(1,2) = 26.667\ MW$

$f(1,3) = 33.333\ MW$

$f(2,3)^+ = 33.333\ MW$

$f(2,3)^- = 0\ MW$

$\delta_{k1}^n(2,3)^+ = 33.333\ MW$

$\delta_{k1}^n(2,3)^- = 0\ MW$

$\gamma' = 10\ S$

$Compensation\ Level = 50\%$

$r(3) = 0\ MW$

$\theta_1 = 3.438°$

$\theta_2 = 1.910°$

$\theta_3 = 0°$

$\Delta\theta(2,3)^+ = 1.910°$

$\Delta\theta(2,3)^- = 0°$
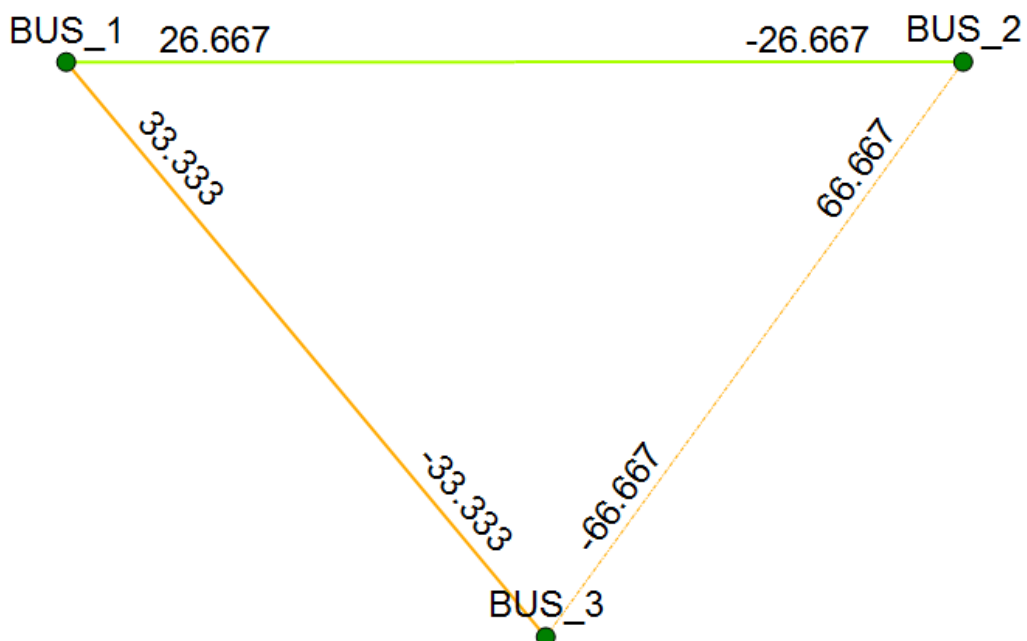
Figure 36: 3-Bus test system: power flow with the positive compensation circuit 2-3

As can be seen in the figure presented above, the addition of the proposed CSCD in the network eliminates the overload in the circuit 1-3.

6.2.5 3-Bus System: Joint Compensation Circuit 1-2

A candidate series compensation device will be attached to circuit 1-2. This candidate enables 50% joint compensation (positive and negative).

Before formulating the expansion problem, we need to calculate $\overline{\gamma}_{k1}$ and $\overline{\gamma}_{k2}$ regarding the compensation levels. $\overline{\gamma}_{k1}$ was already calculated for the positive compensantion circuit 1-2 and is equal to 10. Just $\overline{\gamma}_{k2}$ needs to be calculated as follows:

$$X_{Max}(1,2) = X(1,2) \times (1 + Max.\ Compensation/100) \tag{272}$$

$$X_{Max}(1,2) = 0.1 \times \left(1 + \frac{50}{100}\right) = 0.15\ H \tag{273}$$

$$\gamma_{Min}(1,2) = \frac{1}{X_{Max}(1,2)} \cong 6.667\ S \tag{274}$$

$$\overline{\gamma}_{k2}(1,2) = \gamma(1,2) - \gamma_{Min}(1,2) = 10 - 6.667 = 3.333\ S \tag{275}$$

The MILP formulation for joint compensation proposed by this dissertation is presented below.

$$Objective\ Function = Min\{\delta \times r(3) + c_1 \times x_1 + c_2 \times v_1\} \tag{276}$$

Subject to:

Bus balance equations respectively for buses 1, 2 and 3**:**

$$-f(1,2) - f(1,3) - \delta_{k1}^n(1,2)^+ + \delta_{k1}^n(1,2)^- + \delta_{k2}^n(1,2)^+ - \delta_{k2}^n(1,2)^- = -60 \tag{277}$$

$$f(1,2) - f(2,3)^+ + f(2,3)^- + \delta_{k1}^n(1,2)^+ - \delta_{k1}^n(1,2)^- - \delta_{k2}^n(1,2)^+ + \delta_{k2}^n(1,2)^- = -40 \tag{278}$$

$$f(1,3) + r(3) + f(2,3)^+ - f(2,3)^- = 100 \tag{279}$$

KVL for existing circuits 1-2 and 1-3:

$$f(1,2) = 10 \times (\theta(1) - \theta(2)) \tag{280}$$

$$f(1,3) = 5.556 \times (\theta(1) - \theta(3)) \tag{281}$$

Flow limits for the existing circuit 1-3:

$$-40 \leq f(1,3) \leq 40 \tag{282}$$

Angle constraint for the candidate circuit 2-3:

$$\Delta\theta(2,3) = \Delta\theta(2,3)^+ - \Delta\theta(2,3)^- \tag{283}$$

KVL upper bound for candidate circuit 2-3:

$$f(2,3)^+ \leq 10 \times \Delta\theta(2,3)^+ \tag{284}$$

$$f(2,3)^- \leq 10 \times \Delta\theta(2,3)^- \tag{285}$$

KVL lower bound for candidate circuit 2-3:

$$f(2,3)^+ - 10 \times \Delta\theta(2,3)^+ \geq -M(1 - x_1) \tag{286}$$

$$f(2,3)^- - 10 \times \Delta\theta(2,3)^- \geq -M(1 - x_1) \tag{287}$$

Candidate circuit flow limits:

$$f(2,3)^+ \leq 80 \times x_1 \tag{288}$$

$$f(2,3)^- \leq 80 \times x_1 \tag{289}$$

Angle constraint for the CSCD 1-2:

$$\Delta\theta(1,2) = \Delta\theta(1,2)^+ - \Delta\theta(1,2)^- \tag{290}$$

KVL for the CSCD 1-2 with $\overline{\gamma}_{k1}(1,2) = 10$ and $\overline{\gamma}_{k2}(1,2) = 3.333$:

$$\delta_{k1}^n(1,2)^+ \leq 10 \times \Delta\theta(1,2)^+ \tag{291}$$

97

$$\delta_{k1}^n(1,2)^- \le 10 \times \Delta\theta(1,2)^- \tag{292}$$

$$\delta_{k2}^n(1,2)^+ \le 3.333 \times \Delta\theta(1,2)^+ \tag{293}$$

$$\delta_{k2}^n(1,2)^- \le 3.333 \times \Delta\theta(1,2)^- \tag{294}$$

Flow direction unique existence assurance constraints for the CSCD 1-2:

$$z(1,2)^+ \ge \delta_{k1}^n(1,2)^+/40 \tag{295}$$

$$z(1,2)^- \ge \delta_{k1}^n(1,2)^-/40 \tag{296}$$

$$z(1,2)^+ \ge \delta_{k2}^n(1,2)^+/40 \tag{297}$$

$$z(1,2)^- \ge \delta_{k2}^n(1,2)^-/40 \tag{298}$$

$$\Delta\theta(1,2)^+ \le K(1 - z(1,2)^-) \tag{299}$$

$$\Delta\theta(1,2)^+ \le K(1 - z(1,2)^+) \tag{300}$$

$$z(1,2)^+ + z(1,2)^- \le v_1 \tag{301}$$

$$z(1,2)^+, z(1,2)^- \in \{0,1\}$$

CSCD flow limits:

$$\delta_{k1}^n(1,2)^+ \le 40 \times v_1 \tag{302}$$

$$\delta_{k1}^n(1,2)^- \le 40 \times v_1 \tag{303}$$

$$\delta_{k2}^n(1,2)^+ \leq 40 \times v_1 \tag{304}$$

$$\delta_{k2}^n(1,2)^- \leq 40 \times v_1 \tag{305}$$

ROW 1-2 flow limit, where ROW 1-2 is composed of the existing circuit 1-2 and the CSCD 1-2):

$$-40 \leq f_0^n + \delta_{k1}^n(1,2)^+ - \delta_{k1}^n(1,2)^- - \delta_{k2}^n(1,2)^+ + \delta_{k2}^n(1,2)^- \leq 40 \tag{306}$$

The results are presented below:

$g(1) = 60\ MW$

$g(2) = 40\ MW$

$d(3) = 100\ MW$

$f(1,2) = 12\ MW$

$f(1,3) = 40\ MW$

$\delta_{k1}^n(1,2)^+ = 8\ MW$

$\delta_{k1}^n(1,2)^- = 0\ MW$

$\delta_{k2}^n(1,2)^+ = 0\ MW$

$\delta_{k2}^n(1,2)^- = 0\ MW$

$\gamma' = 6.67\ S$

$Compensation\ Level = 40\%$

$f(2,3)^+ = 60\ MW$

$f(2,3)^- = 0\ MW$

$r(3) = 0\ MW$

$\theta_1 = 0.687°$

$\theta_2 = 0°$

$\theta_3 = -3.478°$

$\Delta\theta(1,2)^+ = 0.687°$

$$\Delta\theta(1,2)^- = 0°$$

$$\Delta\theta(2,3)^+ = 3.478°$$

$$\Delta\theta(2,3)^- = 0°$$

As can be seen in the figure presented above, the addition of the proposed CSCD in the network eliminates the overload in the circuit 1-3.

Moreover, it can be seen that the optimal solution found with the joint compensation in the circuit 1-2 differs from the optimal solution found with the positive compensation formulation. As the proposed has a power flow flexibility and finds an operation setpoint within the compensation range, there might be multiple feasible solutions.

In order to verify if the proposed joint compensation formulation is correct, the optimal solution found with the positive compensation formulation was implemented taking the joint compensation formulation into account, because it must also be a feasible solution and it proved to be.

6.2.6 3-Bus System: Joint Compensation Circuit 1-3

After presenting the formulation of joint compensation for the circuit 1-2, the extension of this formulation to the CSCD 1-3 is intuitive and straightforward. Therefore, in this section, only the results will be presented:

$$g(1) = 60 \; MW$$

$$g(2) = 40 \; MW$$

$$d(3) = 100 \; MW$$

$$f(1,2) = 25.957 \; MW$$

$$f(1,3) = 51.063 \; MW$$

$$\delta_{k2}^n(1,3)^+ = 0 \; MW$$

$$\delta_{k2}^n(1,3)^- = 0 \; MW$$

$$\delta_{k2}^n(1,3)^+ = 17.021 \; MW$$

$$\delta_{k2}^n(1,3)^- = 0 \; MW$$

$$\gamma' = 1.85 \; S$$

$Compensation\ Level = 50\%$

$f(2,3)^+ = 65.957\ MW$

$f(2,3)^- = 0\ MW$

$r(3) = 0\ MW$

$\theta_1 = 5.263°$

$\theta_2 = 3.779°$

$\theta_3 = 0°$

$\Delta\theta(1,3)^+ = 5.266°$

$\Delta\theta(1,3)^- = 0°$

$\Delta\theta(2,3)^+ = 3.779°$

$\Delta\theta(2,3)^- = 0°$

As can been by analyzing the results, the power flow distribution in the network is exactly the same as for the CSCD 1-3 when only negative compensation is allowed.

6.2.7 3-Bus System: Joint Compensation Circuit 2-3

After presenting the formulation of joint compensation for the circuit 1-2, the extension of this formulation to the CSCD 2-3 is intuitive and straightforward. Only one detail about the formulation for a joint compensation candidate should be emphasized when it is connected to a candidate circuit. As explained in the previous chapter, the candidate circuit already determines the flow direction and the flow direction constraints can directly use the candidate circuit power flow. On the other hand, his flow can be greater than $\overline{f_{1k}}$ for the negative compensation and therefore, the following constraints should be represented:

$$z(1,2)^+ \geq f(2,3)^+ / 2\overline{f_{1k}} \tag{307}$$

$$z(1,2)^- \geq f(2,3)^- / 2\overline{f_{1k}} \tag{308}$$

Only two flow direction constraints are needed instead of four equations, i.e., (302), (303), (304) and (305), as shown for the joint compensation circuit 1-2. Taking this detail into account the results can directly be presented:

$g(1) = 60\ MW$

$g(2) = 40\ MW$

$d(3) = 100\ MW$

$f(1,2) = 26.667\ MW$

$f(1,3) = 33.333\ MW$

$f(2,3)^+ = 33.333\ MW$

$f(2,3)^- = 0\ MW$

$\delta_{k1}^n(2,3)^+ = 33.333\ MW$

$\delta_{k1}^n(2,3)^- = 0\ MW$

$\delta_{k2}^n(2,3)^+ = 0\ MW$

$\delta_{k2}^n(2,3)^- = 0\ MW$

$\gamma' = 10\ S$

$Compensation\ Level = 50\%$

$r(3) = 0\ MW$

$\theta_1 = 3.438°$

$\theta_2 = 1.910°$

$\theta_3 = 0°$

$\Delta\theta(2,3)^+ = 1.910°$

$\Delta\theta(2,3)^- = 0°$

As can been by analyzing the results, the power flow distribution in the network is exactly the same as for the CSCD 2-3 when only positive compensation is allowed.

6.3 TEST SYSTEM TS2 – IEEE-24BUS SYSTEM – BENCHMARK EXAMPLE

The IEEE24-Bus system is a test system developed for testing on electrical power systems and presents originally 24 buses, 41 circuits and a load of 8550 MW [49], [50]. The data of the existing and candidate circuits and also the four dispatch scenarios G1, G2, G3 and G4 that will be used in this dissertation were taken from [50].

In order to make the test system even more interesting for the proposed applications, new transmission corridors were generated, i.e., to further increase the number of new candidate right-of-ways in addition to the ones presented in references [49] and [50], the existing circuits between buses 11-13, 16-19, 17-22, 15-21, 12-23, 10-11 and 9-12 were removed, i.e., they turned to be candidate circuits. The configuration of the system under analysis, i.e., the network topology containing existing (solid lines) and candidates (dashed lines) circuits is shown below:
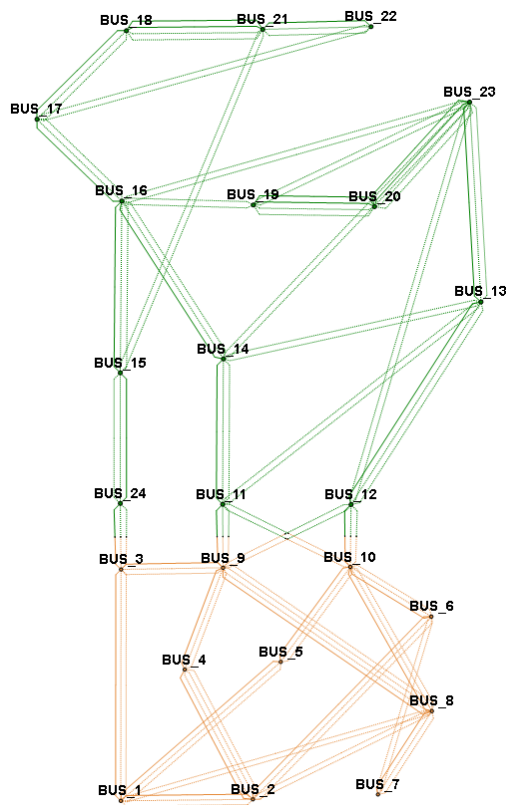
Figure 37: IEEE24-Bus test system under analysis

As can be seen, the system displays 30 existing circuits and 84 candidate circuits 56 being circuit duplication and 28 present in 14 new ROWs. The input data for TS2 is

presented in Appendix D. The green and orange colors are just to differentiate the low and high voltage areas of the system.

First, the transmission expansion planning task will be realized for the TS2 based on the Business As Usual (BAU) approach, i.e., only traditional candidate circuits can be built (transmission lines and transformers).

6.3.1 Expansion Plans Found with the BAU Approach

In order to verify the need for different works for each scenario order (G1, G2, G3 and G4), the proposed model was run for the four dispatch scenarios individually. The figures below consist of the optimal expansion plans found for each scenario, in which the existing circuits are solid lines and the circuits that compose the expansion plan are dashed lines. In addition to that, the net injections of each bus ($g^n - d^n$) are also presented:
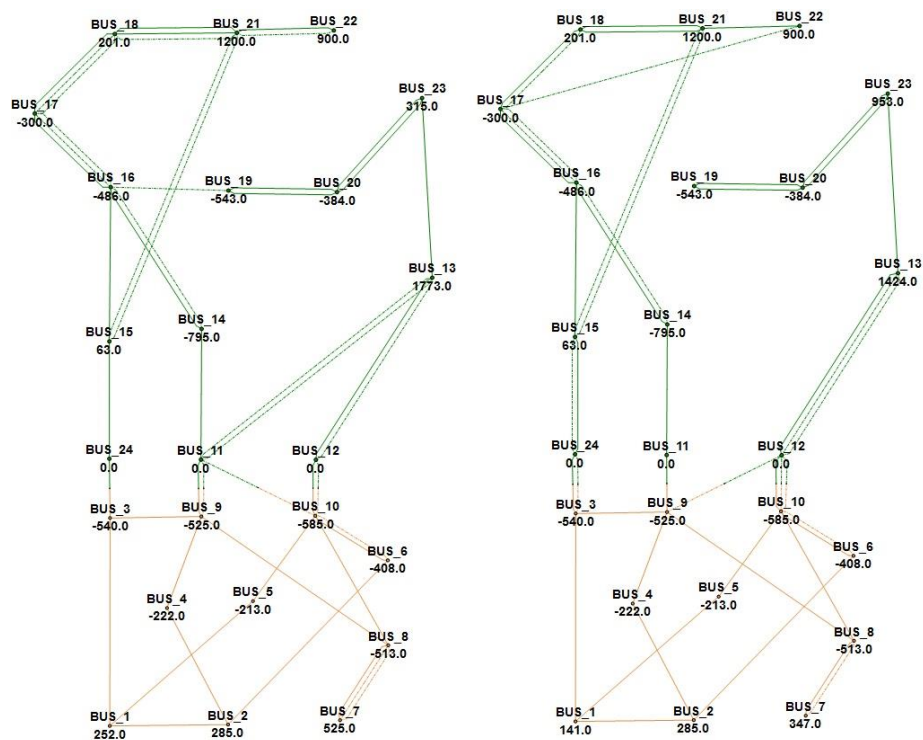
Figure 38: a) G1 plan and b) G2 plan
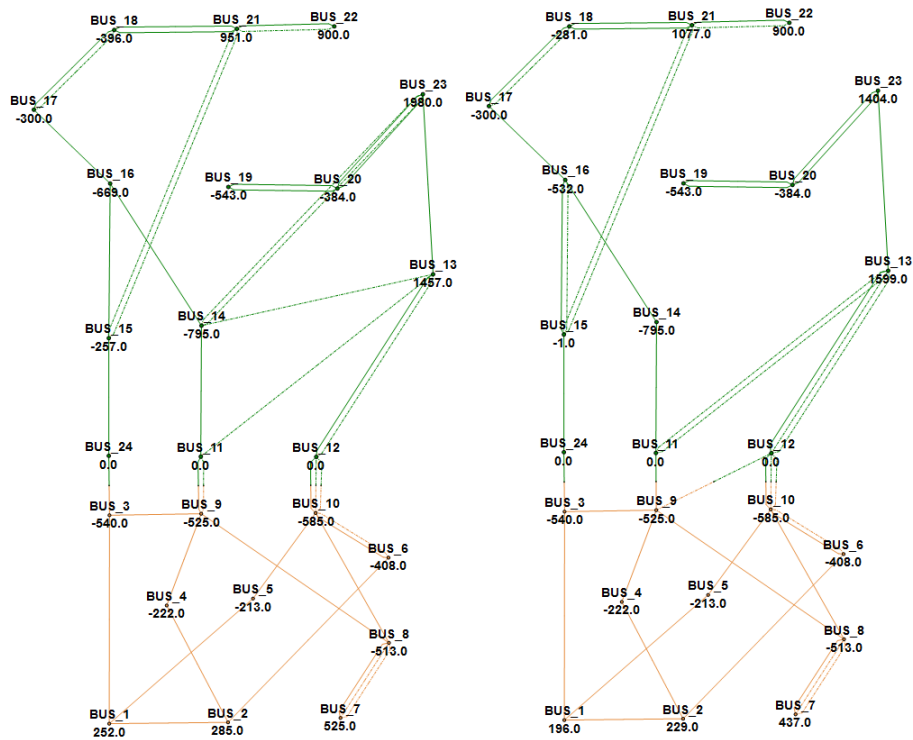
Figure 39: a) G3 plan and b) G4 plan

As can be seen, the network topology of the solutions is different and involves also different levels of investment for each scenario. To emphasize this statement, the total cost of the expansion plans for each scenario (sum of the cost of the circuits), as well as the system average loading are presented in the table below:

Table 3: BAU case – expansion plans for a single dispatch scenario

Scenario	G1	G2	G3	G4
Total Line Additions	16	12	12	12
Total Transformer Additions	3	4	3	3
Total Circuit Additions	19	16	15	15
Expansion Plan Cost [M$]	860	864	814	736
Expansion Plan Cost [%]	117%	117%	111%	100%
CPU Time [Seconds]	5	4	8	4

It can be seen that the expansion plan for the G4 scenario (G4 plan) has the lowest total cost. The G1 plan and G2 plan are approximately 17% more expensive than the G4 plan and finally, the G3 plan is 11%.

Now, the issue associated of having multiple dispatch scenarios will be presented. In this case the expansion model should find a robust plan that meets all

constraints of the problem for the four different dispatch scenarios simultaneously. The resulting expansion plan is shown in the following figure and table.
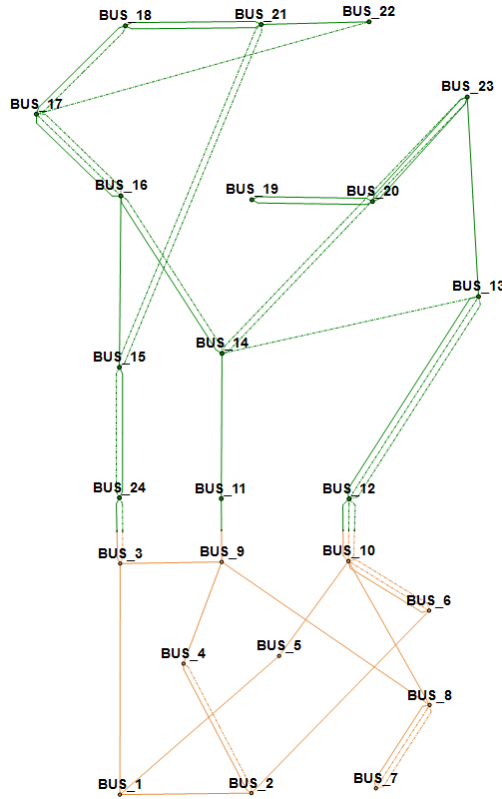
Figure 40: Robust expansion plan for the TS2

Table 4: BAU case – robust expansion plan for all dispatch scenarios

Scenario	All Dispatch Scenarios
Total Line Additions	18
Total Transformer Additions	3
Total Circuit Additions	21
Expansion Plan Cost [M$]	1113
Expansion Plan Cost [%]	151%
CPU Time [Seconds]	520

The total cost of this plan is 1113 million dollars, about 51% more expensive than the plan found only for the G4 scenario, i.e., the least cost expansion plan taking into account just one dispatch scenario. A table specifying which lines and transformers that are part of the robust expansion plan is present in Appendix D of this dissertation.

Another interesting point plausible to present is the system average loading according to each plan:

Table 5: BAU case – network loading

Scenario	G1	G2	G3	G4	Average
Exp. Plan for Single Dispatch Scenario [%]	69.5%	72.8%	70.0%	74.9%	71.8%
Robust Expansion Plan [%]	69.8%	67.2%	62.2%	62.2%	65.3%

The system average loading is equal to 65.3% for the robust expansion plan, i.e., there was a 9% reduction. As would be expected, there was a reduction in the network utilization in comparison to the plans obtained for a single dispatch scenario. With the exception of the G1 plan whose loading was practically the same, there was a percentage reduction in the level of network utilization, respectively equal to 7.6%, 11.1% and 17.0% for G2, G3 and G4 dispatch scenarios.

6.3.2 Expansion Plans Found with CSCDs

As the TS2 is named as benchmark example, the main objective of this test system is to emphasize the technical and economic effects of the proposed methodology. Therefore, a CSCD with 50% maximum compensation level will be attached to all existing and candidate transmission lines with a low cost (1 k$) so that the maximum possible number of CSCDs are added to the expansion plan. Accordingly, in addition to the 84 candidate circuits, there will also be 101 CSCDs attached to transmission lines (27 existing and 74 candidate ones). For these applications, the joint compensation will be chosen, because it consists in the combination of the positive and the negative compensation types and consequently more representative effects are expected.

This case study will be titled BAU + CSCD case. The expansion plans found with CSCDs are shown in the table below. It is worth noting that the results presented in the row "Expansion Plan Cost [%]" for the BAU case had as reference the least cost expansion plan taking into account only a single dispatch scenario, i.e., the G4 plan. When CSCDs are also considered, the reference for each cell of this row is the expansion plan cost from the BAU case taking into account the same dispatch scenario, i.e., for the dispatch scenario G1, the reference cost will be 860 M$, for G2, 864 M$ and so on. This fact is also true when all dispatch scenarios are considered.

Table 6: BAU + CSCD case – expansion plans

Scenario	G1	G2	G3	G4	All Scenarios
Total Line Additions	13	12	12	11	18
Total Transformer Additions	3	3	2	3	3
Total Circuit Additions	16	15	14	14	21
Total CSCD Additions	8	8	12	4	15
Expansion Plan Cost [M$]	790	796	720	728	972
Expansion Plan Cost [%]	92%	92%	88%	99%	87%
CPU Time [Seconds]	305	33	179	10	5266

It is worth to remember that a table specifying which lines, transformers and CSCDs that are part of the expansion plan is also present in Appendix D of this dissertation.

It can be seen that that the expansion plans from the BAU + CSCD case result in cost savings in all situations in relation to the BAU case. Although the number of circuit additions taking into account all dispatch scenarios is the same for the BAU case and the BAU + CSCD case, only 15 circuits (2 transformers and 13 lines) are in both expansion plans. So, when CSCDs are taken into account, the decision of which new circuits should be built is changed and cost savings occur.

It is also plausible to emphasize the impact that the integer variables associated with the flow direction unique existence assurance constraints cause to the computational time required, because each dispatch scenario demands a set of them and the higher the number of scenarios considered, the greater the number of integer variables and therefore the greater the computational time required.

Furthermore, one of the main advantages of the proposed formulation is the power flow flexibility, i.e., the series compensation devices have a specific operating setpoint according to each dispatch scenario and operating conditions, i.e, more representative effects are expected when more than one dispatch scenario are taken into account. As can be seen from the expansion plan robust for all dispatch scenarios, the number of CSCD additions is greater than the number of additions of all plans associated to a single dispatch scenario. Accordingly, the power flow controllability and flexibility is more demanded when more than one dispatch scenario is considered.

More than observing the cost savings, another interesting point to deeply analyze is the power flow flexibility enable by the series compensation devices. Therefore, taking the expansion plan for all dispatch scenarios, the operating setpoint

(compensation level) from all series compensation devices will be shown in each specific dispatch scenario. In addition to the compensation level, the plus (+) or the negative (-) signs will be shown in front of the number to indicate the type of compensation used in each operational situation. When no value is shown, it means that the compensation level is zero. The presented values are also mapped in the color spectrum from green (-50%) to red (+50%), i.e., a "color scale" is used to represent the compensation level.

Table 7: BAU + CSCD case – operating setpoints according to each dispatch scenario

Bus From	Bus To	Circuit #ID	CSCD #ID	G1	G2	G3	G4
1	3	1	5	-7%	+50%	+50%	
1	5	1	5		-50%		
2	4	1	5	-11%	+50%		
2	6	1	5		-50%	-50%	-50%
3	9	1	5		+49%		
5	10	1	5		+50%	+50%	
8	9	1	5		-50%	+50%	
8	10	1	5		+50%		
11	14	1	5		+45%	-46%	
13	23	1	5		+50%	+50%	
14	16	1	5	+40%	+50%	+50%	+46%
15	16	1	5		+50%		
15	21	1	5		-50%		
15	24	1	5	-27%	-25%		-25%
14	16	2	6		+50%	+50%	

The results presented in the table above highlight the power flow flexibility enabled by the proposed formulation and also the potential of the joint compensation which further motivates intense research to develop commercially available Distributed Series Compensators (DSCs).

Finally, it is worth to compare the system average loading between the BAU case and the BAU + CSCD case. This comparison is summarized in the tables presented below. The first table compares the system average loading between the expansion plans when a single dispatch scenario is considered in both cases and the second table compares the loading when all dispatch scenarios are considered in both cases.

Table 8: Network loading – expansion plans found for a single dispatch scenario

Single Dispatch Scenario	G1	G2	G3	G4	Average
BAU Case Network Loading [%]	69.5%	72.8%	70.0%	74.9%	71.8%
BAU + CSCD Case Network Loading [%]	72.6%	76.8%	70.3%	72.8%	73.1%

Table 9: Network loading – expansion plans found for all dispatch scenarios

All Dispatch Scenarios	G1	G2	G3	G4	Average
BAU Case Network Loading [%]	69.8%	67.2%	62.2%	62.2%	65.3%
BAU + CSCD Case Network Loading [%]	67.3%	70.9%	65.9%	65.7%	67.5%

As would be expected, there was an increase in the network utilization in comparison to the plans obtained in the BAU case, i.e., the network average loading is higher when CSCDs are taken into account.

The next test system shows a real and practical application of the proposed formulation.

6.4 TEST SYSTEM TS3 – THE BRAZILIAN SYSTEM – NORTHEAST SYSTEM EXPANSION

The test system 3 is based on a real network, the Brazilian system. The main objective of this test system is to analyze the practical impacts that power flow controllability and flexibility bring to the transmission expansion planning task.

As the Brazilian system presents huge dimensions, one of the four regions should be chosen: south, southeast, north and northeast. The Northeast Region was chosen for the analysis because (i) it is the region with major load growth, (ii) it contains important hydro plants in the region (Paulo Afonso, Xingó, Sobradinho, etc.) and (iii) it contains the regions with most of the technical and economic wind potential as can be seen in chapter 2 of this dissertation. The full Brazilian system and the Northeast Region are shown in Figures 3-a) and 3-b) respectively. The configuration under analysis is December 2016 (5822 buses and 8432 circuits) and the network data were obtained from [51], prepared by the ISO.
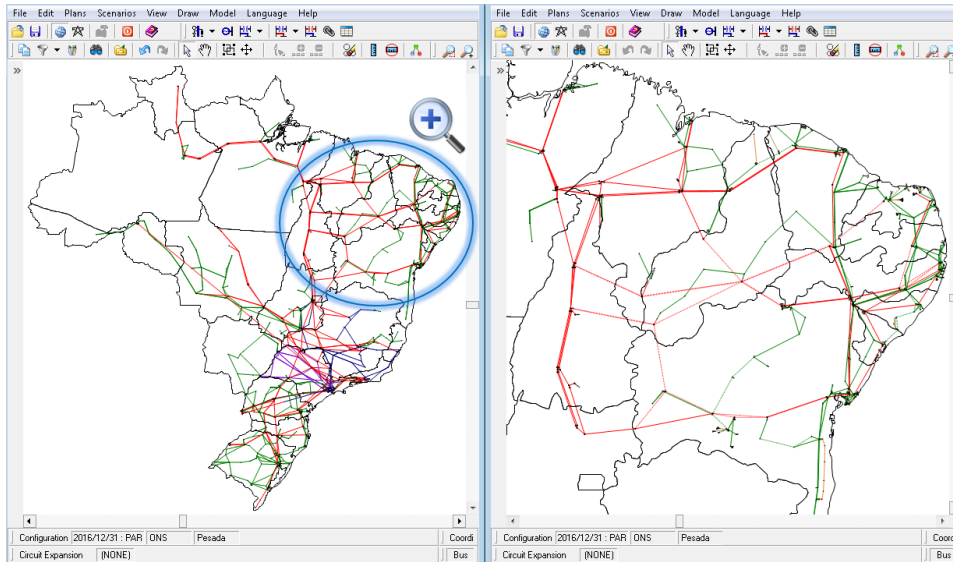
Figure 41: a) Brazilian System and b) Northeast Equivalent System

Before analyzing the Northeast Region, it is necessary to calculate the dispatches for each power plant in the whole Brazilian system for each scenario to be considered. To do so, a simulation called Stochastic Optimization of Multireservoir Hydroelectric System was performed using the SDDP$^{®}$ model with the Data Base obtained from [52], also prepared by the ISO.

Stochastic Dual Dynamic Programming (SDDP) is a commercial simulation tool developed by PSR (website: www.psr-inc.com) that is capable of calculating the minimum cost stochastic operating policy of a hydrothermal system considering operating details of the power plants and transmission system as well as constraints on natural gas supply and stochastic hydrology inflows.

The SDDP considers dispatches generation over a multi-year period while enforcing area interchange limits. In addition to providing power plant dispatches, this simulation provides the data to reduce the system to the Northeast Region, thus reducing the computational effort of the case study analysis.

6.4.1 Dispatch Scenario Selection

In order to consider the variability of generation dispatches in the transmission planning process for the Northeast region, the differences between intra-region dispatches and self-sufficiency of the region's generation are important.

Therefore, having all dispatch scenarios resulting from the SDDP$^{®}$ execution, five were selected according to the following criterion: k-th percentile of the total

northeast generation, i.e., P1, P25, P50, P75 and P100 of the whole probability distribution. More than capturing dispatch variability, this criterion encompasses the case with maximum power import (scenario P1) and also maximum power export (scenario P100). This dispatch scenario selection has proven to be efficient in order to illustrate the proposed methodology as will be seen in the results.

6.4.2 Lines, FACTS and D-FACTS Candidate Selection

When running the DC power flow model with the December 2016 network configuration, the network expansion plan for 2013-2016 is sufficient to eliminate all overloads in the system. While the Brazilian system expansion planning imposes N-1 criterion, this case study imposes no security constraint.

Therefore, the lines of the expansion plan 2013-2016 were considered as candidates. In addition to that, as the main goal of this dissertation is to apply the proposed formulation in order to evaluate the influence of series compensation in the transmission expansion planning task, 500 kV existing lines that include compensation were also considered as candidates. For all candidate lines, the costs were calculated based on the line length using the northeast region costs obtained from the Brazilian Electricity Regulatory Agency [53].

To simplify the planning process, flows on transmission lines of 230 kV or higher will be monitored. Finally, the configuration under analysis is composed of: 1220 buses, 1785 existing circuits (187 monitored lines) and 88 candidate lines (32 being 500 kV lines and 56 being 230 kV lines). The optimal expansion plan will be determined for a single stage, i.e., December 2016.

Finally, it is worth noting that the northeast load is 16.4 GW (approx. 20% of the Brazilian total load).

6.4.2.1 Case Studies Performed with the Test System 3

The table presented below contains the "existing" network diagnosis.

Table 10: "Existing" Network Diagnosis

Scenario	P1	P25	P50	P75	P100
Number of Overloads	8	8	0	1	14
Sum of Overloads [MW]	1406	2635	0	59	5178
Load Shedding [MW]	1032	1221	1032	1032	1501

The first row illustrates the number of overloaded lines and the second shows the sum of overloads on the "existing" network in MW. Nonzero Load Shedding (LS) results occur only if there are unbalanced islands in the system, i.e., new power plants/loads require transmission lines to transport/receive their energy. Despite the P50 scenario does not present overloads, it cannot be neglected because of the LS. Moreover, the overloaded circuits might be different for each dispatch scenario since the power flow distribution is completely different according to each scenario.

In order to eliminate all overloads and LS, the application of the transmission expansion planning proposed formulation will be illustrated for the following case studies:

- Case Study 1 (CS1) ➔ Business as Usual (BAU): allow the proposed model to build new candidate lines;

- Case Study 2 (CS2) ➔ BAU + DSR: allow the model to **a)** build new candidate lines, **b)** deploy DSRs on existing lines or **c)** any combination of **a)** and **b)**;

- Case Study 3 (CS3) ➔ BAU + TCSC + DSR: allow the model to **a)** build new candidate lines without TCSC, **b)** build new candidate lines with TCSC, **c)** deploy DSRs on existing lines or **d)** any combination of **a)** to **c)**.

In the CS2 and CS3, of the 187 monitored existing lines, adding DSRs was cost-effective for 85 of the candidates. For these 85 candidates, adding DSRs was cheaper than building a new line in parallel. Accordingly, a candidate deployment of DSRs was added to each of the 85 lines that were cost-effective. In addition to that, TCSC candidates were added to all candidate lines in the CS3. For all CSCD candidates, the maximum compensation level considered for these simulations is 30%. The cost of a TCSC is modeled as a quadratic function of MVAr and adjusted from $2000 to $2010 using the US Producer Price Index (PPI) [54]. Five DSR models were considered, ranging in ampacity from 500 A to 1500 A and with corresponding inductance values of 39 to 101 μH. The model and number of DSRs for each candidate deployment of DSRs was based on the line ampacity and the typical conductor bundle configuration as specified in [53]. The cost of a single DSR, regardless of model, is the list price of $10,000 for these simulations. All monetary data and results of the TS3 are in US$, as for TS2.

6.4.3 Results Obtained with the Test System 3

In this section, the results obtained with the test system 3 are summarized. The results for the BAU case (CS1) are presented in the table below:

Table 11: Expansion Plan for the BAU Case

Scenario	P1	P25	P50	P75	P100	All Scenarios
Number of Line Additions - 230 [kV]	14	16	15	17	20	20
Number of Line Additions - 500 [kV]	5	3	1	1	6	5
Total Line Additions	19	19	16	18	26	25
Lines in the Robust Exp. Plan	11	15	12	18	18	All
Expansion Plan Cost [M$]	649	529	330	347	727	745
Expansion Plan Cost [%]	197%	161%	100%	105%	221%	226%
CPU Time [Seconds]	35	3	2	2	78	283

First of all, it can be seen that the expansion plans are completely different when only one dispatch scenario is considered. Moreover, the expansion plan robust for all scenarios, shown in the last column of the table above, is different than the plan for any single scenario and is 116% more expensive than the least cost expansion plan taking just one scenario into account (P50).

For further analysis, the robust expansion plan compatible with all dispatch scenarios in the BAU case (CS1) having 25 line additions and a total cost of 745 M$ will be used as reference. The table presented below contains the results for the other case studies proposed in the previous section:

Table 12: Summary of the Results Obtained with TS3

Case Study	Total Line Additions	Lines in the CS1 Exp. Plan	Total CSCD Additions	Investments in Lines [M$]	Investments in CSCDs [M$]	Expansion Plan Cost [M$]	Cost Savings [M$]	CPU Time [Minutes]
CS1	25	All	-	745	-	745	-	5
CS2	24	21	4	695	24	719	26	26
CS3	23	22	4	694	21	715	30	43

First, it is worth to emphasize the impact of the binary variables associated to the construction of the CSCDs and the flow direction unique existence assurance constraints on the computational effort demanded. The computational effort demanded taking into account CSCDs increases representatively.

Furthermore, in CS3, the expansion plan consisted of DSRs totaling 13.6 M$ on three existing lines and 1 TCSC costing 7.4 M$ on a new line. For both CS2 and CS3, adding power flow operational flexibility avoids the construction of 1 and 2 lines

respectively, reducing approximately 50 M$ investment in line construction in both cases. Furthermore, there are 4 lines in the CS2 and 3 lines in the CS3 which are not in the CS1 expansion plan, i.e., in addition to avoiding the construction of new lines, the decision of which new lines should be built is changed.

In addition, as shown in Table 10, there was pre-expansion load shedding and consequently the construction of some lines was necessary to meet reliability requirements. This fact can be seen in the P50 scenario which didn't present pre-expansion overloads and still needed 16 lines to avoid LS.

Finally, both study cases CS2 and CS3 present representative cost savings, being respectively equal to 26 M$ and 30 M$.

7 CONCLUSIONS

In this dissertation, Mixed-Integer Linear Programming (MILP) formulations of the incorporation of the devices which enable power flow controllability and flexibility to the transmission expansion planning problem have been proposed.

The transmission expansion planning problem is formulated as an optimization model based on the linearized power flow and circuit limits where the objective is to minimize the investments in the transmission system.

The first proposed formulation by this dissertation is an alternative hybrid linear model that avoids the nonlinearity present in the Kirchhoff's Voltage Law (KVL) for candidate circuits adding at the same time power controllability to candidate circuits and consequently to the system. This proposed formulation is an improvement of the traditional one because the KVL is enforced but the susceptance presents an operating setpoint which can be between zero and the maximum susceptance value.

From the point of view of power flow controllability and flexibility, instead of explicitly representing a transmission line and a series compensation, this formulation represents a line whose susceptance varies from zero to the maximum value (nominal line susceptance). So, depending on the applications, the proposed formulation can bring interesting results. From the point of view of a relaxed model, i.e., a model which aims to represent conventional lines with less accuracy than the complete formulation, it is expected that the proposed formulation demands more computational effort but with

better results than the traditional hybrid model, in other words, with results closer to the full model with KVL being represented through the disjunctive formulation.

The second proposed formulation models Candidate Series Compensation Devices (CSCDs) which are able to increase and/or decrease the line reactance and consequently control the power flow in the target transmission line. The devices which enable such control are presented in the third chapter of this dissertation. The traditional FACTS devices are well known and their control capabilities also. Their major applications are for positive compensation, assuming the conventions defined in this master thesis. The proposed formulation enables the positive compensation representation.

On the other hand, it is plausible to emphasize that the Distributed-FACTS contemplated by this dissertation are new devices which present also new control capabilities. Based on the conventions defined in this master thesis, the Distributed Series Reactors (DSRs) enable the negative compensation while the Distributed Series Compensators (DSCs) enable the joint compensation. Accordingly, more than helping to broadcast this new knowledge, this dissertation proposes the MILP formulation to incorporate these devices in the DC OPF and consequently in the transmission expansion planning task and these are valuable contributions brought by this work.

Focusing on the proposed formulation, more than defining the susceptance variation range provided by the CSCD, the compensation type may also be set, i.e., the proposed formulation enables the application of three compensation types. These are also valuable contributions brought by this dissertation.

As shown above, the maximum compensation level achieved by each CSCD is arbitrarily defined as input data. In addition to that, the proposed formulation has the capability of presenting a specific operating setpoint according to each dispatch scenario and operating conditions. This feature promotes the power flow controllability and flexibility demanded by systems with increasing RES.

The proposed formulations were applied to several case studies in chapter 6. The analysis of results of these case studies allowed showing the applicability of the proposed formulations and discussing its features and characteristics.

Furthermore, this dissertation has shown that a robust expansion plan compatible with all dispatch scenarios in the Business as Usual (BAU) case, i.e., traditional

transmission equipment (lines and transformers), results in a lower average loading, needs more reinforcements in the system, and is more expensive. FACTS and D-FACTS are very important for transmission expansion planning by providing an operational flexibility to different dispatch scenarios and consequently increasing asset utilization and existing transmission capacity, capabilities that are vital in systems with high penetration of renewable energy sources. Therefore, the faculty of postponing transmission upgrades and saving transmission investments has been analyzed in this work.

The proposed formulation was clearly and didactically shown through Test System 1.

The technical benefits on the system operation were shown through the case studies developed on Test System 2. It was shown that when all dispatch scenarios are considered, more CSCDs are demanded and their effects are also more representative. Furthermore, the power flow flexibility provided by the proposed formulation was also shown, i.e., the formulation enables different operating setpoints according to each dispatch scenario.

On the other hand, it is worth to emphasize that the computational effort demanded when CSCDs are taken into account increases representatively because of the impact of the binary variables associated to the construction of the CSCDs and the flow direction unique existence assurance constraints. Each dispatch scenario demands a set of the flow direction unique existence assurance constraints and the higher the number of scenarios considered, the greater the number of integer variables and therefore the greater the computational time required.

It is worth to emphasize the complete example that was given through test system 3, the real Brazilian system. This case study started with a simulation called Stochastic Optimization of Multireservoir Hydroelectric System in order to determine the dispatches from all power plants in Brazil. Afterwards, a dispatch scenario selection for the transmission expansion task was performed. Then, line, FACTS and D-FACTS candidates were created. Finally, the proposed MILP formulation was applied to the BAU case and taking also CSCDs into account. Practical results with a real system were shown and it could be noticed that the model meets the goals of effectiveness and computational effort.

Other practical advantage of the MILP formulation is that the solution techniques for mixed-integer linear programs are notably mature, allowing the treatment of large-scale optimization problems with robustness and speed. In other words, the problem can be solved to global optimality with the use of widely employed and commercially available mixed-integer linear optimization solvers. The possibility of using commercial solvers is an attractive feature for industry applications, as it essentially translates into guarantees of longevity. Finally, it is worth mentioning that the MILP formulations have been coded and executed with FICO Xpress Mosel ® Version 3.4.1.

7.1 RECOMMENDATIONS FOR FUTURE WORK

As the first recommendation for future work, investigations in order to reduce the computational effort demanded consist in an important research topic. As shown in this dissertation, the existing circuit flow variables are represented through free variables in the DC OPF model. It is suggested as future work to model the existing circuit flow directly with positive and negative variables as is done in the proposed formulation for candidate circuits. The objective of this suggested formulation is to represent the existing circuit flow variables directly in the second set of flow direction unique existence assurance constraints for CSCDs being attached to existing circuits, as this dissertation already proposed for candidate circuits. This will reduce the number of constraints needed for the joint compensation and also when more than one CSCD are in the same ROW. On the other hand, the number of variables represented in the problem will increase. A comparative analysis of the computational time could be performed to see if this new formulation would bring representative gains.

More than investigations, improvements in order to reduce the computational effort demanded consist in an important research topic. As explained in this dissertation, each dispatch scenario demands a set of the flow direction unique existence assurance constraints and the higher the number of scenarios considered, the greater the number of integer variables and therefore the greater the computational time required. Efforts should be devoted in order to propose a formulation in which the introduction of binary variables associated to the flow direction unique existence assurance constraints is avoided.

Furthermore, in the proposed formulation, the maximum compensation level achieved by each CSCD is arbitrarily defined as input data. Another recommendation would be to further investigate the relationship between the compensation level achieved by each device (FACTS or D-FACTS) and the respective cost, i.e., the shape of these curves (if they are linear, concave or convex). Having these curves, efforts should be devoted to formulate the transmission expansion planning problem with the model deciding the maximum compensation level of the CSCDs that will be installed in the network, i.e., the optimization model will be responsible for calculating the trade-off between compensation level and cost taking into account the technical needs of the network. Therefore, further research on this topic is highly recommended.

Another approach for further research is to further analyze and develop models to increase network's power flow controllability and flexibility. First, existing and candidate phase shifters should also be taken into consideration in the transmission expansion planning MILP formulation. Their effects and combined effects with CSCDs should be investigated.

It is worth noting that the Distributed-FACTS devices also contain useful sensors to monitor the condition of the line. As explained in the third chapter of this dissertation, with this information available in the future, more efforts should be devoted in order to produce an accurate Real-time Dynamic Thermal Rating (RTDR). As explained in [28], the maximum thermal capacity of the line dynamically changes and if RTDR curves could be inferred, there could be a power flow increase through a line by 10 to 30% for 90 to 98 % of the time compared to "state-of-art" techniques. This would also increase the system power flow flexibility, i.e., coupled with power flow control, this would allow a utility to re-route power through uncongested lines and further increase system transfer capability.

Although these effects have direct application in the system operation, it is believed that this information will also bring additional information to the planning task. Accordingly, more than determining the RTDR curves, their impacts on the transmission expansion planning task is also suggested for future work. As line thermal limits are nowadays very conservative, more realistic and still safe thermal limits of lines may be the result of research in this area. In addition to determining more realistic values, this research could bring varied thermal limits according, for example, to operating conditions, dispatch scenarios, climate seasons, etc. For such applications, the

proposed formulation can directly be applied incorporating only the necessary changes, i.e., one thermal limit for each dispatch scenario, or one thermal limit for each season in multi-stage planning, etc. More than increasing system transfer capability, further research in this area could also help to postpone transmission upgrades and save transmission investments.

This dissertation proposes formulation to incorporate power flow controllability and flexibility in the DC OPF. Another topic of system operation flexibility which is gaining strength is the DC breakers. This topic involves intense research nowadays and there are many practical industry applications, because these devices will enable better protection schemes for Multi-terminal DC links and DC networks. Accordingly, the DC network representation with Kirchhoff's Current and also Voltage Laws in the DC OPF as a MILP formulation consists in a suggestion for future work. In this approach, DC candidate circuits and also binary variables associated with the switching process of DC breakers could be represented. The latter item would also enable power flow controllability and flexibility in the DC OPF as the DC network configuration and operating setpoints would change according to the operating conditions.

8 REFERENCES

[1] Secretaria de Planejamento e Desenvolvimento Energético, Ministério de Minas e Energia, "Plano Decenal de Expansão de Energia 2022", 2013.

[2] B. Bezerra, L. A. Barroso, M. V. Pereira, "Bidding Strategies with Fuel Supply Uncertainty in Auctions of Long-Term Energy Call Options", IEEE Power and Energy Society General Meeting, 2011.

[3] Estação Triunfo (PE), Dados horários de velocidade do vento de Janeiro/2007, Projeto SONDA http://sonda.ccst.inpe.br/infos/index.html.

[4] NCAR/NCEP, "Global Reanalysis Project Data base".

[5] MERRA, "Modern Era Retrospective Analysis for Research and Applications", Meteorological Data Base.

[6] Camargo Schubert, http://www.camargoschubert.com.br/.

[7] M.V.F. Pereira and L. M. V. G. Pinto, "Stochastic Optimization of Multireservoir Hydroelectric System – a Decomposition Approach", Water Resource Research, Vol 21 No 6, 1985.

[8] S. Granville, G. C. Oliveira, L. M. Thomé, N. Campodónico, M. L. Latorre, M. Pereira, L. A. Barroso, "Stochastic Optimization of Transmission Constrained and Large Scale Hydrothermal Systems in a Competitive Framework," Proceedings of the IEEE General Meeting, Toronto, 2003.

[9] E. Acha, C. R. Fuente-Esquivel, H. Ambriz-Perez, C. Angeles-Camacho, "FACTS: Modelling and Simulation in Power Systems", John Wiley & Sons Inc., 2004.

[10] J. Arrillaga, N. R. Watson, "Computer Modelling of Electrical Power Systems", John Wiley & Sons Inc., 2001.

[11] V. Kakkar, N. K. Agarwal, "Recent Trends on FACTS and D-FACTS", Modern Electric Power Systems (MEPS), 2010 Proceedings of the International Symposium, pp. 1–8, 2010.

[12] R. Adapa, *et alii*, FACTS Overview, IEEE Power Engineering Society, pp. 2.1–2.4, 1995.

[13] E. H.Watanabe, P. G. Barbosa, K. C. Almeida, G. N. Taranto, "Tecnologia FACTS – Tutorial", SBA Controle & Automação, vol. 9, no. 1, jan., feb., mar. and april, 1998.

[14] E. H. Watanabe, M. Aredes, P. G. Barbosa, F. K. de Araújo Lima, R. F. da Silva Dias, G. Santos Jr., "Flexible AC Transmission Systems", Power Electronics Handbook, Third Edition, pp. 851–877, Burlington, 2011.

[15] D. Divan, W. Brumsickle, R. Schneider, B. Kranz, R. Gascoigne, D. Bradshaw, M. Ingram, I. Grant, "A Distributed Static Series Compensator System for Realizing Active Power Flow Control on Existing Power Lines", IEEE Transactions on Power Delivery, Volume: 22 , issue 1, 2007, pp. 642-649.

[16] R. M. Marthur, R. K. Varma, "Thyristor Based FACTS Controllers for Electrical Transmission Systems", John Wiley & Sons Inc., 2002.

[17] S. Meikandasivam, R. K. Nema, S. K. Jain, "Performance of Installed TCSC Projects, IEEE Power Electronics (IICPE), 2010 India International Conference, pp.1-8, 2011.

[18] N. G. Hingorani, L. Gyugyi, "Understanding FACTS", IEEE press, 1999.

[19] A. J. F. Deri, B. J. Ware, R. A. Byron, A. S. Mehraban, M. Chamia, P. Halvarsson, L. Ängquist, "Improving transmission system performance using controlled series capacitors," Cigré Joint Session 14/37/38-07, Paris, France, 1992.

[20] F. L. Lirio, "Modelagem tensorial de SVC e TCSC no domínimio s para análise linear de transitórios eletromagnéticos e harmônicos", PhD, COPPE/UFRJ, 2007.

[21] C. Gama, "Brazilian north–south interconnection control application and operating experience with a TCSC", IEEE – PES Summer Meeting, vol. 2, pp. 1103–1108, 1999.

[22] L. Gyugyi, C. D. Schauder, K.K. Sen, "Static synchronous series compensator: a solid-state approach to the series compensation of transmission lines", IEEE Transactions on Power Delivery, vol. 12, issue 1, Jan. 1997, pp. 406-417.

[23] H. Johal, "Distributed Series Reactance: A New Approach to Realize Grid Power Flow Control", PhD, Georgia Institute of Technology, 2008.

[24] J. Verboomen, D. Van Hertem, P.H. Schavemaker, W.L. Kling, and R. Belmans, "Phase shifting transformers: principles and applications", International Conference on Future Power Systems, Nov. 2005.

[25] D. M. Falcão, "Análise de Redes Elétricas", Universidade Federal do Rio de Janeiro, 2003.

[26] A. A., Hossam-Eldin, H. Elrefaie, G. K. Mohamed, "Study and Simulation of the Unified Power Flow Controller Effect on Power Systems", The Eleventh International Middle East Power Systems Conferece, MPECON ,Department of Electrical Eng., Alexandria University, Egypt, 2006.

[27] Electricity Today´s Smart Grid Cybersecurity Forum, Expanded Digital Magazine July/August 2013, Volume 26, No. 6, Nov. 13th ,14th ,15th, 2013.

[28] F. Kreikebaum, D. Das,Y. Yang, F. Lambert, D. Divan, "Smart Wires – A Distributed, Low-Cost Solution for Controlling Power Flows and Monitoring Transmission Lines", Innovative Smart Grid Technologies Conference Europe (ISGT Europe), 2010 IEEE PES, pp. 1-8.

[29] H. Johal, D. Divan, "Design Considerations for Series-Connected Distributed FACTS Converters", IEEE Transactions on Industry Applications, Vol. 45, No. 6, 2007, pp. 1609-1618.

[30] D. Das, F. Kreikebaum, D. Divan, F. Lambert, "Reducing Transmission Investment to Meet Renewable Portfolio Standards Using Smart Wires", IEEE PES Transmission and Distribution Conference and Exposition, 2010, pp. 1-7.

[31] D. Divan, "Distributed Intelligent Power Networks – A New Concept for Improving T&D System Utilization and Performance", Electricity Transmission Conference in Deregulated Markets: Challenges, Opportunities, and Necessary R&D Agenda, 2004.

[32] F. Kreikebaum, M. Imayavaramban, D. Divan, "Active Smart Wires: An Inverter-less Static Series Compensator", IEEE Energy Conversion Congress and Exposition (ECCE), 2010, pp. 3626 -3630.

[33] D. Divan, H. Johal, "Distributed FACTS—A New Concept for Realizing Grid Power Flow Control", IEEE Transactions on Power Electronics, vol. 22, no. 6, pp. 2253-2260, 2007.

[34] G. Latorre, R.D. Cruz, J.M. Areiza, and A. Villegas, "Classification of Publications and Models on Transmission Expansion Planning", IEEE Transactions on Power Systems, vol. 18, no. 2, pp. 938-945, May 2003.

[35] E. Nery, "Mercados e Regulação de Energia Elétrica", Cigré Brasil & Editora Interciência, Rio de Janeiro, RJ, Brazil, 2012.

[36] R. Gomes, "A Gestão do Sistema de Transmissão do Brasil", Editora FGV, Rio de Janeiro, RJ, Brazil, 2012.

[37] S. Binato, G. C. Oliveira, "A heuristic approach to cope with multi-year transmission expansion planning", Proceedings of the IEEE Stockholm Power Tech Conference, Stockholm, Sweden 1995.

[38] L. Bahiense, G. C. Oliveira, M. V. Pereira, S. Granville, "A mixed integer disjunctive model for transmission network expansion", IEEE Transactions on Power Systems, Vol 16, No. 3, 2001.

[39] PSR, "OPTNET – Network Transmission Expansion Planning and Analysis – Methodology Manual", Version 2.7, Rio de Janeiro, RJ, Brazil, November 2012.

[40] S. Binato, "Expansão ótima de sistemas de transmissão através de decomposição de Benders e técnicas de planos cortantes", Tese de Doutorado, COPPE, UFRJ, Rio de Janeiro, RJ, Brazil, April 2000.

[41] S. Granville, M. V. F. Pereira, G. B. Dantzig, B. Avi-Itzhak, M. Avriel, A. Monticelli, and L. M. V. G. Pinto. Mathematical decomposition techniques for power system expansion planning - analysis of the linearized power flow model using the Benders decomposition technique. Technical Report RP 2473-6, EPRI, 1988.

[42] S. Binato, M. Pereira and S. Granville, "A New Benders Decomposition Approach to Solve Power Transmission Network Design Problems", IEEE Transactions on Power Systems, Vol 16, No. 2, 2001.

[43] P. Tsamasphyrou, A. Renaud, P. Carpentier, "Transmission Network Planning: An Efficient Benders Decomposition Scheme", Proceedings of the 13th Power System Computation Conference (PSCC), pp. 487-494, Trondheim, Norway, Jun.-Jul. 1999.

[44] M. Pereira, L. Pinto, S. Cunha and G. Oliveira. A decomposition approach to automated generation-transmission expansion planning. IEEE Transactions on PAS, Vol. 104, No. 11, 1985.

[45] F. Thomé, "Aplicação de Técnica de Decomposição com o Cálculo de Multiplicadores Implícitos no Planejamento da Expansão da Geração e Rede de Transmissão de Sistemas Elétricos", Dissertação de Mestrado, COPPE, UFRJ, Rio de Janeiro, RJ, Brazil, March 2008.

[46] R. C. Perez, S. Binato, M. V. Pereira, G. C. Oliveira, F. Thomé, L. M. Thomé, "Modelo de Planejamento de Redes de Transmissão Aplicado à Expansão do Sistema do WECC nos Estados Unidos", XII Symposium of Specialists in Electric Operational and Expansion Planning (XII SEPOPE), Rio de Janeiro, RJ, Brazil, May 2012.

[47] G. N. Taranto, L. M. V. G. Pinto, M.V.F Pereira, "Representation of FACTs Devices in Power System Economic Dispatch", IEEE Transactions on Power Systems, Vol. 7, No. 2, May 1992, pp.572-576.

[48] R. C. Perez, D. M. Falcão, G. C. Oliveira, "Análise do Impacto da Inclusão de FACTs e Smart Wires no Planejamento da Expansão da Transmissão", XII Symposium of Specialists in Electric Operational and Expansion Planning (XII SEPOPE), Rio de Janeiro, RJ, Brazil, May 2012.

[49] R. Fang, D. J. Hill, "A new Strategy for Transmission Expansion Planning in Competitive Electricity Markets", IEEE Transactions on Power Systems, Vol. 18, No. 1, February 2003, pp. 374-380.

[50] R. Romero, C. Rocha, J.R.S Mantovani, I. G. Sánches, "Constructive Heuristic Algorithm for the DC Model in Network Transmission Expansion Planning", IEEE Proc.-Gener. Transm. Distrib., Vol. 152, No. 2, March 2005, pp. 277-282.

[51] ONS, Operador Nacional do Sistema (National System Operator), "Plano de Ampliação e Reforços (PAR) Data Base", available at www.ons.org.br.

[52] ONS, Operador Nacional do Sistema (National System Operator), "Programa Mensal da Operação (PMO) Data Base", available at www.ons.org.br.

[53] ANEEL, Agência Nacional de Energia Elétrica (Brazilian Electricity Regulatory Agency), "Base de Preços de Referência - Ref. 06/2013", Brazil, 2013.

[54] L. J. Cai, et al., "Optimal choice and allocation of FACTS devices in deregulated electricity market using genetic algorithms," in IEEE PES Power Systems Conference and Exposition, New York, NY, 2004, pp. 201-207.

[55] B. Sttot, O. Alsac, "Fast Decoupled Load Flow", IEEE Transactions on Power Apparatus and Systems, v. 93, pp. 859-869, 1974.

[56] B. Sttot, "Review of Load Flow Calculation Methods", Proceedings of the IEEE", v. 62, pp. 916-929, 1974.

9 APPENDIX A: LINEARIZED POWER FLOW

9.1 INTRODUCTION

The main objective of a power flow calculation essentially consists in determining the state of the network, i.e., bus voltage and angle and also the power flow distribution (active and reactive power in transmission lines) through the solution of a set of nonlinear algebraic equations which is used to represent a static configuration of the system.

In electrical power systems under normal operation conditions, present a flat voltage profile, i.e., the voltage magnitude at all buses stays nearly its nominal value (1 p.u.) meaning that the reactive power flow through transmission lines and transformers is relatively small. In addition to that, the active power losses in the transmission lines are also relatively small. Finally, as described in section 3.1 of this dissertation, the real power flow depends structurally on the phase angle difference.

The aforementioned facts enable the utilization of an approximate model entitled linearized power flow – proposed by Stott [55], [56] – for many applications. This model allows the estimation of the active power flow distribution with a low computational cost and acceptable accuracy for many applications.

The linearized power flow is presented as follows.

9.2 DC POWER FLOW FORMULATION

The active power flow through a transmission line is determined by the following equation:

$$P_{ij} = V_i^2 g_{ij} - V_i V_j g_{ij} \cos(\theta_{ij}) - V_i V_j b_{ij} \cos(\theta_{ij}) \tag{309}$$

where:

$$g_{ij} = \frac{r_{ij}}{r_{ij}^2 + x_{ij}^2} \tag{310}$$

$$b_{ij} = \frac{-x_{ij}}{r_{ij}^2 + x_{ij}^2} \tag{311}$$

where:

r_{ij} Series resistance of the transmission line;

x_{ij} Series reactance of the transmission line.

Neglecting transmission losses, i.e., assuming $r_{ij} \approx 0$:

$$g_{ij} \approx 0 \tag{312}$$

$$b_{ij} = \frac{-1}{x_{ij}} \tag{313}$$

Considering that the phase angle difference between buses i and j is sufficient small that enables the following approximation:

$$\sin(\theta_{ij}) \approx \theta_{ij} \tag{314}$$

Finally, as initially described in the introduction of this appendix, considering that the voltage magnitude at all buses is approximately equal to the nominal voltage:

$$V_i \approx V_j \approx 1 \; p.u. \tag{315}$$

In consequence of all aforementioned approximations, the active power flow equation according to the Kirchhoff's Second Law, i.e., Kirchhoff's Voltage Law (KVL), in the linearized model becomes:

$$P_{ij} = \frac{\theta_{ij}}{x_{ij}} = \frac{(\theta_i - \theta_j)}{x_{ij}} = \gamma_{ij}(\theta_i - \theta_j) \tag{316}$$

where:

$$\gamma_{ij} = \frac{1}{x_{ij}} \tag{317}$$

where:

γ_{ij} Series susceptance of the transmission line;

In addition to the KVL, the linearized power flow model represents also Kirchhoff's First Law that is also entitled Kirchhoff's First Law (KCL). The active power injection in each bus is equal to the flow sum that leaves the bus, i.e.:

$$P_i = \sum_{j \in \Omega_i} \gamma_{ij}(\theta_i - \theta_j) \tag{318}$$

where:

Ω_i Set of circuits directly connected to bus i.

9.3 PHASE SHIFTER REPRESENTATION

In the case of phase shifters, the active power flow is defined as follows:

$$P_{ij} = V_i^2 g_{ij} - V_i V_j g_{ij} \cos(\theta_{ij} + \alpha_{ij}) - V_i V_j b_{ij} \sin(\theta_{ij} + \alpha_{ij}) \tag{319}$$

where:

α_{ij} Phase displacement introduced by the phase-shifting transformer.

Introducing the same approximations (used for transmission lines), the phase shifter's active power flow in the linearized model is defined as follows:

$$P_{ij} = \frac{\theta_{ij} + \alpha_{ij}}{x_{ij}} \tag{320}$$

The Figure presented below summarizes the phase shifter model:
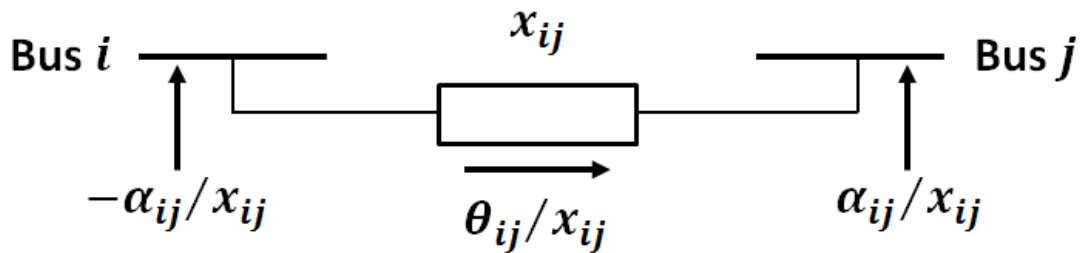
Figure 42: Phase shifter model for linearized power flow

10 APPENDIX B: Big M – THE DISJUNCTIVE CONSTANT

The disjunctive constant was proposed by [41]. This subject was further studied in [43], however the proposed disjunctive constant value was still a very large numerical value. In [40] and in [42] a significant reduction to the constant value was achieved. This calculation is presented below.

Let $k \in \Omega_k^1$ be a candidate circuit represented in the problem by the following linear constraints:

$$f_k^1 - \gamma_k^1\big(\theta(i_k) - \theta(j_k)\big) \le M_k(1 - x_k) \tag{321}$$

$$f_k^1 - \gamma_k^1\big(\theta(i_k) - \theta(j_k)\big) \ge -M_k(1 - x_k) \tag{322}$$

$$-\overline{f_k^1}x_k \le f_k^1 \le \overline{f_k^1}x_k \tag{323}$$

Where M_k is a very big constant ("big M") associated to each candidate circuit k. The disjunctive constraints can be interpreted as follows: if $x_k = 1$, Kirchhoff's second law is enforced to the candidate circuit k, i.e., $f_k = \gamma_k\big(\theta(i_k) - \theta(j_k)\big)$ and the disjunctive constant does not present any effect. Otherwise, if $x_k = 0$, and the following effect is obtained in the flow limit constraints:

$$0 \le f_k^1 \le 0 \tag{324}$$

So, $f_k^1 = 0$. Substituting $f_k^1 = 0$ and $x_k = 0$ in the disjunctive constraints one obtains:

$$-\gamma_k^1\big(\theta(i_k) - \theta(j_k)\big) \le M_k \tag{325}$$

$$-\gamma_k^1\big(\theta(i_k) - \theta(j_k)\big) \ge -M_k \tag{326}$$

As can be seen, these constraints insert a limit on the angular aperture between buses i_k and j_k. The value of M_k must be such that this limit is never reached, otherwise an artificial limit will be inserted in the problem which does not present any physical existence reason.

In order to facilitate reader's interpretation, only conventional candidate circuits (lines and transformers) will be taken into account. First, a circuit duplication will be analyzed. The constraints associated to the existing circuit $k \in \Omega_k^0$ are:

$$f_k^0 - \gamma_k^0\big(\theta(i_k) - \theta(j_k)\big) = 0 \tag{327}$$

$$-\overline{f_k^0} \le f_k^0 \le \overline{f_k^0} \tag{328}$$

Substituting the first into the second equation, one obtains:

$$-\overline{f_k^0}\Big/\gamma_k^0 \le \big(\theta(i_k) - \theta(j_k)\big) \le \overline{f_k^0}\Big/\gamma_k^0 \tag{329}$$

Which is also a limit imposed by the existing network on the angular aperture between buses of the candidate circuit k. Considering this effect in the disjunctive constraints, we obtain:

$$M_k \ge \gamma_k^1 * \overline{f_k^0}\Big/\gamma_k^0 \tag{330}$$

Therefore, it can be concluded that when candidate circuit k is a circuit duplication, the disjunctive constant M_k can be adjusted to a value which is a function of the characteristics of the existing circuit and also the candidate circuit itself.

Now, a candidate circuit that is not a duplication should be considered. For this analysis, it is assumed that the buses at which the circuit is connected belong to an interconnected network. So, there is at least a sequence of existing circuits that connect these buses. Be $W_k = \{k_1, k_2, k_3, \dots, k_w\}$ a path of existing circuits connecting candidate circuit terminal buses. In the same way as for the circuit duplication, there already is a

limit on the angular aperture between these buses. On the other hand, this limit is not given by just one existing circuit but a set of them:

$$-\sum_{k \in W_k} \overline{f_k^0}\Big/{\gamma_k^0} \leq \left(\theta(i_k) - \theta(j_k)\right) \leq \sum_{k \in W_k} \overline{f_k^0}\Big/{\gamma_k^0} \tag{331}$$

So the problem becomes how to find the minimum path W_{Min}, where $W_{Min} \in W_k$, composed by existing circuits that interconnects candidate circuit's bus terminals. In other words, to calculate the lower limit imposed by the existing network to the angular aperture between buses i_k and j_k, the aforementioned shortest path problem needs to be solved in order to determine W_{Min}.

Following the same reasoning used above and replacing the limit W_{Min} encountered for $\left(\theta(i_k) - \theta(j_k)\right)$ in the disjunctive representation from a candidate circuit that is not a duplication, the following statement can be made:

$$M_k \geq \gamma_k^1 * W_{Min} \tag{332}$$

In summary, since there may be several paths connecting buses i_k and j_k, the smallest value of M_k will be the candidate's reactance times the "length" of the shortest path between i_k and j_k, where circuit "length" can be defined as the ratio of its capacity and its reactance [42]. Finally, for practical applications, the length of the shortest path between any pair of buses is calculated by Dijkstra's algorithm.

It is worth to emphasize that the value of M_k for candidate k depends on the network topology and the reactance values present in the network. Furthermore, it is also worth to remember that the main job of M_k is to avoid inserting an artificial limit in the problem which does not present any physical existence reason. So, if Candidate Series Compensation Devices are taken into account, they will present effects on the network and therefore they should also be considered in this determination. As an illustration, considering a CSCD with negative compensation which is attached to an existing circuit, if it is actually added to the network, the equivalent reactance of the Right-Of-Way will increase and its "length" will also increase. If the shortest path W_{Min} is still the same, an increase in M_k will consequently be needed. Finally, the algorithm

must always consider the worst situation to avoid that artificial bounds are inserted into the optimization problem.

11 APPENDIX C: WHY IS THE $\Delta\theta^+$ OR $\Delta\theta^-$ UNIQUE EXISTENCE ASSURANCE IMPORTANT?

11.1 Hybrid Candidate Circuit 2-3

In this appendix, the simplest test system from the case study section with 3 buses, 2 existing branches and 1 hybrid candidate circuit will also be used.

$g(1) \le 60$ $\gamma(1,2) = 10$ $g(2) \le 40$

BUS_1 $f(1,2) \le 40$ BUS_2

$\gamma(1,3) = 5.556$ $\gamma(2,3) = 10$

$f(1,3) \le 40$ $f(2,3) \le 80$

BUS_3

$d(3) = 100$
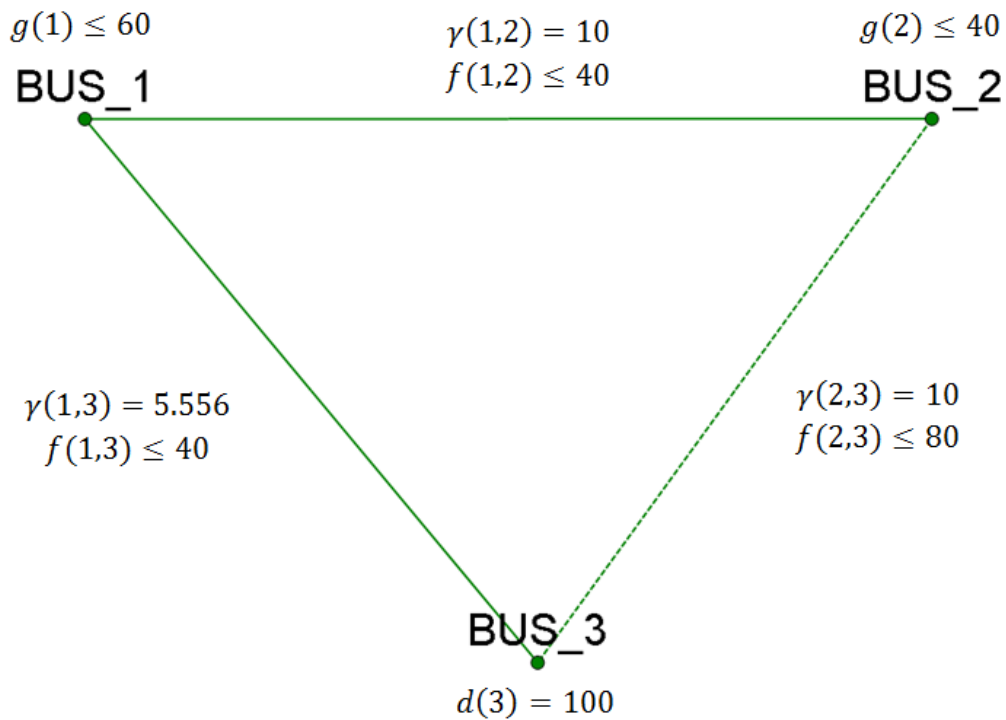
Figure 43: 3-Bus test system

As can be seen in the figure presented above, existing transmission lines are represented through a continuous line while the hybrid candidate line is represented through a dashed line.

First the expansion planning problem will be formulated having the hybrid candidate circuit 2-3 and neglecting the flow direction unique assurance constraints:

$$Objective\ Function = Min\{\delta \times r(3) + c_1 \times x_1\} \tag{333}$$

Subject to:

Bus balance equations respectively for buses 1, 2 and 3**:**

$$-f(1,2) - f(1,2) - f(1,3) = -60 \tag{334}$$

$$f(1,2) - f(2,3)^+ + f(2,3)^- = -40 \tag{335}$$

$$f(1,3) + r(3) + f(2,3)^+ - f(2,3)^- = 100 \tag{336}$$

KVL for existing circuits 1-2 and 1-3:

$$f(1,2) = 10 \times (\theta(1) - \theta(2)) \tag{337}$$

$$f(1,3) = 5.556 \times (\theta(1) - \theta(3)) \tag{338}$$

Flow limits for the existing circuit 1-2 and 1-3:

$$-40 \leq f(1,2) \leq 40 \tag{339}$$

$$-40 \leq f(1,3) \leq 40 \tag{340}$$

Angle constraint for the candidate circuit 2-3:

$$\Delta\theta(2,3) = \Delta\theta(2,3)^+ - \Delta\theta(2,3)^- \tag{341}$$

KVL upper bound for candidate circuit 2-3:

$$f(2,3)^+ \leq 10 \times \Delta\theta(2,3)^+ \tag{342}$$

$$f(2,3)^- \leq 10 \times \Delta\theta(2,3)^- \tag{343}$$

Flow limit constraints for the hybrid candidate circuit 2-3:

$$f(2,3)^+ \leq 80 \times x_1 \tag{344}$$

$$f(2,3)^- \leq 80 \times x_1 \tag{345}$$

The results are presented below:

$$f(1,2) = 40 \; MW$$

$$f(1,3) = 20 \; MW$$

$$f(2,3)^+ = 80 \; MW$$

$$f(2,3)^- = 0 \; MW$$

$$r(3) = 0 \; MW$$

$$\theta_1 = 0°$$

$$\theta_2 = -0.04 \; rad = -2.292°$$

$$\theta_3 = -0.036 \; rad = -2.063°$$

$$\Delta\theta(2,3)^+ = 0.08°$$

$$\Delta\theta(2,3)^- = 0.084°$$

As can be seen, in this solution $\Delta\theta(2,3)^+$ and $\Delta\theta(2,3)^-$ are both simultaneously nonzero and consequently:

$$f(2,3)^+ - f(2,3)^- = 80 \neq 10 \times (\theta(2)^0 - \theta(3)^0) = 10 \times (0.04) * 100 = 4 \tag{346}$$

The values inside the model are calculated in p.u. and that is the reason we need to multiply by 100. In summary, the hybrid candidate flow does not respect Kirchhoff's second law. This problem occurred because there is no constraint that forces that only one of the variables $\Delta\theta(2,3)^+$ and $\Delta\theta(2,3)^-$ can be nonzero in the optimal solution of the problem.

Now, if we consider the flow direction unique existence assurance constraints for the hybrid candidate circuit 2-3:

$$\Delta\theta(2,3)^+ \leq K \times z(2,3) \tag{347}$$

$$\Delta\theta_k^{n-} \leq M \times (1 - z(2,3)) \tag{348}$$

$$z(2,3) \in \{0,1\}$$

The following results are obtained:

$f(1,2) = 16\ MW$

$f(1,3) = 40\ MW$

$f(2,3)^+ = 56\ MW$

$f(2,3)^- = 0\ MW$

$r(3) = 4\ MW$

$\theta_1 = 0°$

$\theta_2 = -0.016\ rad = -0.917°$

$\theta_3 = -0.072\ rad = -4.125°$

$\Delta\theta(2,3)^+ = 0.056 = 3.209°$

$\Delta\theta(2,3)^- = 0°$

In this case, $\Delta\theta(2,3)^+$ and $\Delta\theta(2,3)^-$ cannot simultaneously be nonzero. As consequence, the following equation is now met:

$$f(2,3)^+ - f(2,3)^- = 56 = 10 \times (\theta(2)^0 - \theta(3)^0) = 10 \times (0.056) * 100 = 56 \quad (349)$$

It is worth to emphasize that if the improved flow direction constraints proposed by this dissertation – that are shown below – are used instead of (347) and (348), the results are exactly the same.

$$z(2,3)^+ \geq f(2,3)^+ / 80 \tag{350}$$

$$z(2,3)^- \geq f(2,3)^- / 80 \tag{351}$$

$$\Delta\theta(2,3)^+ \leq K(1 - z(2,3)^-) \tag{352}$$

$$\Delta\theta(2,3)^- \leq K(1 - z(2,3)^+) \tag{353}$$

$$z(2,3)^+ + z(2,3)^- \leq x_1 \tag{354}$$

$$z(2,3)^+, z(2,3)^- \in \{0,1\}$$

The same analysis can be done for the positive or negative compensation when a candidate series compensation device (CSCD) is attached to an existing or candidate circuit. The effect of non-compliance with the KVL is exactly the same.

11.2 JOINT COMPESANTION

As the joint compensation presents intrinsically in its formulation both positive and negative compensations, may not be necessary the representation of the flow direction unique existence assurance constraints. The purpose of this section is to deeply investigate this issue.

First, the joint compensation circuit 1-2 will be analyzed. It is the same test system and also the same CSCD 1-2 that are used in the case study section.

11.2.1   3-Bus System: Joint Compensation Circuit 1-2

A CSCD will be attached to circuit 1-2. This candidate enables 50% joint compensation (positive and negative). So, $\overline{\gamma}_{k1} = 10$ and $\overline{\gamma}_{k2} = 3.333$.

The MILP formulation for joint compensation without the flow direction unique existence assurance constraints is presented below:

$$Objective\ Function = Min\{\delta \times r(3) + c_1 \times x_1 + c_2 \times v_1\} \tag{355}$$

Subject to:

Bus balance equations respectively for buses 1, 2 and 3**:**

$$-f(1,2) - f(1,3) - \delta_{k1}^n(1,2)^+ + \delta_{k1}^n(1,2)^- + \delta_{k2}^n(1,2)^+ - \delta_{k2}^n(1,2)^- = -60 \tag{356}$$

$$f(1,2) - f(2,3)^+ + f(2,3)^- + \delta_{k1}^n(1,2)^+ - \delta_{k1}^n(1,2)^- - \delta_{k2}^n(1,2)^+ + \delta_{k2}^n(1,2)^- = -40 \tag{357}$$

$$f(1,3) + r(3) + f(2,3)^+ - f(2,3)^- = 100 \tag{358}$$

KVL for existing circuits 1-2 and 1-3:

$$f(1,2) = 10 \times (\theta(1) - \theta(2)) \tag{359}$$

$$f(1,3) = 5.556 \times (\theta(1) - \theta(3)) \tag{360}$$

Flow limits for the existing circuit 1-3:

$$-40 \leq f(1,3) \leq 40 \tag{361}$$

Angle constraint for the candidate circuit 2-3:

$$\Delta\theta(2,3) = \Delta\theta(2,3)^+ - \Delta\theta(2,3)^- \tag{362}$$

KVL upper bound for candidate circuit 2-3:

$$f(2,3)^+ \leq 10 \times \Delta\theta(2,3)^+ \tag{363}$$

$$f(2,3)^- \leq 10 \times \Delta\theta(2,3)^- \tag{364}$$

KVL lower bound for candidate circuit 2-3:

$$f(2,3)^+ - 10 \times \Delta\theta(2,3)^+ \geq -M(1 - x_1) \tag{365}$$

$$f(2,3)^- - 10 \times \Delta\theta(2,3)^+ \geq -M(1 - x_1) \tag{366}$$

Candidate circuit flow limits:

$$f(2,3)^+ \leq 80 \times x_1 \tag{367}$$

$$f(2,3)^- \leq 80 \times x_1 \tag{368}$$

Angle constraint for the CSCD 1-2:

$$\Delta\theta(1,2) = \Delta\theta(1,2)^+ - \Delta\theta(1,2)^- \tag{369}$$

KVL for the CSCD 1-2 with $\overline{\gamma}_{k1}(1,2) = 10$ and $\overline{\gamma}_{k2}(1,2) = 3.333$:

$$\delta_{k1}^n(1,2)^+ \leq 10 \times \Delta\theta(1,2)^+ \tag{370}$$

$$\delta_{k1}^n(1,2)^- \leq 10 \times \Delta\theta(1,2)^- \tag{371}$$

$$\delta_{k2}^n(1,2)^+ \leq 3.333 \times \Delta\theta(1,2)^+ \tag{372}$$

$$\delta_{k2}^n(1,2)^- \leq 3.333 \times \Delta\theta(1,2)^- \tag{373}$$

CSCD flow limits:

$$\delta_{k1}^n(1,2)^+ \leq 40 \times v_1 \tag{374}$$

$$\delta_{k1}^n(1,2)^- \leq 40 \times v_1 \tag{375}$$

$$\delta_{k2}^n(1,2)^+ \leq 40 \times v_1 \tag{376}$$

$$\delta_{k2}^n(1,2)^- \leq 40 \times v_1 \tag{377}$$

ROW 1-2 flow limit, where ROW 1-2 is composed of the existing circuit 1-2 and the CSCD 1-2):

$$-40 \quad \leq f_0^n + \delta_{k1}^n(1,2)^+ - \delta_{k1}^n(1,2)^- - \delta_{k2}^n(1,2)^+ + \delta_{k2}^n(1,2)^- \leq 40 \tag{378}$$

The results are presented below:

$f(1,2) = 0 \; MW$

$f(1,3) = 35.714 \; MW$

$\delta_{k1}^n(1,2)^+ = 24.286 \; MW$

$\delta_{k1}^n(1,2)^- = 0 \; MW$

$\delta_{k2}^n(1,2)^+ = 0 \; MW$

$\delta_{k2}^n(1,2)^- = 0 \; MW$

$$f(2,3)^+ = 64.286 \ MW$$

$$f(2,3)^- = 0 \ MW$$

$$\theta_1 = 0°$$

$$\theta_2 = 0°$$

$$\theta_3 = -3.683°$$

$$\Delta\theta(1,2)^+ = 1.392°$$

$$\Delta\theta(1,2)^- = 1.392°$$

$$\Delta\theta(2,3)^+ = 3.683°$$

$$\Delta\theta(2,3)^- = 0°$$

As can be seen, in this solution $\Delta\theta(1,2)^+$ and $\Delta\theta(1,2)^-$ are both simultaneously nonzero and $f(1,2)$, θ_1 and θ_2 are all equal to zero. Consequently, the KVL for the CSCD 1-2 is not met and the power flow distribution is not correct.

As explained throughout this thesis, to obtain the same percentage of compensation in terms of the reactance ($X\%$), $\overline{\gamma}_{k1}(1,2)$ must be different from $\overline{\gamma}_{k2}(1,2)$. Another interesting conjecture to consider is: what happens to the model when $\overline{\gamma}_{k1}(1,2)$ is equal to $\overline{\gamma}_{k2}(1,2)$. This test was performed and the results were exactly equal to the results previously obtained and above mentioned, which proves that the conjecture of $\overline{\gamma}_{k1}(1,2)$ being equal to $\overline{\gamma}_{k2}(1,2)$ or not does not present any connection with the need of the flow direction unique existence assurance. In other words, the constraints that ensure that $\Delta\theta(1,2)^+$ and $\Delta\theta(1,2)^-$ are never simultaneously nonzero should be represented independently if $\overline{\gamma}_{k1}(1,2)$ is equal or not to $\overline{\gamma}_{k2}(1,2)$.

11.2.2   3-Bus System: Joint Compensation Circuit 1-3

A CSCD will be attached to circuit 1-3. This candidate enables 50% joint compensation (positive and negative). So, $\overline{\gamma}_{k1} = 5.556$ and $\overline{\gamma}_{k2} = 1.852$.

The MILP formulation for joint compensation without the flow direction unique existence assurance constraints is presented below:

$$Objective \ Function = Min\{\delta \times r(3) + c_1 \times x_1 + c_2 \times v_1\} \tag{379}$$

Subject to:

Bus balance equations respectively for buses 1, 2 and 3:

$$-f(1,2) - f(1,3) - \delta_{k1}^n(1,3)^+ + \delta_{k1}^n(1,3)^- + \delta_{k2}^n(1,3)^+ - \delta_{k2}^n(1,3)^- = -60 \quad (380)$$

$$f(1,2) - YLT(2,3)^+ + YLT(2,3)^- = -40 \quad (381)$$

$$f(1,3) + r(3) + YLT(2,3)^+ - YLT(2,3)^- + \delta_{k1}^n(1,3)^+ - \delta_{k1}^n(1,3)^- - \delta_{k2}^n(1,3)^+ + \delta_{k2}^n(1,3)^- = 100 \quad (382)$$

KVL for existing circuits 1-2 and 1-3:

$$f(1,2) = 10 \times (\theta(1) - \theta(2)) \quad (383)$$

$$f(1,3) = 5.556 \times (\theta(1) - \theta(3)) \quad (384)$$

Flow limits for the existing circuit 1-3:

$$-40 \leq f(1,3) \leq 40 \quad (385)$$

Angle constraint for the candidate circuit 2-3:

$$\Delta\theta(2,3) = \Delta\theta(2,3)^+ - \Delta\theta(2,3)^- \quad (386)$$

KVL upper bound for candidate circuit 2-3:

$$f(2,3)^+ \leq 10 \times \Delta\theta(2,3)^+ \quad (387)$$

$$f(2,3)^- \leq 10 \times \Delta\theta(2,3)^- \quad (388)$$

KVL lower bound for candidate circuit 2-3:

$$f(2,3)^+ - 10 \times \Delta\theta(2,3)^+ \geq -M(1 - x_1) \quad (389)$$

$$f(2,3)^- - 10 \times \Delta\theta(2,3)^+ \geq -M(1 - x_1) \quad (390)$$

Candidate circuit flow limits:

$$f(2,3)^+ \leq 80 \times x_1 \tag{391}$$

$$f(2,3)^- \leq 80 \times x_1 \tag{392}$$

Angle constraint for the CSCD 1-3:

$$\Delta\theta(1,3) = \Delta\theta(1,3)^+ - \Delta\theta(1,3)^- \tag{393}$$

KVL for the CSCD 1-3 with $\overline{\gamma}_{k1}(1,3) = 5{,}556$ and $\overline{\gamma}_{k2}(1,3) = 1{,}852$:

$$\delta_{k1}^n(1,3)^+ \leq 5{,}556 \times \Delta\theta(1,3)^+ \tag{394}$$

$$\delta_{k1}^n(1,3)^- \leq 5{,}556 \times \Delta\theta(1,3)^- \tag{395}$$

$$\delta_{k2}^n(1,3)^+ \leq 1{,}852 \times \Delta\theta(1,3)^+ \tag{396}$$

$$\delta_{k2}^n(1,3)^- \leq 1{,}852 \times \Delta\theta(1,3)^- \tag{397}$$

CSCD flow limits:

$$\delta_{k1}^n(1,3)^+ \leq 40 \times v_1 \tag{398}$$

$$\delta_{k1}^n(1,3)^- \leq 40 \times v_1 \tag{399}$$

$$\delta_{k2}^n(1,3)^+ \leq 40 \times v_1 \tag{400}$$

$$\delta_{k2}^n(1,3)^- \leq 40 \times v_1 \tag{401}$$

ROW 1-2 flow limit, where ROW 1-2 is composed of the existing circuit 1-2 and the CSCD 1-2):

$$-40 \le f_0^n + \delta_{k1}^n(1,3)^+ - \delta_{k1}^n(1,3)^- - \delta_{k2}^n(1,3)^+ + \delta_{k2}^n(1,3)^- \le 40 \tag{402}$$

The results are presented below:

$f(1,2) = 40 \; MW$

$f(1,3) = 66.667 \; MW$

$\delta_{k1}^n(1,3)^+ = 0 \; MW$

$\delta_{k1}^n(1,3)^- = 40 \; MW$

$\delta_{k2}^n(1,3)^+ = 6.667 \; MW$

$\delta_{k2}^n(1,3)^- = 0 \; MW$

$YLT(2,3)^+ = 80 \; MW$

$YLT(2,3)^- = 0 \; MW$

$\theta_1 = 6.875°$

$\theta_2 = 4.537°$

$\theta_3 = 0°$

$\Delta\theta(1,3)^+ = 0.336 \; rad = 11°$

$\Delta\theta(1,3)^- = 0.216 \; rad = 4.125°$

$\Delta\theta(2,3)^+ = 4.537°$

$\Delta\theta(2,3)^- = 0°$

As can be seen, in this solution $\Delta\theta(1,3)^+$ and $\Delta\theta(1,3)^-$ are both simultaneously nonzero. Consequently, the KVL for the CSCD 1-3 is not met. To illustrate that fact, it is interesting to analyze the resultant $\gamma(1,3)$ achieved by the CSCD 1-3 for the whole ROW 1-3:

$$\gamma(1,3) = \frac{\left[f(1,3) + \delta_{k1}^n(1,3)^+ - \delta_{k1}^n(1,3)^- - \delta_{k2}^n(1,3)^+ + \delta_{k2}^n(1,3)^-\right]}{\Delta\theta(1,3)} = \frac{0.2 \; p.u.}{0.12} = 1.667 \; S \tag{403}$$

From the aforementioned equation can be noticed that the resultant $\gamma(1,3)$ does not represent anymore the physical result of series compensation, since the minimum achievable value for $\gamma(1,3)$ is 3.704 ($\gamma(1,3) - \overline{\gamma}_{k2}(1,3) = 5.556 - 1.852$).

The same test having $\overline{\gamma}_{k1}(1,3)$ is equal to $\overline{\gamma}_{k2}(1,3)$ was also performed for this example. The results were exactly equal to the results previously obtained, except for the following variables:

$\Delta\theta(1,3)^+ = 19.251\,°$

$\Delta\theta(1,3)^- = 12.376°$

$\Delta\theta(1,3)^+$ and $\Delta\theta(1,3)^-$ are different from the above mentioned ones, but both are still simultaneously nonzero. Accordingly, the constraints that ensure that $\Delta\theta(1,3)^+$ and $\Delta\theta(1,3)^-$ are never simultaneously nonzero should be represented independently if $\overline{\gamma}_{k1}(1,3)$ is equal or not to $\overline{\gamma}_{k2}(1,3)$.

When the flow direction unique existence assurance constraints are used, it can be seen that the minimum susceptance is achieved. Taking the results of the case study entitled "Joint Compensation Circuit 1-3" into account, the resultant $\gamma(1,3)$ for the ROW 1-3 can be calculated as follows:

$$\gamma_{CSCD}(1,3) = \frac{0.170213\ p.u.}{0.091914} = 1.852 \tag{404}$$

$$\gamma(1,3) = 5.556 - 1.852 = 3.704 \tag{405}$$

As can be seen, $\overline{\gamma}_{k2}$ limit is achieved and the ROW 1-3 operates with its minimum allowed $\gamma(1,3)$ value.

12 APPENDIX D: INPUT DATA FOR THE TEST SYSTEM 2 – IEEE-24BUS SYSTEM

12.1 INTRODUCTION

The IEEE24-Bus system is a test system developed for testing on electrical power systems and presents originally 24 buses, 41 circuits and a load of 8550 MW [49], [50]. The data of the existing and candidate circuits and also the four dispatch scenarios G1, G2, G3 and G4 that will be used in this dissertation were taken from [50].

It is worth to remember that in order to make the test system even more interesting for the proposed applications, new transmission corridors were generated, i.e., to further increase the number of new candidate right-of-ways in addition to the ones presented in references [49] and [50], the existing circuits between buses 11-13, 16-19, 17-22, 15-21, 12-23, 10-11 and 9-12 were removed, i.e., they turned to be candidate circuits. The configuration of the system under analysis is presented in the following section.

12.2 DATA USED IN THE TEST SYSTEM 2

Table 13: TS2 – Dispatch Scenarios

Dispatch Scenario	Buses									
	1	2	7	13	15	16	18	21	22	23
G1	576	576	900	1773	645	465	1200	1200	900	315
G2	465	576	722	1424	645	465	1200	1200	900	953
G3	576	576	900	1457	325	282	603	951	900	1980
G4	520	520	812	1599	581	419	718	1077	900	1404

Table 14: TS2 – Loads

Load [MW]	Buses																	
	1	2	3	4	5	6	7	8	9	10	14	15	16	17	18	19	20
	324	291	540	222	213	408	375	513	525	585	795	582	951	300	999	543	384

Table 15: TS2 – Existing circuits

Bus From	Bus To	Circuit #ID	Circuit Type	Resistance [%]	Reactance [%]	Nominal Capacity [MW]
1	2	1	Line	2.60	1.39	175
1	3	1	Line	5.46	21.12	175
1	5	1	Line	2.18	8.45	176
2	4	1	Line	3.28	12.67	175
2	6	1	Line	4.97	19.20	175
3	9	1	Line	3.08	11.90	175
4	9	1	Line	2.68	10.37	175
5	10	1	Line	2.28	8.83	175
6	10	1	Line	1.39	6.05	175
7	8	1	Line	1.59	6.14	175
8	9	1	Line	4.27	16.51	175
8	10	1	Line	4.27	16.51	175
11	14	1	Line	0.54	4.18	500
12	13	1	Line	0.61	4.76	500
13	23	1	Line	1.11	8.65	500
14	16	1	Line	0.50	3.89	500
15	16	1	Line	0.22	1.73	500
15	24	1	Line	0.67	5.19	500
16	17	1	Line	0.33	2.59	500
17	18	1	Line	0.18	1.44	500
18	21	1	Line	0.33	2.59	500
18	21	2	Line	0.33	2.59	500
19	20	1	Line	0.51	3.96	500
19	20	2	Line	0.51	3.96	500

20	23	1	Line	0.28	2.16	500
20	23	2	Line	0.28	2.16	500
21	22	1	Line	0.87	6.78	500
3	24	1	Transformer	0.23	8.39	400
9	11	1	Transformer	0.23	8.39	400
10	12	1	Transformer	0.23	8.39	400

Table 16: TS2 – Candidate circuits

Bus From	Bus To	Circuit #ID	Circuit Type	Resistance [%]	Reactance [%]	Nominal Capacity [MW]	Cost [M$]
1	2	2	Line	2.60	1.39	175	3
1	3	2	Line	5.46	21.12	175	55
1	5	2	Line	2.18	8.45	176	22
1	2	3	Line	2.60	1.39	175	3
1	3	3	Line	5.46	21.12	175	55
1	5	3	Line	2.18	8.45	176	22
1	8	1	Line	3.48	13.44	500	35
1	8	2	Line	3.48	13.44	500	35
2	4	2	Line	3.28	12.67	175	33
2	6	2	Line	4.97	19.20	175	50
2	4	3	Line	3.28	12.67	175	33
2	6	3	Line	4.97	19.20	175	50
2	4	4	Line	3.28	12.67	175	33
2	8	1	Line	3.28	12.67	500	33
2	8	2	Line	3.28	12.67	500	33
3	9	2	Line	3.08	11.90	175	31
3	9	3	Line	3.08	11.90	175	31
4	9	2	Line	2.68	10.37	175	27
4	9	3	Line	2.68	10.37	175	27

5	10	2	Line	2.28	8.83	175	23
5	10	3	Line	2.28	8.83	175	23
6	10	2	Line	1.39	6.05	175	16
6	10	3	Line	1.39	6.05	175	16
6	7	1	Line	4.97	19.20	175	50
6	7	2	Line	4.97	19.20	175	50
7	8	2	Line	1.59	6.14	175	16
7	8	3	Line	1.59	6.14	175	16
8	9	2	Line	4.27	16.51	175	43
8	10	2	Line	4.27	16.51	175	43
8	9	3	Line	4.27	16.51	175	43
8	10	3	Line	4.27	16.51	175	43
8	9	4	Line	4.27	16.51	175	43
11	13	1	Line	0.61	4.76	500	66
11	14	2	Line	0.54	4.18	500	58
11	13	2	Line	0.61	4.76	500	66
11	14	3	Line	0.54	4.18	500	58
12	13	2	Line	0.61	4.76	500	66
12	23	1	Line	1.24	9.66	500	134
12	13	3	Line	0.61	4.76	500	66
12	23	2	Line	1.24	9.66	500	134
13	23	2	Line	1.11	8.65	500	120
13	23	3	Line	1.11	8.65	500	120
13	14	1	Line	0.57	4.47	500	62
13	14	2	Line	0.57	4.47	500	62
14	16	2	Line	0.50	3.89	500	54
14	16	3	Line	0.50	3.89	500	54
14	23	1	Line	0.80	6.20	500	86
14	23	2	Line	0.80	6.20	500	86
15	16	2	Line	0.22	1.73	500	24
15	21	1	Line	0.63	4.90	500	68
15	24	2	Line	0.67	5.19	500	72

15	16	3	Line	0.22	1.73	500	24
15	21	2	Line	0.63	4.90	500	68
15	24	3	Line	0.67	5.19	500	72
16	17	2	Line	0.33	2.59	500	36
16	19	1	Line	0.30	2.31	500	32
16	17	3	Line	0.33	2.59	500	36
16	19	2	Line	0.30	2.31	500	32
16	23	1	Line	1.05	8.22	500	114
16	23	2	Line	1.05	8.22	500	114
17	18	2	Line	0.18	1.44	500	20
17	22	1	Line	1.35	10.53	500	146
17	18	3	Line	0.18	1.44	500	20
17	22	2	Line	1.35	10.53	500	146
18	21	3	Line	0.33	2.59	500	36
18	21	4	Line	0.33	2.59	500	36
19	20	3	Line	0.51	3.96	500	55
19	20	4	Line	0.51	3.96	500	55
19	23	1	Line	0.78	6.06	500	84
19	23	2	Line	0.78	6.06	500	84
20	23	3	Line	0.28	2.16	500	30
20	23	4	Line	0.28	2.16	500	30
21	22	2	Line	0.87	6.78	500	94
21	22	3	Line	0.87	6.78	500	94
3	24	2	Transformer	0.23	8.39	400	50
3	24	3	Transformer	0.23	8.39	400	50
9	11	2	Transformer	0.23	8.39	400	50
9	12	2	Transformer	0.23	8.39	400	50
9	11	3	Transformer	0.23	8.39	400	50
9	12	3	Transformer	0.23	8.39	400	50
10	11	2	Transformer	0.23	8.39	400	50
10	12	2	Transformer	0.23	8.39	400	50
10	11	3	Transformer	0.23	8.39	400	50

| 10 | 12 | 3 | Transformer | 0.23 | 8.39 | 400 | 50 |

Table 17: TS2 – Candidate Series Compensation Devices

Bus From	Bus To	Circuit #ID	CSCD #ID	Comp. Level [%]	Nominal Capacity [MW]
1	2	1	5	50	175
1	3	1	5	50	175
1	5	1	5	50	176
1	8	1	5	50	500
2	4	1	5	50	175
2	6	1	5	50	175
2	8	1	5	50	500
3	9	1	5	50	175
4	9	1	5	50	175
5	10	1	5	50	175
6	7	1	5	50	175
6	10	1	5	50	175
7	8	1	5	50	175
8	9	1	5	50	175
8	10	1	5	50	175
11	13	1	5	50	500
11	14	1	5	50	500
12	13	1	5	50	500
12	23	1	5	50	500
13	14	1	5	50	500
13	23	1	5	50	500
14	16	1	5	50	500
14	23	1	5	50	500
15	16	1	5	50	500
15	21	1	5	50	500
15	24	1	5	50	500
16	17	1	5	50	500

16	19	1	5	50	500
16	23	1	5	50	500
17	18	1	5	50	500
17	22	1	5	50	500
18	21	1	5	50	500
19	20	1	5	50	500
19	23	1	5	50	500
20	23	1	5	50	500
21	22	1	5	50	500
1	2	2	6	50	175
1	3	2	6	50	175
1	5	2	6	50	176
1	8	2	6	50	500
2	4	2	6	50	175
2	6	2	6	50	175
2	8	2	6	50	500
3	9	2	6	50	175
4	9	2	6	50	175
5	10	2	6	50	175
6	7	2	6	50	175
6	10	2	6	50	175
7	8	2	6	50	175
8	9	2	6	50	175
8	10	2	6	50	175
11	13	2	6	50	500
11	14	2	6	50	500
12	13	2	6	50	500
12	23	2	6	50	500
13	14	2	6	50	500
13	23	2	6	50	500
14	16	2	6	50	500
14	23	2	6	50	500
15	16	2	6	50	500
15	21	2	6	50	500
15	24	2	6	50	500

16	17	2	6	50	500
16	19	2	6	50	500
16	23	2	6	50	500
17	18	2	6	50	500
17	22	2	6	50	500
18	21	2	6	50	500
19	20	2	6	50	500
19	23	2	6	50	500
20	23	2	6	50	500
21	22	2	6	50	500
1	2	3	7	50	175
1	3	3	7	50	175
1	5	3	7	50	176
2	4	3	7	50	175
2	6	3	7	50	175
3	9	3	7	50	175
4	9	3	7	50	175
5	10	3	7	50	175
6	10	3	7	50	175
7	8	3	7	50	175
8	9	3	7	50	175
8	10	3	7	50	175
11	14	3	7	50	500
12	13	3	7	50	500
13	23	3	7	50	500
14	16	3	7	50	500
15	16	3	7	50	500
15	24	3	7	50	500
16	17	3	7	50	500
17	18	3	7	50	500
18	21	3	7	50	500
19	20	3	7	50	500
20	23	3	7	50	500
21	22	3	7	50	500
2	4	4	8	50	175

8	9	4	8	50	175
18	21	4	8	50	500
19	20	4	8	50	500
20	23	4	8	50	500

12.3 EXPANSION PLANS OBTAINED THROUGH THE PROPOSED FORMULATION

Table 18: TS2 – BAU case: expansion plan

Bus From	Bus To	Circuit #ID	Circuit Type	Resistance [%]	Reactance [%]	Nominal Capacity [MW]	Cost [M$]
2	4	2	Line	3.28	12.67	175	33
6	10	2	Line	1.39	6.05	175	16
6	10	3	Line	1.39	6.05	175	16
7	8	2	Line	1.59	6.14	175	16
7	8	3	Line	1.59	6.14	175	16
12	13	2	Line	0.61	4.76	500	66
12	13	3	Line	0.61	4.76	500	66
13	14	1	Line	0.57	4.47	500	62
14	16	2	Line	0.50	3.89	500	54
14	23	1	Line	0.80	6.20	500	86
14	23	2	Line	0.80	6.20	500	86
15	21	1	Line	0.63	4.90	500	68
15	24	2	Line	0.67	5.19	500	72
15	21	2	Line	0.63	4.90	500	68
16	17	2	Line	0.33	2.59	500	36
16	17	3	Line	0.33	2.59	500	36
17	18	2	Line	0.18	1.44	500	20
17	22	1	Line	1.35	10.53	500	146
3	24	2	Transformer	0.23	8.39	400	50
10	12	2	Transformer	0.23	8.39	400	50

Bus From	Bus To	Circuit #ID	Circuit Type	Resistance [%]	Reactance [%]	Nominal Capacity [MW]	Cost [M$]
10	12	3	Transformer	0.23	8.39	400	50

Table 19: TS2 – BAU + CSCD case: lines and transformers in the expansion plan

Bus From	Bus To	Circuit #ID	Circuit Type	Resistance [%]	Reactance [%]	Nominal Capacity [MW]	Cost [M$]
6	10	2	Line	1.39	6.05	175	16
7	8	2	Line	1.59	6.14	175	16
7	8	3	Line	1.59	6.14	175	16
12	13	2	Line	0.61	4.76	500	66
12	13	3	Line	0.61	4.76	500	66
13	14	1	Line	0.57	4.47	500	62
14	16	2	Line	0.50	3.89	500	54
14	23	1	Line	0.80	6.20	500	86
15	21	1	Line	0.63	4.90	500	68
15	21	2	Line	0.63	4.90	500	68
16	17	2	Line	0.33	2.59	500	36
16	19	1	Line	0.30	2.31	500	32
16	17	3	Line	0.33	2.59	500	36
17	18	2	Line	0.18	1.44	500	20
17	18	3	Line	0.18	1.44	500	20
18	21	3	Line	0.33	2.59	500	36
20	23	3	Line	0.28	2.16	500	30
21	22	2	Line	0.87	6.78	500	94
9	12	2	Transformer	0.23	8.39	400	50
10	12	2	Transformer	0.23	8.39	400	50
10	12	3	Transformer	0.23	8.39	400	50

Table 20: TS2 – BAU + CSCD case: CSCDs in the expansion plan

Bus From	Bus To	Circuit #ID	CSCD #ID
1	3	1	5
1	5	1	5
2	4	1	5
2	6	1	5
3	9	1	5
5	10	1	5
8	9	1	5
8	10	1	5
11	14	1	5
13	23	1	5
14	16	1	5
15	16	1	5
15	21	1	5
15	24	1	5
14	16	2	6